2011

Data mixing at the source, relay, and in the air in multiple-access relay networks

Young Jin Chun
Iowa State University

Data mixing at the source, relay, and in the air

in multiple-access relay networks

by

Young Jin Chun

A dissertation submitted to the graduate faculty

in partial fulfillment of the requirements for the degree of

DOCTOR OF PHILOSOPHY

Major: Electrical Engineering

Program of Study Committee:

Sang Wu Kim, Major Professor

Zhengdao Wang

Aditya Ramamoorthy

Ahmed E. Kamal

Jennifer Davidson

Iowa State University

Ames, Iowa

2011

TABLE OF CONTENTS

LIST OF TABLES

LIST OF FIGURES

ACKNOWLEDGEMENTS

This dissertation would not have been possible without the guidance and the help of several individuals who in one way or another contributed and extended their valuable assistance in the preparation and completion of this study.

First and foremost, I offer my sincerest gratitude to my supervisor, Dr. Sang Wu Kim, who has supported me thoughout my thesis with his patience and knowledge. I want to thank him for his inquisitiveness, insight, and inspiration. I have benefited tremendously from his countless efforts and undaunting dedication to the intellectual and personal growth of his graduate students. I would also like to thank Dr. Zhengdao Wang, Dr. Aditya Ramamoorthy, Dr. Ahmed Kamal, and Dr. Jennifer Davidson for serving on my dissertation committee and for contributing their broad perspective in refining the ideas in this thesis.

Last but not the least, I would like to thank my family. Their love, support, and encouragement have been with me every single moment. This dissertation is dedicated to them as an inadequate but sincere expression of appreciation and love.

ABSTRACT

The concept of cooperative relay is an essential technique for future cellular networks such as wireless mesh networking or wireless ad-hoc networking. In a practical relay network, channel coding, network coding, and antenna arrays, will coexist and yet the joint optimization of these conventional coding schemes and cooperative relay is not well understood. To build a design guideline for relay network, this dissertation develop a joint optimization methodology for multiple coding schemes in multiple access relay network.

There are four major contributions in this thesis: First, we jointly optimize conventional coding schemes and radio resources of multiple access relay network with multiple antennas. The combined design of MIMO transmission modes, channel coding at the source, network coding at the relay have been investigated. We develop optimal design rule that minimize the end-to-end error probability. Second, we derive the fundamental tradeoff between achievable rate and reliability of multiple access relay network with multiple antennas. We consider three MIMO transmission modes, spatial multiplexing (SM), Alamouti coding as transmit diversity (TD), and Golden Coding, and random linear network coding at the relay. We compare the average decoding error probability of each transmission mode. Third, we present an interference cancellation scheme for multi-user MIMO. The proposed Log-likelihood-ratio (LLR) ordered successive interference cancellation (SIC) scheme provides $1 \sim 3$dB gain over the conventional SNR-ordered SIC and the gain increases with increasing number of users. Finally, we present a new architecture for MIMO receivers that cancel the co-channel interference (CCI) using a single radio frequency (RF) and baseband (BB) chain, while still achieving nearly the same bit error rate that can be provided by the conventional receiver requiring multiple RF/BB chains.

CHAPTER 1. INTRODUCTION

1.1 Motivation

The evolution of wireless communication technology has been dramatic over the past decades. A new mobile generation has appeared every decade since the first 1G system (NMT) was introduced in 1981, 2G (GSM) system that started to roll out in 1992, and 3G (W-CDMA/FOMA) which appeared in 2001. Pre-4G technologies such as WiMAX and 3G Long term evolution (LTE) have been on the market since 2006 and 2009 respectively. As the mobile technology progresses, the mobile data traffic is also growing at an explosive rate; the mobile traffic was reported to be two hundred thousand terabyte at 2003, six hundred thousand terabyte at 2010, and is expected to reach 1.4 million terabyte at 2020. The explosive growth in mobile communication has reached to a point where researchers have begun to develop wireless network architecture instead of the traditional point-to-point based communication with central controlling base station.

One example of this trend is the multiple-access relay network where multiple sources communicate to a common destination with the help of cooperating relays. This new research trend is based on the recognition that any wireless transmission from each transmitter can be received and processed at other nodes to achieve a performance gain, rather than being considered as interference. The basic relaying techniques, including amplify and forward (AF), decode and forward (DF), and selective relaying, for cooperative relay was first introduced by Laneman and Wornell in their seminal paper [1] which triggered interest in the study of cooperative relay networks. Conventional coding schemes, such as channel coding, network coding, and antenna array, has been applied to the cooperative relay in order to further improve the system performance. However, it seems we are only beginning to understand about the joint optimization of

multiple coding schemes within cooperative network and practical ways to approach them. In order to have a design guideline for relay network, development of comprehensive optimization theory among multiple coding schemes based on the relaying strategy is essential.

In this dissertation, we jointly optimize conventional coding schemes and radio resources of multiple access relay network with multiple antennas. We investigate the combined design of the MIMO transmission modes, channel coding at the source node, network coding strategy at the relay, node location, and transmit power. We develop optimal design rule that minimize the end-to-end error probability. In the present work, We consider four MIMO transmission modes (spatial multiplexing (SM), beamforming and Alamouti coding as transmit diversity (TD), and Golden Coding), three types of network coding (NC) scheme at the relay (deterministic NC, adaptive NC, and random NC), and two different error probability measures (outage probability and decoding error probability). We also present two practical MIMO receiver schemes. First, Log-likelihood-ratio (LLR) ordered successive interference cancellation (SIC) scheme is analyzed in multi-user, multi-mode system which provides $1 \sim 3$dB gain over the conventional SNR-ordered SIC in multiuser MIMO system and the gain increases with increasing number of users. Second, we present a new architecture for MIMO receivers that cancel the co-channel interference (CCI) using a single radio frequency (RF) and baseband (BB) chain, while still achieving nearly the same bit error rate that can be provided by the conventional receiver requiring multiple RF/BB chains.

1.2 Article Survey

Information theoretic study on the multiple access relay channel (MARC) was first introduced in [2]. Outer bounds on the capacity of the MARC has been studied in [3], the diversity-multiplexing tradeoff (DMT) has been developed in [4], [5], [6], and an outage minimizing relaying strategy has been studied in [7]. Among many literatures, the authors in [8] and [9] analyzed DMT of single-relay system with single antenna nodes for half-duplexing relays. MIMO relay channels were studied in [10] and [11] where the authors in [10] present the DMT lower bound of nonorthogonal amplify and forward protocol and the authors in [11] consider the DMT of decode and forward (DF) and compress-and-forward (CF) protocols for

both full-duplex and half-duplex relays.

In recent years, several network coding techniques for the MARC have been studied. Authors in [12] investigated the cooperative diversity gain offered by the network coding, assuming that the relays are able to decode all source messages reliably. Authors in [13] proposed a network coding scheme based on low-density parity-check (LDPC) codes that accounts for the lossy nature of wireless networks and showed that a significant coding/diversity gain can be achieved. Hausl et. al. proposed a joint network-channel coding scheme based on turbo codes for the case of two sources and one relay [18]. Authors in [19] presented LDPC code design for decode-and-forward relaying in single-source single-destination scenario. Author in [16] investigated the tradeoff between reliability and rate as a function of node density and SNR, and showed how the energy and node density can be traded in achieving a given reliability-rate pair in single antenna case. [17] analyzed an network coded cooperation that adaptively matchs networks-on-graphs to the well-known class of codes-on-graphs such as LDPC codes, which enables real-time adaptation of network codes to variant link states and changing network topologies.

Network coding for multiple antennas have been studied for special network geometries in [18], [19]: [18] proposed a cross-layer design employing multiple antenna techniques and network coding called a MIMO two-way relay for one dimensional mesh network and [19] investigated the performance of MIMO network coding in the bi-directional relay network. An adaptive relay protocol has been proposed for a network with single antenna relays in [20] - [22] and for a network with multiple antennas using amplify and forward protocol in [23], [24]. Authors in [24] proposed an adaptive antenna selection scheme at both the relay and the source for half-duplex MIMO amplify and forward relay protocol. Rate optimization for relay network has been addressed in [25] and [26]: [25] proposed a throughput optimal control policy for the parallel relay network with decode and forward protocol. Authors in [26] analyzed the performance of variable-rate two phase collaborative diversity protocols and optimized the transmission rate based on the node location.

1.3 Outline of The Dissertation

This dissertation is organized as follows: Chapter 2 summarizes the basic relaying techniques of cooperative network and review space-time coding performance. Our main discussion and results are contained in Chapter 3-4 and we investigate the combined design of the MIMO transmission modes, coding rate, network coding strategy at the relay, node location, and transmit power. Chapter 3 treats deterministic network coding and adaptive network coding at the relay, and Chapter 4 treats the fundamental tradeoff between achievable rate and reliability using random network coding. In Chapter 5 and 6, we present practical MIMO receiver schemes. Chapter 5 treats LLR ordered SIC scheme for multi-user, multi-mode MIMO system, whereas Chapter 6 cover a new architecture for MIMO receivers that cancel the co-channel interference using a single RF/BB chain. Finally, Chapter 7 summarizes our conclusions and points to areas for future research.

CHAPTER 2. BACKGROUND AND RELATED LITERATURE

2.1 Cooperative Relay Protocols

In this chapter, we review cooperation strategies for relay network and compare space-time coding performance. For relay network, we consider a simplified three node model as shown in Fig. 2.1. and assume that source and relay transmit same energy $E = E_s = E_r$. The communication protocol consists of two orthogonal phases. In the first phase, a source sends information to its destination, and the information is also received by the relay at the same time. The received signals at the destination and the relay in the first phase are given by

$$\begin{aligned} \mathbf{y}_{ds} &= \sqrt{E}\, h_{ds} x + \mathbf{n}_{ds} \\ \mathbf{y}_{rs} &= \sqrt{E}\, h_{rs} x + \mathbf{n}_{rs} \end{aligned} \tag{2.1}$$

where h_{ij} indicate the channel gain between node i and j, n_{ij} is the additive noise, and x is the transmitted symbol. For Rayleigh fading, h_{ij} is modeled as a Gaussian random variance with mean zero and variance 0.5 per dimension. The additive complex Gaussian noise n_{ij} has mean zero and variance $N_0/2$ per dimension. In the second phase, the relay forwards a processed version of the source's signal to the destination which can be modeled as

$$\mathbf{y}_{dr} = \sqrt{E}\, h_{dr} q\left(y_{rs}\right) + \mathbf{n}_{dr} \tag{2.2}$$

and the function $q(\cdot)$ depends on the utilized relaying protocol.

2.1.1 Amplify and Forward relaying (AF)

In AF protocol, the relay transmits an amplified version of y_{rs} to the destination. The relay amplify the received signal by a factor β that is inversely proportional to the received power,

so that the signal from the relay $q(y_{rs})$ has transmit energy E.

$$q\left(y_{rs}\right)=\beta y_{rs},\quad \beta=\frac{\sqrt{E}}{\sqrt{E|h_{rs}|^2+N_0}} \tag{2.3}$$

The received signal at the destination in the second phase according to (2.2) is given by

$$\begin{aligned}\mathbf{y}_{dr}&=\frac{\sqrt{E}}{\sqrt{E|h_{rs}|^2+N_0}}h_{dr}y_{rs}+n_{dr}\\&=\frac{\sqrt{E}}{\sqrt{E|h_{rs}|^2+N_0}}\sqrt{E}h_{dr}h_{rs}x+n'_{dr}\end{aligned} \tag{2.4}$$

where n'_{dr} is a complex Gaussian random variable with mean zero and variance N'_0.

$$N'_0=N_0\left(1+\frac{E|h_{dr}|^2}{E|h_{rs}|^2+N_0}\right) \tag{2.5}$$

The destination receives two representation of the signal x through the source link and relay link and apply maximal ratio combining (MRC) as follows.

$$y=a_1y_{ds}+a_2y_{dr} \tag{2.6}$$

The combining factors a_1 and a_2 are choosen to to maximize the combined SNR.

$$a_1=\frac{\sqrt{E}h^*_{ds}}{N_0},\quad a_2=\frac{\sqrt{\frac{E}{E|h_{rs}|^2+N_0}}\sqrt{E}h^*_{dr}h^*_{rs}}{N'_0} \tag{2.7}$$

By assuming that the symbol x has unit energy, the received SNR of the MRC output is

$$\gamma=\gamma_1+\gamma_2 \tag{2.8}$$

where

$$\gamma_1=\frac{|a_1\sqrt{E}h_{ds}|^2}{|a_1|^2N_0}=\frac{E|h_{ds}|^2}{N_0}=\Gamma|h_{ds}|^2,\quad \Gamma=\frac{E}{N_0} \tag{2.9}$$

and

$$\begin{aligned}\gamma_2&=\frac{|a_2\sqrt{\frac{E}{E|h_{rs}|^2+N_0}}\sqrt{E}h_{dr}h_{rs}|^2}{|a_2|^2N'_0}=\frac{1}{N_0}\frac{E^2|h_{dr}|^2|h_{rs}|^2}{E\left(|h_{rs}|^2+|h_{dr}|^2\right)+N_0}\\&=\frac{\Gamma^2|h_{dr}|^2|h_{rs}|^2}{\Gamma\left(|h_{rs}|^2+|h_{dr}|^2\right)+1}\end{aligned} \tag{2.10}$$

Hence, the mutual information for amplify-and-forward relaying is given by

$$I_{AF}=\frac{1}{2}\log\left(1+\gamma_1+\gamma_2\right)=\frac{1}{2}\log\left(1+\Gamma|h_{ds}|^2+f(\Gamma|h_{rs}|^2,\Gamma|h_{dr}|^2)\right) \tag{2.11}$$

where

$$f(x,y) \triangleq \frac{xy}{x+y+1} \tag{2.12}$$

The outage probability can also be obtained by averaging over the Rayleigh fading which can be simplified at high SNR as follows

$$P\left[I_{AF} < R\right] \simeq \left(\frac{2^{2R}-1}{\Gamma}\right)^2 \tag{2.13}$$

We note that AF protocol achieves diversity order 2.

2.1.2 Decode and Forward relaying (DF)

In DF protocol, the relay decode the received signal, re-encode it, and then retransmit it to the receiver. We denote the decoded signal at the relay as $\hat{x}$ and the transmitted signal from the relay as $\sqrt{E}\hat{x}$. The end-to-end mutual information of DF protocol is limited by the mutual information of the weakest link between the sourcerelay and the combined channel from the sourcedestination and relaydestination as follows.

$$I_{DF} = \frac{1}{2}\min\left\{\log(1+\Gamma|h_{rs}|^2), \log(1+\Gamma|h_{ds}|^2+\Gamma|h_{dr}|^2)\right\} \tag{2.14}$$

The outage probability for DF protocol is given by $P[I_{DF} < R]$ and can be written as

$$P[I_{DF} < R] = P\left\{|h_{rs}|^2 < \frac{2^{2R}-1}{\Gamma}\right\} + P\left\{|h_{rs}|^2 > \frac{2^{2R}-1}{\Gamma}\right\} P\left\{|h_{ds}|^2 + |h_{dr}|^2 < \frac{2^{2R}-1}{\Gamma}\right\} \tag{2.15}$$

At high SNR, the outage probability can be simplified as follows

$$P[I_{DF} < R] \simeq \frac{2^{2R}-1}{\Gamma} \tag{2.16}$$

We note that DF protocol provides diversity order 1, because the performance of the system is limited by the worst link from the source to relay and the source to destination.

2.2 Space-time coding performance comparison

In this section, we consider a space-time (ST) coded MIMO system with M_t transmit and M_r receive antennas as shown in Fig. 2.2. The ST encoder divides input data stream into k

bit long blocks and, for each block, selects one ST codeword from the codeword set of size 2^k. The selected codeword is then transmitted through the channel over the M_t transmit antennas and T time slots. Each codeword can be represented as a $T \times M_t$ matrix

$$C = \begin{bmatrix} c_1^1 & c_1^2 & \cdots & c_1^{M_t} \\ c_2^1 & c_2^2 & \cdots & c_2^{M_t} \\ \vdots & \vdots & \ddots & \vdots \\ c_T^1 & c_T^2 & \cdots & c_T^{M_t} \end{bmatrix} \tag{2.17}$$

where c_t^i denotes the transmitted symbol from i th antenna at time t. We assume that the codewords satisfy energy constraint $E[||C||_F^2] = M_t T$, and the channel is frequency flat, quasi-static fading. The channel state information (CSI) is available at the receiver, but not at the sender. The received signal y_t^j at j th antenna at time t can be expressed as

$$y_t^j = \sqrt{\frac{E}{M_t}} \sum_{i=1}^{M_t} c_t^i h_{ij} + z_t^j \tag{2.18}$$

where z_t^j is the complex Gaussian noise at receive antenna j at time t and E is the average received SNR at each receive antenna. (2.18) can be rewritten as follows

$$Y = \sqrt{\frac{E}{M_t}} CH + Z \tag{2.19}$$

where $Y = y_t^j$ is the received signal matrix of size $T \times M_r$, $H = h_{ij}$ is the channel coefficient matrix of size $M_t \times M_r$, and $Z = z_t^j$ is the noise matrix of size $T \times M_r$. The receiver decode the transmitted matrix using ML decoding as follows.

$$\hat{C} = \arg\min_C ||Y - \sqrt{\frac{E}{M_t}} CH||_F^2 \tag{2.20}$$

The average pairwise error probability given that codeword C_a is transmitted and C_b is detected is determined as follows.

$$\begin{aligned} P(C_a \to C_b) &= \mathrm{E}_H \left[Q\left(\sqrt{\frac{E}{2M_t}} ||C_a - C_b||_F \right) \right] \\ &\leq \frac{1}{2} \prod_{i=1}^{r} \left(1 + \frac{E\lambda_i}{4M_t} \right)^{-M_t} \leq \frac{1}{2} \left(\frac{E}{4M_t} \right)^{-rM_t} \left(\prod_{i=1}^{r} \lambda_i \right)^{-M_t} \end{aligned} \tag{2.21}$$

where $r = \mathrm{rank}(C_a - C_b)$ and λ_i are the non-zero eigenvalues of $(C_a - C_b)(C_a - C_b)^H$. Two ST code design criteria can be developed based on the upper bound (2.21).

- Rank criterion: The minimum rank of the code difference matrix $C_a - C_b$ should be as large as possible. If the matrix $C_a - C_b$ has full rank, the corresponding ST code achieves full diversity.

- Product criterion: The minimum value of $\prod_{i=1}^{r} \lambda_i$ should be as large as possible. This quantity is referred to as the coding gain achieved by the ST code.

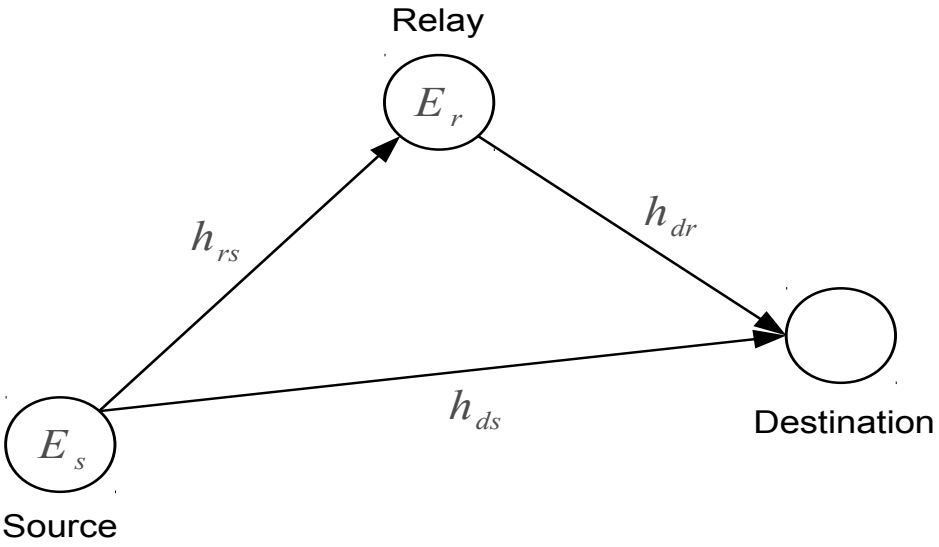

Figure 2.1 Three node relay network.

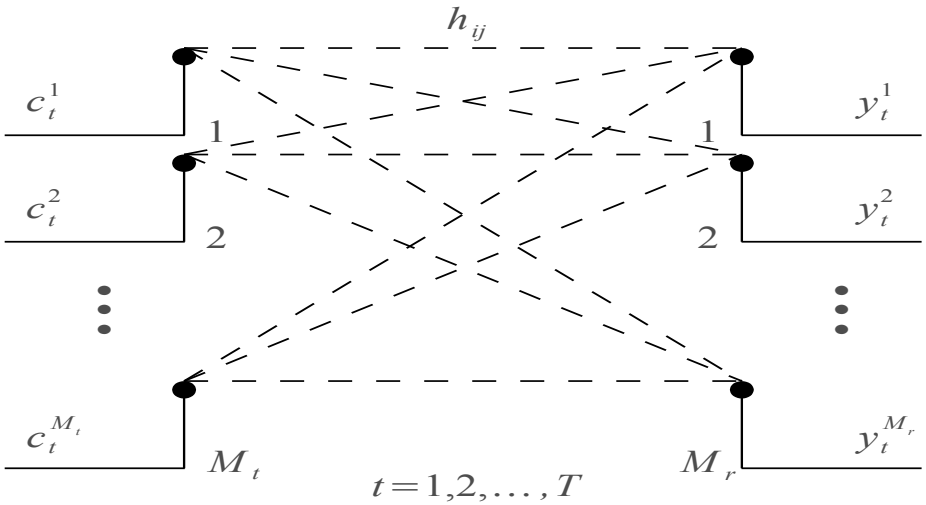

Figure 2.2 MIMO system with M_t transmit and M_r receive antennas

CHAPTER 3. MIMO NETWORK CODING

In this chapter, we consider a multiple access relay network where multiple source nodes send independent packets to a common destination with the assistance from a relay node. We assume that the relay node is equipped with multiple antennas and is allowed to choose either spatial multiplexing (SM) or beam forming mode as transmit diversity (TD). We develop a combined design methodology for MIMO transmission, network coding at the relay node, and channel coding rate at the source nodes that minimizes the end-to-end outage probability.

3.1 Introduction

We consider a multiple access relay network where multiple source nodes send independent packets to a common destination with the assistance from a relay node. We assume that the relay node is equipped with multiple antennas and is allowed to choose either spatial multiplexing (SM) or beam forming mode as transmit diversity (TD). The main objective of this chapter is to propose a transmission mode selection scheme at the relay which optimize these three linear combinations concurrently.

There are numerous works that optimize either the network coding, the MIMO transmission modes, or the data rates in multiple access relay channel. Network coding techniques for single antenna relay network have been studied in [84] - [30]. The cooperative diversity gain offered by the network coding has been investigated in [84]. [85] proposed a network coding scheme based on low-density parity-check (LDPC) codes that accounts for the lossy nature of wireless networks and showed that a significant coding/diversity gain can be achieved. Authors in [86] investigated the tradeoff between reliability and rate as a function of node density and SNR, and showed how the energy and node density can be traded in achieving a given

reliability-rate pair in single antenna case. [30] analyzed an network coded cooperation which adaptively match networks-on-graphs to the well-known class of codes-on-graphs such as LDPC codes. This approach enables real-time adaptation of network codes to variant link states and changing network topologies. Network coding for multiple antennas have been studied for special network geometries in [87], [88]. [87] proposed a cross-layer design employing multiple antenna techniques and network coding called a MIMO two-way relay for one dimensional mesh network and [88] investigated the performance of MIMO network coding in the bi-directional relay network. An adaptive relay protocol has been proposed for a network with single antenna relays in [89] - [91] and for a network with multiple antennas using amplify and forward protocol in [92], [93]. Authors in [93] proposed an adaptive antenna selection scheme at both the relay and the source for half-duplex MIMO amplify and forward relay protocol. Rate optimization for relay network has been addressed in [38], [39]. [38] proposed a throughput optimal control policy for the parallel relay network with decode and forward protocol. Authors in [39] analyzed the performance of variable-rate two phase collaborative diversity protocols and optimized the transmission rate based on the node location.

These previous works solve optimization problem for the specific linear combination. They either optimize the network coding and MIMO, adapt the relay protocol for different network model, or optimize network coding and channel coding. However, if multiple linear combinations coexist in the network, these approaches provide a suboptimal solution. With this motivation, we analyze a multiple access relay network where three types of linear combinations coexist and optimize these combinations concurrently. To that end, we derive the outage probability with the maximum likelihood decoding at the destination, and investigate the effect of the MIMO transmission modes at the relay, coding rates from each source, relay locations, and different network coding schemes on the outage probability. Throughout the outage probability analysis, we propose an optimal MIMO mode selection scheme which depends on channel codings from the source, the network coding at the relay, and the MIMO transmission modes. This mode selection scheme serves as a design guideline for an optimal relay network.

The remainder part of this chapter is organized as follows. A system model is described in Section II and the outage probability is derived in Section III, and Section IV presents the

optimum MIMO mode selection scheme. Section V provides numerical results and Section VI concludes the chapter.

3.2 System Model

Consider a multiple access relay network shown in Fig. 3.1, where K sources send distinct messages to a common destination with the assistance by a relay. The communication protocol consists of two phases. In the first phase, each source is assigned an orthogonal channel, and transmits its message to the destination after channel coding. Let $\mathbf{u}_i$ denote the message of the i-th source and $\mathbf{x}_i = (x_{i1}, x_{i2}, \cdots, x_{in})$ denote the transmitted channel codeword of $\mathbf{u}_i$. Due to the broadcast nature of the wireless medium, the relay may also overhear the codewords $\mathbf{x}_1, \mathbf{x}_2, \cdots, \mathbf{x}_K$ possibly with some errors. If the relay successfully decodes all K codeword [1], it makes a linear combination of decoded words, encodes the network coded data, and sends the result to the destination. If at least one codeword is received in error at the relay, it remains silent during the second phase.

We assume that the relay is equipped with two antennas and may choose one of two MIMO transmission modes: spatial multiplexing (SM) and transmit diversity (TD). In the SM mode, the decoded words $\mathbf{u}_1, \cdots, \mathbf{u}_K$ are divided into two groups and decoded words in each group are linearly combined to yield two network encoded vectors

$$\text{SM}: \ \mathbf{v}_1 = \sum_{i=1}^{K/2} a_i \mathbf{u}_i, \quad \mathbf{v}_2 = \sum_{i=K/2+1}^{K} b_i \mathbf{u}_i \tag{3.1}$$

where the coefficients a_i, b_i are elements in GF(M). Then, $\mathbf{v}_1$ and $\mathbf{v}_2$ are channel encoded and the resulting codewords $\mathbf{p}_1$ and $\mathbf{p}_2$ are sent to the destination. In the TD mode, the decoded words $\mathbf{u}_1, \cdots, \mathbf{u}_K$ are linearly combined to yield a network coded vector

$$\text{TD}: \ \mathbf{v}_0 = \sum_{i=1}^{K} c_i \mathbf{u}_i \tag{3.2}$$

Then, $\mathbf{v}_0$ is channel encoded and the resulting channel codeword $\mathbf{p}_0$ is sent to the destination after applying a proper weighting factors for beamforming.

[1] The relay uses cyclic redundancy check (CRC) code for error checking.

We assume that each source is located at unit distance from the destination ($d_{ds} = 1$) and the relay is located at distance $d_{dr} \in [0, 1]$ from the destination. The distance d_{ri} between i-th source and the relay is given by

$$d_{ri} = \sqrt{d_{dr}^2 + d_{ds}^2 - 2d_{dr}d_{ds}\cos\theta_i}\ , \quad i = 1, \cdots, K \tag{3.3}$$

where the angle θ_i is shown in Fig. 3.1. The channel gain between nodes i and j, h_{ij}, is given by

$$h_{ij} = \sqrt{d_{ij}^{-\alpha}} \cdot z_{ij} \tag{3.4}$$

where d_{ij} is the distance between nodes i and j, α is the path loss exponent and z_{ij} captures the channel fading characteristic. For Rayleigh fading, z_{ij} is modeled as a Gaussian random variable with mean zero and variance 0.5 per dimension.

The received signals at the destination and the relay in the first phase when $\mathbf{x}_i$ is sent by the i-th source are given by

$$\begin{aligned} \mathbf{y}_{di} &= h_{di}\mathbf{x}_i + \mathbf{n}_{di} \\ \mathbf{y}_{ri} &= h_{ri}\mathbf{x}_i + \mathbf{n}_{ri} \end{aligned} \tag{3.5}$$

where $\mathbf{n}_{ij}$ is the complex Gaussian vector with mean zero and variance $N_0/2$ per dimension. The received signals at the destination in the second phase are given by

$$\begin{aligned} \mathbf{y}_{dr}\big|_{\mathrm{SM}} &= g_1\mathbf{p}_1 + g_2\mathbf{p}_2 + \mathbf{n}_{dr} \\ \mathbf{y}_{dr}\big|_{\mathrm{TD}} &= (|g_1|^2 + |g_2|^2)\mathbf{p}_0 + \mathbf{n}_{dr} \end{aligned} \tag{3.6}$$

where g_r, $r = 1, 2$ is the channel gain between the r-th antenna of the relay and the destination.

The frame structures are compared in Fig. 3.2. Without relay, each source transmits its packet during T seconds. With relay, each source and relay transmits its packet during T_c seconds, where $T_c = TK/(K+1)$. To achieve the effective rate of R bps/Hz, R has to be changed to $R_c = R(K+1)/K$ for the network with relay.

In this section, we derive the outage probability with the maximum likelihood (ML) decoding at the destination. We derive four users case ($K = 4$) first and extend the result to K users in general.

3.2.1 Link Outage Probability

For notational simplicity, we denote the link outage of $\mathbf{x}_i$ as $\overline{\mathbf{x}}_i$. Similarly, the link outage of $\mathbf{p}_l$, $l = 0, 1, 2$ is denoted by $\overline{\mathbf{p}}_l$. The link outage probability for $\mathbf{x}_i$ is given by

$$\begin{aligned} p_{ds} \triangleq P(\overline{\mathbf{x}}_i) &= P(\mathrm{I}(\mathbf{x}_i : \mathbf{y}_{di}) < R_c) \\ &= 1 - \exp\left(-\frac{2^{R_c} - 1}{\gamma_s}\right) \end{aligned} \tag{3.7}$$

where $\gamma_s = d_{ds}^{-\alpha} E_s / N_0$ is the received SNR of the source symbol at the destination [2]. For $S_i \to R$ channel with MRC at the relay, the link outage probability at the relay is given by

$$\begin{aligned} p_{ri} \triangleq P(\mathrm{I}(\mathbf{x}_i : \mathbf{y}_{ri}) < R_c) \\ = 1 - \left(1 + \frac{2^{R_c} - 1}{\gamma_{ri}}\right) \exp\left(-\frac{2^{R_c} - 1}{\gamma_{ri}}\right) \end{aligned} \tag{3.8}$$

where $\gamma_{ri} = d_{ri}^{-\alpha} E_s / N_0$ is the received SNR of the i-th source symbol at the relay. The link outage probability of $R \to D$ channel in TD (beamforming) mode is given by

$$\begin{aligned} p_{\mathrm{TD}} \triangleq P(\overline{\mathbf{p}}_0) &= P(\mathrm{I}(\mathbf{p}_0 : \mathbf{y}_{dr}) < R_c) \\ &= 1 - \left(1 + \frac{2^{R_c} - 1}{\gamma_r}\right) \exp\left(-\frac{2^{R_c} - 1}{\gamma_r}\right) \end{aligned} \tag{3.9}$$

where $\gamma_r = d_{dr}^{-\alpha} E_r / N_0$ is the received SNR of the relay provided symbol at the destination. The proof of (3.7), (3.8), (3.9) are in [94]. The link outage probability for $R \to D$ channel in SM mode is given by

$$\begin{aligned} p_{\mathrm{SM}} \triangleq P(\overline{\mathbf{p}}_1) &= P\left(\mathrm{I}(\mathbf{p}_1 : \mathbf{y}_{dr}) < R_c\right) \\ &= 1 - \left(1 + \frac{2^{2R_c} - 2^{R_c}}{\gamma_r}\right) \exp\left(-\frac{2^{2R_c} - 1}{\gamma_r}\right) \end{aligned} \tag{3.10}$$

which is the outage probability for $\mathbf{p}_1$. Proof of (3.10) is provided by the Appendix A. At high SNR, it follows from the approximation $\exp(x) \backsimeq 1 - x$ for $x \ll 1$ that (3.7)-(3.10) can be approximated as

$$\begin{aligned} p_{ds} \doteq \left(\frac{2^{R_c} - 1}{\gamma_s}\right), \quad p_{ri} \doteq \left(\frac{2^{R_c} - 1}{\gamma_{ri}}\right)^2 \\ p_{\mathrm{TD}} \doteq \left(\frac{2^{R_c} - 1}{\gamma_r}\right)^2, \quad p_{\mathrm{SM}} \doteq \left(\frac{2^{R_c} - 1}{\gamma_r}\right) \end{aligned} \tag{3.11}$$

[2] (3.7) is same for all sources, since all source are located at unit distance from the destination.

3.2.2 End-to-End Outage Probability

We derive the end-to-end outage probability for $\mathbf{x}_1$. The end-to-end outage probability for other sources can similarly be derived. The outage event for $\mathbf{x}_1$ depends on whether the relay decodes $\mathbf{x}_1, \cdots, \mathbf{x}_4$ (denoted as r) or not (denoted as nr). Given the event r occurs, the end-to-end outage in SM mode occurs if and only if $\overline{\mathbf{x}}_1$ occurs and $\overline{\mathbf{x}}_2$ or $\overline{\mathbf{p}}_1$ occurs. Therefore, the end-to-end outage probability for $\overline{\mathbf{x}}_1$ given r is

$$P(\text{out}|r) = P(\overline{\mathbf{x}}_1) \times P(\overline{\mathbf{x}}_2 \cup \overline{\mathbf{p}}_1) \tag{3.12}$$

In TD mode, the end-to-end outage for $\overline{\mathbf{x}}_1$ occurs if and only if $\overline{\mathbf{x}}_1$ occurs and $\overline{\mathbf{x}}_2$ or $\overline{\mathbf{x}}_3$ or $\overline{\mathbf{x}}_4$ or $\overline{\mathbf{p}}_0$ occurs. Therefore,

$$P(\text{out}|r) = P(\overline{\mathbf{x}}_1) \times P(\overline{\mathbf{x}}_2 \cup \overline{\mathbf{x}}_3 \cup \overline{\mathbf{x}}_4 \cup \overline{\mathbf{p}}_0) \tag{3.13}$$

in TD mode.

$P(\text{out}|r)$ indicates that even if $\mathbf{x}_1$ fails from the direct transmission, the destination may still recover $\mathbf{x}_1$ by combining $\mathbf{x}_2$ and $\mathbf{p}_1$ in SM mode or by combining $\mathbf{x}_2$, $\mathbf{x}_3$, $\mathbf{x}_4$ and $\mathbf{p}_0$ in TD mode. The last term in (3.12)-(3.13) can be further simplified by using an addition rule of probability $P(A_1 \cup A_2) = P(A_1) + P(A_2) - P(A_1 \cap A_2)$ and the independence of events (i.e., independence of the channel) as follows.

$$\begin{aligned} P(\text{out}|r)_{\text{SM}} &= p_{ds}\ p_{\text{SM}} + (1 - p_{\text{SM}})p_{ds}^2 \\ P(\text{out}|r)_{\text{TD}} &= p_{ds}\ p_{\text{TD}} + (1 - p_{\text{TD}})p_{ds}^2\left[p_{ds}^2 - 3p_{ds} + 3\right] \end{aligned} \tag{3.14}$$

Given the event nr occurs, the end-to-end outage occurs if the direct link is in outage. Hence, we obtain

$$P(\text{out}|nr) = P(\overline{\mathbf{x}}_1) = p_{ds} \tag{3.15}$$

Therefore, the end-to-end outage probability for $\mathbf{x}_1$ is given by

$$P(\text{out}) = P(\text{out}|nr)P(nr) + P(\text{out}|r)P(r) \tag{3.16}$$

where $P(r) = \prod_{i=1}^{4}(1 - p_{ri})$ is the probability that $\mathbf{x}_1, \cdots, \mathbf{x}_4$ are correctly decoded at the relay and $P(nr) = 1 - P(r)$.

Although TD mode provides a diversity order of 2 for the relay-to-destination channel, four codewords ($\mathbf{x}_2$, $\mathbf{x}_3$, $\mathbf{x}_4$, and $\mathbf{p}_0$) have to be correctly received at the destination in order to recover $\mathbf{x}_1$ from $\mathbf{p}_0$, whereas in SM mode two codewords ($\mathbf{x}_2$ and $\mathbf{p}_1$) have to be correctly received at the destination. For this reason, if the source-to-destination channel is noisy, then SM mode provides a lower outage probability than TD mode. However, if the source-to-destination channel is reliable, the probability of $\overline{\mathbf{x}}_i$ is small and the diversity order of $\overline{\mathbf{p}}_l$ plays an important role. Thus, TD mode provides a lower outage probability than SM mode.

3.2.3 Generalization to Multiple Sources and Relays

First, if there are K sources and a single relay,

$$P(r) = \prod_{i=1}^{K}(1 - p_{ri}), \quad P(nr) = 1 - P(r) \tag{3.17}$$

and the second term in (3.12)-(3.13) becomes

$$P\left(\overline{\mathbf{x}}_2^{K/2} \cup \overline{\mathbf{p}}_1\right) = 1 - (1 - p_{\mathrm{SM}})(1 - p_{ds})^{K/2-1} \tag{3.18}$$

in SM mode and

$$P\left(\overline{\mathbf{x}}_2^{K} \cup \overline{\mathbf{p}}_0\right) = 1 - (1 - p_{\mathrm{TD}})(1 - p_{ds})^{K-1} \tag{3.19}$$

in TD mode where

$$\overline{\mathbf{x}}_2^{K} \triangleq \overline{\mathbf{x}}_2 \cup \overline{\mathbf{x}}_3 \cup \cdots \cup \overline{\mathbf{x}}_K \tag{3.20}$$

Proof of (3.18), (3.19) is provided in Appendix B. Then, the outage probability $P(\mathrm{out})$ for multi sources, single relay case can be calculated by substituting (3.17)-(3.19) into (3.16).

Second, if there are K sources and R relays,

$$P(r) = \prod_{r=1}^{R}\prod_{i=1}^{K}(1 - p_{ri}), \quad P(nr) = 1 - P(r). \tag{3.21}$$

For simplicity, we ssume that power control is applied to each relay, so that the received SNR γ_r of the relay provided codeword at the destination is identical. We denote the r-th relay's

network coded codeword as $\mathbf{p}_{1r}$, $\mathbf{p}_{2r}$ for SM mode where r indicate the r-th relay and the network encoding rules are given as follows.

$$\text{SM}: \ \mathbf{v}_{1r} = \sum_{i=1}^{n} a_i \mathbf{u}_i, \quad \mathbf{v}_{2r} = \sum_{i=n+1}^{K} b_i \mathbf{u}_i \tag{3.22}$$

If $\mathbf{x}_1$ fails from the direct transmission, the destination may still recover $\mathbf{x}_1$ by combining $(\mathbf{x}_2, \mathbf{x}_3, \cdots, \mathbf{x}_n, \mathbf{p}_{11}, \cdots, \mathbf{p}_{1R})$ where each $\mathbf{p}_{1r}$ is linearly independent. Hence, the end-to-end outage in SM mode occurs if and only if $\overline{\mathbf{x}}_1$ occurs and any l $(l \geq R)$ out of $R + (n-1)$ codewords $(\mathbf{x}_2, \mathbf{x}_3, \cdots, \mathbf{x}_n, \mathbf{p}_{11}, \cdots, \mathbf{p}_{1R})$ are in outage.

$$\begin{aligned} P(\text{out}|r)_{\text{SM}} &= P(\overline{\mathbf{x}}_1) \times P\left(\ \forall\ l \text{ out of } R+(n-1) \text{ codewords are in outage, } l \geq R\ \right) \\ &= p_{ds}\left[\sum_{i_1=0}^{n-1}\sum_{i_2=R-i_1}^{R}\binom{n-1}{i_1}\binom{R}{i_2} p_{ds}^{i_1}\left(1-p_{ds}\right)^{(n-1)-i_1} p_{\text{SM}}^{i_2}\left(1-p_{\text{SM}}\right)^{R-i_2}\right], \text{ if } R \geq n-1 \\ &= p_{ds}\Bigg[\sum_{i_1=0}^{R-1}\sum_{i_2=R-i_1}^{R}\binom{n-1}{i_1}\binom{R}{i_2} p_{ds}^{i_1}\left(1-p_{ds}\right)^{(n-1)-i_1} p_{\text{SM}}^{i_2}\left(1-p_{\text{SM}}\right)^{R-i_2} \\ &\quad + \sum_{l=R}^{n-1}\binom{n-1}{l} p_{ds}^{l}\left(1-p_{ds}\right)^{(n-1)-l}\Bigg], \text{ if } R < n-1 \end{aligned} \tag{3.23}$$

where $p_{ds} = P(\overline{\mathbf{x}}_i)$, $p_{\text{SM}} = P\left(\overline{\mathbf{p}}_{1r}\right)$ are given in (3.7) and (3.10), respectively.

For TD mode, the r-th relay's network coded codeword $\mathbf{p}_{0r}$ is generated as follows.

$$\text{TD}: \ \mathbf{v}_{0r} = \sum_{i=1}^{K} c_i \mathbf{u}_i \tag{3.24}$$

The end-to-end outage occurs if and only if $\overline{\mathbf{x}}_1$ occurs and any l $(l \geq R)$ out of $R + (K-1)$ codewords $(\mathbf{x}_2, \mathbf{x}_3, \cdots, \mathbf{x}_K, \mathbf{p}_{01}, \cdots, \mathbf{p}_{0R})$ are in outage. Hence, $P(\text{out}|r)_{\text{TD}}$ can be similarly derived by replacing n to K in (3.23) and p_{SM} to p_{TD}. We note that the diversity order of $P(\text{out}|r)$ in (3.23) is $R+1$ for a fixed received SNR per information bit $\gamma_b = (K\gamma_s + 2R\gamma_r)/K$.

$$\begin{aligned} P(\text{out}|r)_{\text{SM}} &\doteq p_{ds}\left[\ p_{ds}^{i_1} p_{\text{SM}}^{i_2}\ \right] \\ &\doteq \frac{1}{\gamma_s}\left[\ \frac{1}{\gamma_s^{i_1}}\frac{1}{\gamma_r^{i_2}}\ \right] \\ &\doteq \frac{1}{\gamma_b^{\min(i_1+i_2)+1}} = \frac{1}{\gamma_b^{R+1}} \end{aligned} \tag{3.25}$$

3.3 Combined Design Rule

In this section, we develop a combined design rule that determines the MIMO transmission mode, network coding at the relay, and code rate R at the source that minimizes the end-to-end outage probability.

$$P(\text{out})_{\text{SM}} \underset{SM}{\overset{TD}{\gtrless}} P(\text{out})_{\text{TD}} \tag{3.26}$$

If the terms with diversity order greater than 1 are ignored, (3.26) can be simplified to

$$\left(\frac{K}{2}-1\right) p_{ds} + p_{\text{SM}} \underset{SM}{\overset{TD}{\gtrless}} (K-1)\, p_{ds} \tag{3.27}$$

which is equivalent to

$$f(K, R_c, \gamma_s, \gamma_r) \underset{SM}{\overset{TD}{\gtrless}} \frac{K}{2} - 1 \tag{3.28}$$

and

$$\begin{aligned} f(K, R_c, \gamma_s, \gamma_r) \triangleq \frac{K}{2} \exp\left(-\frac{2^{R_c}-1}{\gamma_s}\right) \\ - \left(1 + \frac{2^{2R_c} - 2^{R_c}}{\gamma_r}\right) \exp\left(-\frac{2^{2R_c}-1}{\gamma_r}\right) \end{aligned} \tag{3.29}$$

At high SNR, it can be shown from (3.11) that the MIMO mode selection rule in (3.28) is equivalent to

$$\frac{\gamma_r}{\gamma_s} \underset{SM}{\overset{TD}{\lessgtr}} \frac{2}{K} \tag{3.30}$$

We note that as the number of users K increase, SM mode provides better performance than TD. This is because for large K, the right-hand side of (3.27) is much bigger than the left-hand side p_{SM}, so the end-to-end outage probability of SM provides lower value than that of TD.

3.4 Adaptive Network Coding

In this section, we relax the relaying condition in Section III (i.e., the relay combine correctly received codewords, and cooperate even in the case with detection error.), and derive the end-to-end outage probability as well as the decoding error probability for $K = 4$ case.

3.4.1 End-to-End Outage Probability

We apply the network coding rule presented in Table 3.1. The error event $e_i = 0$ indicates that the corresponding codeword is correctly decoded at the relay, whereas $e_i = 1$ indicates decoding error. The outage probability $P(\text{out}|\mathbf{e}_1)$ for error pattern $\mathbf{e}_1$ is given by (3.14)

$$\begin{aligned} P(\text{out}|\mathbf{e}_1)_{\text{SM}} &= p_{ds}\Big[1-(1-p_{\text{SM}})\cdot(1-p_{ds})\Big] \\ P(\text{out}|\mathbf{e}_1)_{\text{TD}} &= p_{ds}\Big[1-(1-p_{\text{TD}})\cdot(1-p_{ds})^3\Big] \end{aligned} \tag{3.31}$$

and the outage probability for other error patterns are presented in Table C.17. Hence, the end-to-end outage probability of adaptive network coding is given by

$$P(\text{out})_{\text{SM } or \text{ TD}} = \sum_{\mathbf{e}_i, i=1}^{16} P(\mathbf{e}_i)\cdot P(\text{out}|\mathbf{e}_i)_{\text{SM } or \text{ TD}}. \tag{3.32}$$

3.4.2 Decoding Error Probability

For this section only, we assume that each source node transmit a binary bit $x_i \in \{0,1\}$, $i = 1, \cdots, 4$ to the destination over orthogonal channels. The received signal at the destination and the relay in the first phase when x_i is sent by the i th source are given by

$$\begin{aligned} y_{di} &= h_{di}(-1)^{x_i}\sqrt{d_{ds}^{-\alpha}E_s} + n_{di} \\ y_{ri} &= h_{ri}(-1)^{x_i}\sqrt{d_{ri}^{-\alpha}E_r} + n_{ri} \end{aligned} \tag{3.33}$$

where y_{di} and y_{ri} are complex scalars. Based on y_{ri}, the relay decode x_i as $\hat{x}_i = x_i \oplus e_i$ with decoding error e_i where the decoding error probability $p(e_i = 1)$ depends on the receiver scheme at the relay such as maximal-ratio combining (MRC) or equal-gain combining (EGC).

After decoding, the relay check for errors using CRC code and exclude the symbols with error from parity generation. The relay partition the source nodes into subgroup and generate the parity bit using only the symbols from the corresponding subgroup as shown in Table 3.1. For example, if the relay use SM mode, there are two subgroups; $\{x_1, x_2\}$, $\{x_3, x_4\}$. The relay generate two parity bits p_1, p_2 using the symbols out of each subgroup as follows.

$$p_1 = x_1 \oplus x_2, \quad p_2 = x_3 \oplus x_4 \tag{3.34}$$

when all symbol are correctly decoded at the relay. If x_2 has a detection error (i.e., $e_2 = 1$), the generated parity bits are given by

$$p_1 = x_1, \quad p_2 = x_3 \oplus x_4. \tag{3.35}$$

If both symbol in a subgroup has detection error (e.g., x_1, x_2 are both in error), the corresponding parity bit forwards same parity bit from the other subgroup as follows

$$p_1 = p_2 = x_3 \oplus x_4. \tag{3.36}$$

For TD mode, the relay use all 4 symbols $\{x_1, x_2, x_3, x_4\}$ to generate a parity bit $p_0 = x_1 \oplus x_2 \oplus x_3 \oplus x_4$ and transmit it using beamforming. The received signals at the destination in the second phase are given by

$$\begin{aligned} y_{dr}|_{\text{SM}} &= (g_1(-1)^{p_1} + g_2(-1)^{p_2}) \sqrt{d_{dr}^{-\alpha} E_r} + n_{dr} \\ y_{dr}|_{\text{TD}} &= (|g_1|^2 + |g_2|^2) p_0 \sqrt{d_{dr}^{-\alpha} E_r} + n_{dr} \end{aligned} \tag{3.37}$$

The destination decode the transmitted codeword using ML decoding based on the received signals $(y_{d1}, y_{d2}, y_{d3}, y_{d4}, y_{dr})$ during two consecutive phase.

The adaptive network coding rule for multiple access relay network is presented in Table 3.1 and the codebook for each error pattern $\mathbf{e}_i = (e_1, e_2, e_3, e_4)$ is given in Appendix C. First, we derive the union bound of decoding error probability for a particular error pattern $\underline{e}_1$. Let $\mathbf{c}_a = (x_{a,1}, \cdots, x_{a,4}, p_{a,1}, p_{a,2})$ and $\mathbf{c}_b = (x_{b,1}, \cdots, x_{b,4}, p_{b,1}, p_{b,2})$ be two distinct codewords. The conditional pairwise error probability with ML decoding is given by

$$\begin{aligned} Pr\left(\mathbf{c}_a \to \mathbf{c}_b\right) &= \mathrm{E}\left[Q\left(\sqrt{ (\sum_{i=1}^{4} ||y_{a,di} - y_{b,di}||^2 + ||y_{a,dr} - y_{b,dr}||^2)/2N_0 } \right) \right] \\ &\leq \frac{1}{2} \prod_{i=1}^{4} \mathrm{E}_{h_{di}} \left[\exp\left(-\frac{||y_{a,di} - y_{b,di}||^2}{4N_0} \right) \right] \quad \mathrm{E}_{g_r} \left[\exp\left(-\frac{||y_{a,dr} - y_{b,dr}||^2}{4N_0} \right) \right] \end{aligned} \tag{3.38}$$

For Rayleigh fading channel h_{di} and g_r, we have

$$\mathrm{E}_{h_{di}} \left[\exp\left(-||y_{a,di} - y_{b,di}||^2 / 4N_0 \right) \right] = \left[\frac{1}{1 + d_{ds}^{-\alpha} (x_{a,i} \oplus x_{b,i}) E_s / N_0} \right] \tag{3.39}$$

which is proved in [56] for point-to-point channel and

$$\mathrm{E}_{g_r} \left[\exp\left(-||y_{a,dr} - y_{b,dr}||^2 / 4N_0 \right) \right] = \prod_{n=1}^{n_r} \left[\frac{1}{1 + d_{dr}^{-\alpha} \lambda_n E_r / N_0} \right] \tag{3.40}$$

which is derived in [57] for $n_r \times 1$ MISO channel and λ_n are the eigenvalues of code-difference matrix. The eigenvalues for TD mode are given by $\lambda_1 = \lambda_2 = (p_{a,0} \oplus p_{b,0})$ where $p_{a,0} = x_1 \oplus x_2 \oplus x_3 \oplus x_4$ and that for SM mode are given by $\lambda_1 = \sum_{i=1}^{2}(p_{a,i} \oplus p_{b,i})$ and $\lambda_2 = 0$ where $p_{a,i}$ are defined in (4.5). Then, (4.10) can be expressed as

$$\begin{aligned} Pr\left(\mathbf{c}_a \to \mathbf{c}_b\right)^{\text{SM}} &\leq \frac{1}{2}\prod_{i=1}^{4}\frac{1}{1+(x_{a,i}\oplus x_{b,i})\gamma_s}\cdot\left[\frac{1}{1+\sum_{i=1}^{2}(p_{a,i}\oplus p_{b,i})\gamma_r}\right] \\ Pr\left(\mathbf{c}_a \to \mathbf{c}_b\right)^{\text{TD}} &\leq \frac{1}{2}\prod_{i=1}^{4}\frac{1}{1+(x_{a,i}\oplus x_{b,i})\gamma_s}\cdot\left[\frac{1}{1+(p_{a,0}\oplus p_{b,0})\gamma_r}\right]^2 \end{aligned} \tag{3.41}$$

where $\oplus$ denotes mod-2 addition (XOR) and $\gamma_s = d_{ds}^{-\alpha}E_s/N_0$, $\gamma_r = d_{dr}^{-\alpha}E_r/N_0$ are the receive signal-to-noise ratio at the destination from the source node and relay node, respectively. The union bound on the probability of decoding error, for a given error pattern $\underline{e}_1$, is given by

$$P_E\left(\mathbf{e}_1\right)^{\text{SM } or \text{ TD}} \leq \sum_{\mathbf{c}_b \neq \mathbf{c}_a} Pr\left(\mathbf{c}_a \to \mathbf{c}_b\right)^{\text{SM } or \text{ TD}} \tag{3.42}$$

Averaging (4.16) over all possible codeword in Table C.1 yields

$$\begin{aligned} P_E\left(\mathbf{e}_1\right)^{\text{SM}} \leq\ & 4\left(\frac{1}{1+\bar{\gamma}_s}\right)\left(\frac{1}{1+\bar{\gamma}_r}\right) + 2\left(\frac{1}{1+\bar{\gamma}_s}\right)^2 \\ & + 4\left(\frac{1}{1+\bar{\gamma}_s}\right)^2\left(\frac{1}{1+2\bar{\gamma}_r}\right) + 4\left(\frac{1}{1+\bar{\gamma}_s}\right)^3\left(\frac{1}{1+\bar{\gamma}_r}\right) + \left(\frac{1}{1+\bar{\gamma}_s}\right)^4 \\ P_E\left(\mathbf{e}_1\right)^{\text{TD}} \leq\ & 4\left(\frac{1}{1+\bar{\gamma}_s}\right)\left(\frac{1}{1+\bar{\gamma}_r}\right)^2 + 6\left(\frac{1}{1+\bar{\gamma}_s}\right)^2 \\ & + 4\left(\frac{1}{1+\bar{\gamma}_s}\right)^3\left(\frac{1}{1+\bar{\gamma}_r}\right)^2 + \left(\frac{1}{1+\bar{\gamma}_s}\right)^4 \end{aligned} \tag{3.43}$$

where the error event $\mathbf{e}_1$ occurs with probability $P(\mathbf{e}_1) = \prod_{i=1}^{4}(1-p_{e,ri})$ and $p_{e,ri} = P(e_i = 1)$ indicate the link error probability between i th source and the relay.

The union bound for other error patterns are presented in Appendix C. Hence, the average decoding error probability for adaptive network coding is given by

$$P(E)_{\text{SM } or \text{ TD}} = \sum_{\mathbf{e}_i, i=1}^{16} P(\mathbf{e}_i)\cdot P_E(\mathbf{e}_i)^{\text{SM } or \text{ TD}}. \tag{3.44}$$

where $P_E(\mathbf{e}_i)^{\text{SM } or \text{ TD}}$ and $P(\mathbf{e}_i)$ are derived in (C.1)-(C.31). Based on the decoding error probability analysis, we observe that for TD mode, we can control the dominant term in the error probability and eventually determine the diversity order of the system by changing the

SNR ratio between relay and source $G_D = \gamma_r/\gamma_s$. For example, consider the union bound for error pattern $\mathbf{e}_1$ in (3.38). At high SNR, the two dominant terms in $P_E(\mathbf{e}_1)^{\mathrm{TD}}$ are given as follows

$$\begin{aligned} P_E(\mathbf{e}_1)^{\mathrm{TD}} &\leq 4\left(\frac{1}{1+\gamma_s}\right)\left(\frac{1}{1+\gamma_r}\right)^2 + 6\left(\frac{1}{1+\gamma_s}\right)^2 \\ &\leq \left(\frac{1}{1+\gamma_s}\right)\left[4\left(\frac{1}{1+\gamma_r}\right)^2 + 6\left(\frac{1}{1+\gamma_s}\right)\right]. \end{aligned} \tag{3.45}$$

If $\frac{4}{(1+\gamma_r)^2} < \frac{6}{(1+\gamma_s)}$ (i.e, $(1+\gamma_r)^2/(1+\gamma_s) \geq 2/3 \rightarrow \gamma_r^2/\gamma_s \geq 2/3$ at high SNR), then the second term is dominant and the diversity order $P_E(\mathbf{e}_1)^{\mathrm{TD}}$ is 2. However, if $4/(1+\gamma_r)^2 > 6/(1+\gamma_s)$ (i.e, $(1+\gamma_r)^2/(1+\gamma_s) < 2/3 \rightarrow \gamma_r^2/\gamma_s < 2/3$ at high SNR), then the first term is dominant and the diversity order $P_E(\mathbf{e}_1)^{\mathrm{TD}}$ become 3. This characteristic of TD mode is well captured in Fig. 3.4. We note that $\gamma_r^2/\gamma_s = G_D^2 \times \gamma_b/(1+0.5G_D)$ is a strictly increasing function of the SNR ratio $G_D = \gamma_r/\gamma_s$ for a fixed γ_b. For SNR ratio G_D above a threshold, the decoding error probability curve decrease with diversity order 2, whereas for G_D below the threshold, the decoding error probability decrease with diversity order higher than 2. The reason why we have this type of characteristic can be explained as follows. For coding perspective, the codebook Table C.1 has minimum distance $d_{\min} = 2$, so we have coding diversity 2. For path diversity perspective, however, each information bit x_i has overall path diversity 3, because the source to destination link provide diversity 1 and relay to destination link provide additional diversity 2 by using beamforming. Since coding diversity 2 term and path diversity 3 term co-exist in the decoding error probability of TD mode, we can control the dominant term in the error probability and determine the diversity order of the system by changing the SNR ratio $G_D = \gamma_r/\gamma_s$. However, for SM mode, each information bit x_i has path diversity 2 since the relay to destination link provides diversity 1, and the coding diversity is still 2 (i.e., $d_{\min} = 2$). Hence, the decoding error probability curve for SM mode decrease with diversity order 2 regardless to the SNR ratio G_D as illustrated in Fig. 3.5.

3.5 Numerical Results

In this section, we present numerical results, assuming that each source is located at unit distance from the destination, and at angle $\underline{\theta} = (\theta_1, \theta_2, \theta_3, \theta_4) = (\frac{-\pi}{6}, \frac{-\pi}{3}, \frac{\pi}{3}, \frac{\pi}{6})$. We assume

that the transmit energy per information bit $E_b = (4E_s + 2E_r)/4$ is fixed and the path loss exponent is $\alpha = 4$.

Fig. 3.6. shows the end-to-end outage probability versus $\gamma_r/(\gamma_r + \gamma_s)$ for two values of received SNR per information bit γ_b (dB). We can see that for $\gamma_r/(\gamma_r + \gamma_s)$ above a threshold $(0.3 \sim 0.4)$, SM is better than TD. This is because the additional improvement of reliability on the relay-to-destination link offered by TD mode does not help much in reducing the end-to-end outage probability when the relay-to-destination link SNR γ_r is high enough. For a given γ_b, an increase of γ_r requires a decrease of γ_s which makes p_{SM} negligible than p_{ds} in (3.27). Hence, it is better to combine two source nodes at a time and send the encoded data in SM mode to have a smaller end-to-end outage probability.

Fig. 3.7. shows the end-to-end outage probability versus received SNR per information bit $\gamma_b = (4\gamma_s + 2\gamma_r)/4$ with γ_r/γ_s optimized for each γ_b. We can see that if γ_b is above a threshold SM provides a lower end-to-end outage probability while for γ_b below the threshold, the outage probability can be lowered by not using the relay. Fig. 3.8. compares adaptive network coding in (3.32) to convectional network coding in (3.1), (3.2) for the same network in Fig. 3.7. The end-to-end outage probability of adaptive network coding is lower than conventional case, but the SNR advantage is not significant (i.e., less than 0.2 dB).

Fig. 3.9. shows that the end-to-end outage probability versus the rate R. We can see that for R below a threshold SM provides a lower outage probability than TD while for R above the threshold TD provides a lower outage probability than SM.

Fig. 3.10. shows the decoding error probability versus source transmit energy E_s/N_0 at several relay location. We see that once the relay is located near the destination node, SM mode provides more reliability than TD mode. As the relay move closer to the source node, the error probability of TD mode becomes smaller than that of SM mode. For target error $P_E = 10^{-4}$, TD mode obtain 3 dB SNR gain per each source node comparing to SM mode at $d_{dr} = 0.5$ and 5 dB SNR gain at $d_{dr} = 0.9$. The x-axis in Fig. 3.10. represent the source to relay channel quality. As E_s/N_0 decrease, the source to relay channel becomes more noisy, and vice versa. We note that for noisy $S \to R$ channel (i.e., $E_s/N_0 \downarrow$), the optimal transmission mode is SM mode, whereas for reliable $S \to R$ channel (i.e., $E_s/N_0 \uparrow$), the optimal transmission mode

is TD mode.

Fig. 3.11, shows the decoding error probability versus relay location d_{dr} for several source transmit energy E_s/N_0. We observe the same trend as the previous figure that SM mode is optimal for small d_{dr} and TD mode becomes optimal for large d_{dr}. The x-axis in Fig. 3.11. represent the relay to destination channel quality. As d_{dr} increase, the path lose between relay and destination increases and the channel becomes noisy. We note that for noisy $R \rightarrow D$ channel (i.e., $d_{dr} \uparrow$), the optimal transmission mode is TD mode, whereas for reliable $R \rightarrow D$ channel (i.e., $d_{dr} \downarrow$), the optimal transmission mode is SM mode.

3.6 Conclusion

We considered a multiple access relay network where once each source transmits a channel coded packet, the relay decodes the transmitted packet, generates network coded packet, and re-transmits it. We assumed multiple antennas at the relay and considered two MIMO transmission modes at the relay; spatial multiplexing (SM) and beamforming as transmit diversity (TD). We applied different network coding schemes depending on the MIMO transmission modes. We derived the outage probability with the maximum likelihood decoding at the destination, and investigated the effect of MIMO transmission modes at the relay, coding rate from each source, relay locations, and different network coding schemes on the outage probability. We proposed an optimal MIMO mode selection sheme which depends on channel coding from the source, network coding at the relay, and MIMO transmission modes.

Table 3.1 Adaptive parity generation rule

Error Pattern					SM		TD
$\underline{e}_i = (e_1, e_2, e_3, e_4)$					p_1	p_2	p_0
$\underline{e}_1$:	0	0	0	0	$x_1 \oplus x_2$	$x_3 \oplus x_4$	$x_1 \oplus x_2 \oplus x_3 \oplus x_4$
$\underline{e}_2$:	0	0	0	1	$x_1 \oplus x_2$	x_3	$x_1 \oplus x_2 \oplus x_3$
$\underline{e}_3$:	0	0	1	0	$x_1 \oplus x_2$	x_4	$x_1 \oplus x_2 \oplus x_4$
$\underline{e}_4$:	0	1	0	0	x_1	$x_3 \oplus x_4$	$x_1 \oplus x_3 \oplus x_4$
$\underline{e}_5$:	1	0	0	0	x_2	$x_3 \oplus x_4$	$x_2 \oplus x_3 \oplus x_4$
$\underline{e}_6$:	0	0	1	1	$x_1 \oplus x_2$	$x_1 \oplus x_2$	$x_1 \oplus x_2$
$\underline{e}_7$:	0	1	0	1	x_1	x_3	$x_1 \oplus x_3$
$\underline{e}_8$:	1	0	0	1	x_2	x_3	$x_2 \oplus x_3$
$\underline{e}_9$:	0	1	1	0	x_1	x_4	$x_1 \oplus x_4$
$\underline{e}_{10}$:	1	0	1	0	x_2	x_4	$x_2 \oplus x_4$
$\underline{e}_{11}$:	1	1	0	0	$x_3 \oplus x_4$	$x_3 \oplus x_4$	$x_3 \oplus x_4$
$\underline{e}_{12}$:	1	1	1	0	x_4	x_4	x_4
$\underline{e}_{13}$:	1	1	0	1	x_3	x_3	x_3
$\underline{e}_{14}$:	1	0	1	1	x_2	x_2	x_2
$\underline{e}_{15}$:	0	1	1	1	x_1	x_1	x_1
$\underline{e}_{16}$:	1	1	1	1	$\varnothing$	$\varnothing$	$\varnothing$

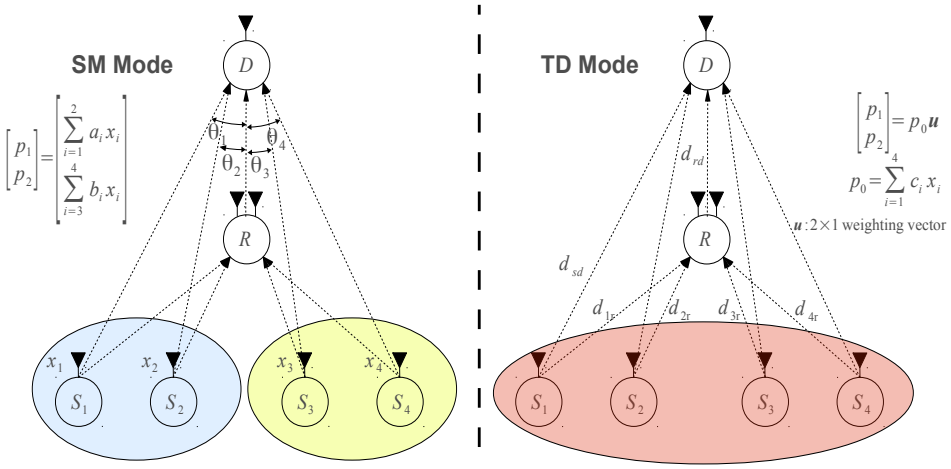

Figure 3.1 Symmetric multiple access relay network.

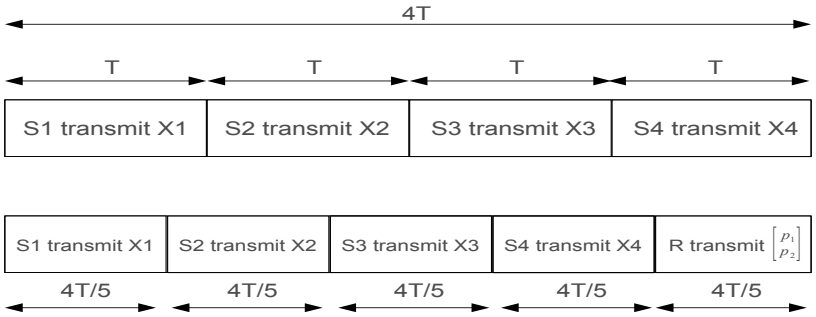

Figure 3.2 Frame structure of non-cooperative network and cooperative relay network, K = 4.

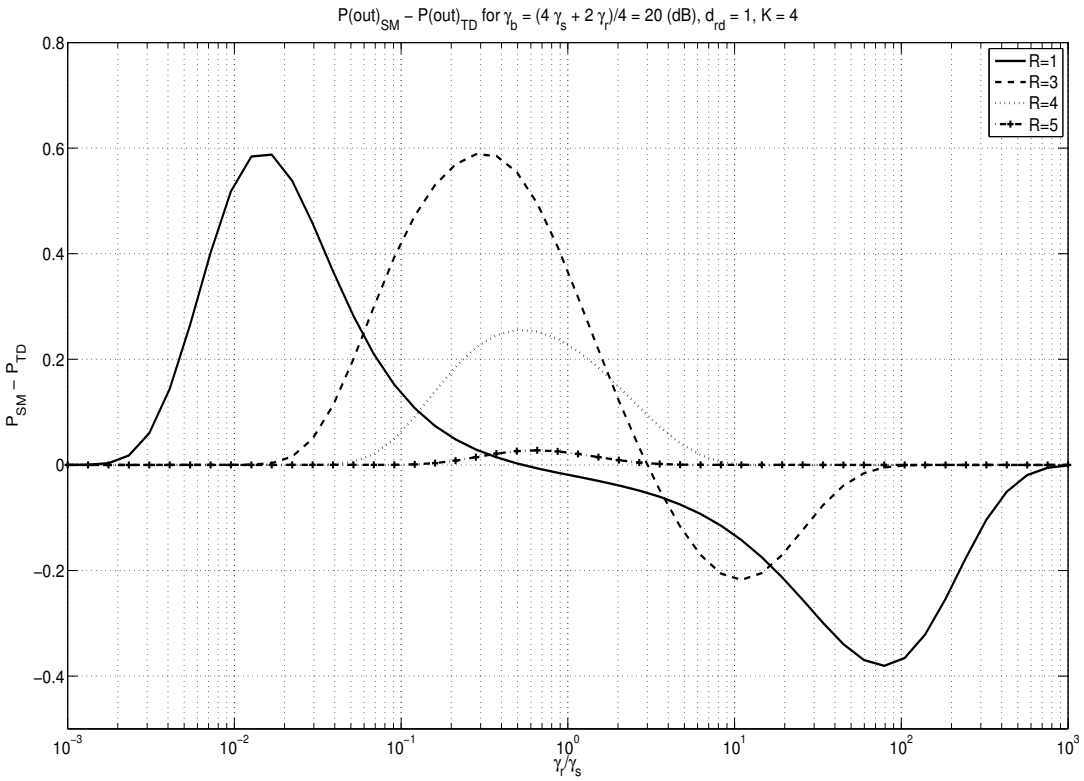

Figure 3.3 $P(\text{out})_{\text{SM}} - P(\text{out})_{\text{TD}}$ versus γ_r/γ_s for fixed received SNR $\gamma_b = (4\gamma_s + 2\gamma_r)/4 = 20$ (dB), $d_{dr} = 1$, $K = 4$.

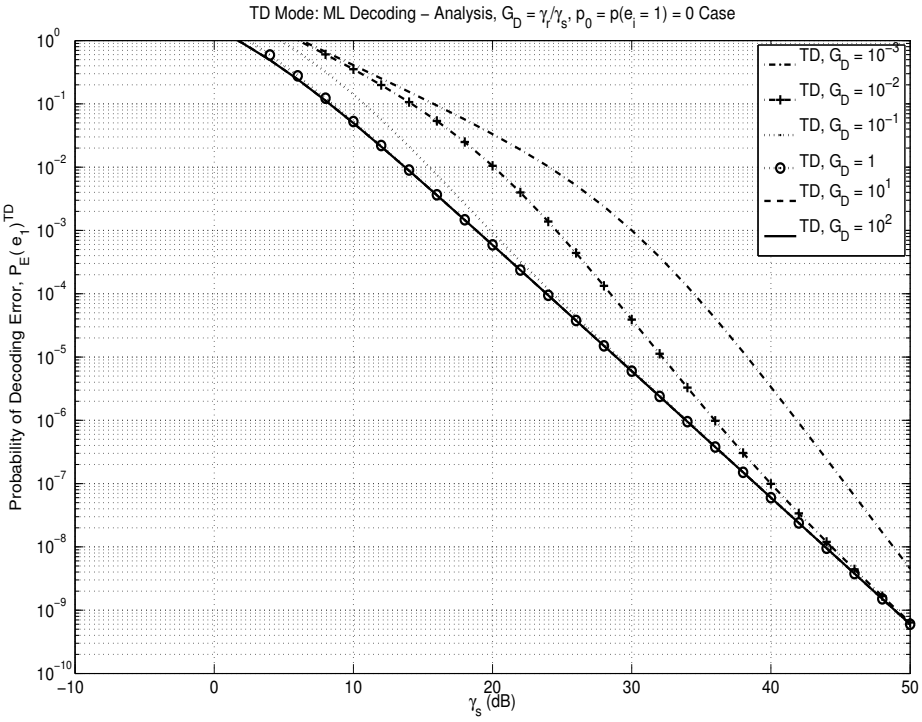

Figure 3.4 Decoding error probability of TD mode for several power ratio $G_D = \gamma_r/\gamma_s$

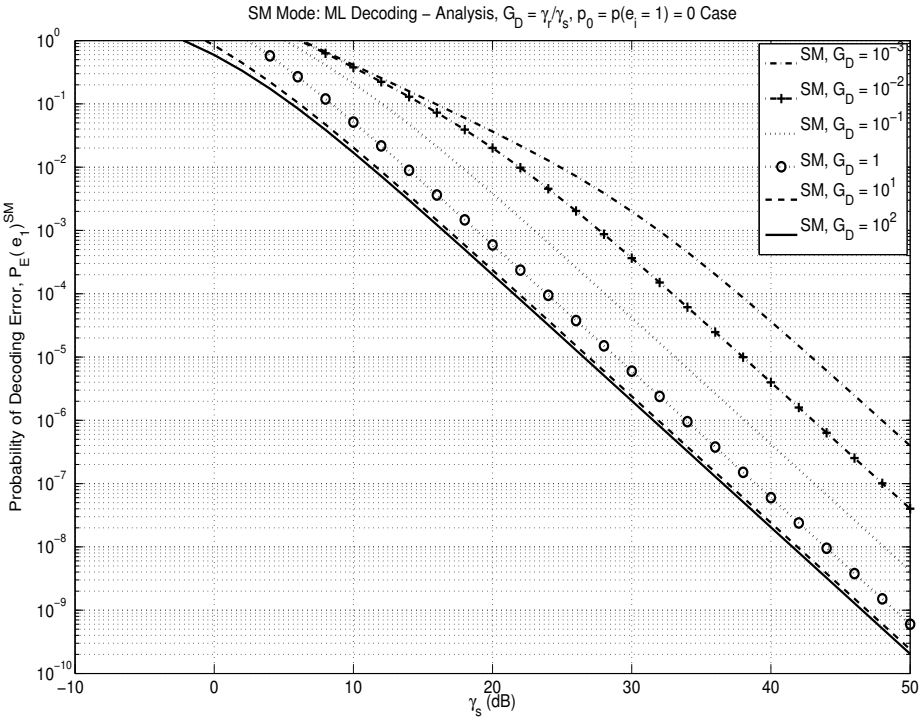

Figure 3.5 Decoding error probability of SM mode for several power ratio $G_D = \gamma_r/\gamma_s$

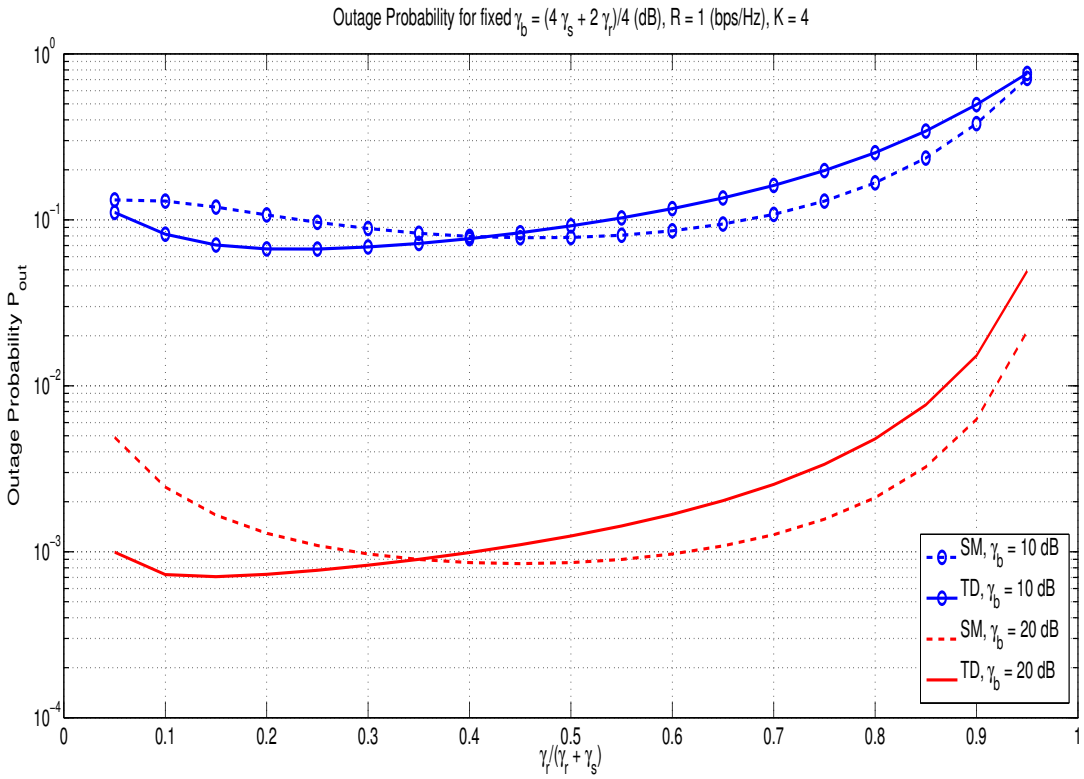

Figure 3.6 Outage probability versus $\gamma_r/(\gamma_r + \gamma_s)$ for fixed received SNR $\gamma_b = (4\gamma_s + 2\gamma_r)/4$ (dB), $R = 1$ (bps/Hz), $d_{dr} = 1$, $K = 4$.

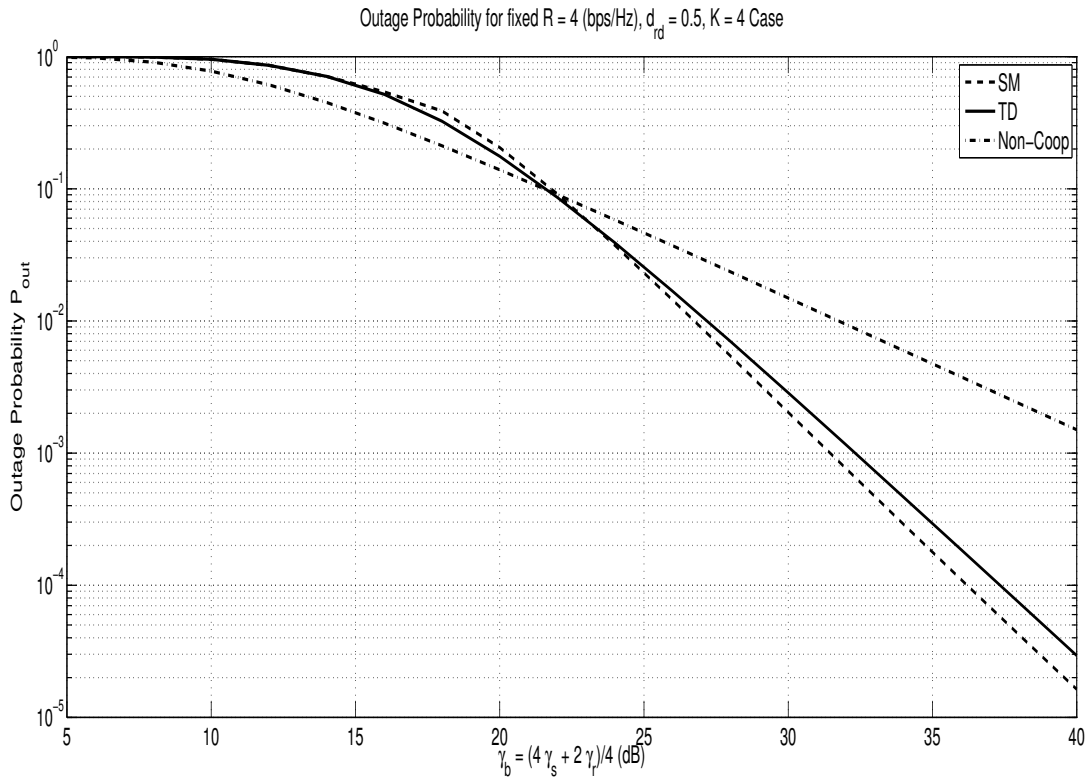

Figure 3.7 Outage probability versus received SNR γ_b with γ_r/γ_s optimized, $R = 4$ (bps/Hz), $d_{dr} = 0.5$, $K = 4$.

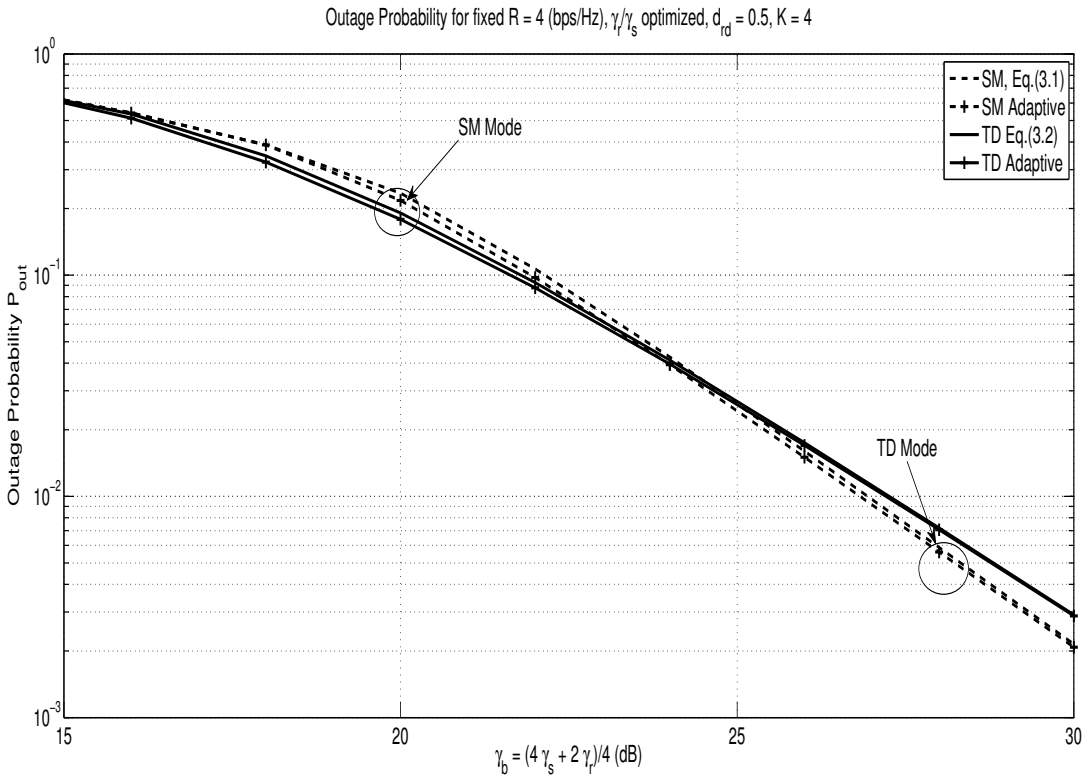

Figure 3.8 Comparison of adaptive and conventional network coding with γ_r/γ_s optimized, $R = 4$ (bps/Hz), $d_{dr} = 0.5$, $K = 4$.

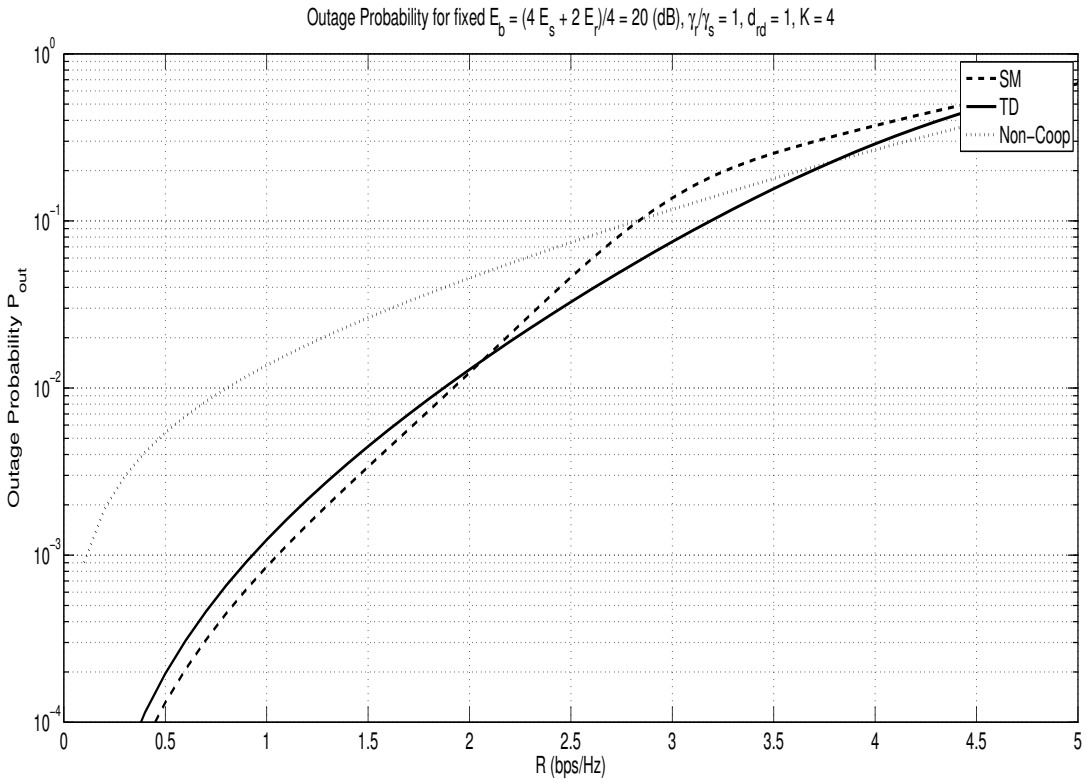

Figure 3.9 Outage error probability versus transmission rate R for fixed received SNR $\gamma_b = 20(dB)$, $d_{dr} = 1$, $\gamma_r/\gamma_s = 1$, $K = 4$

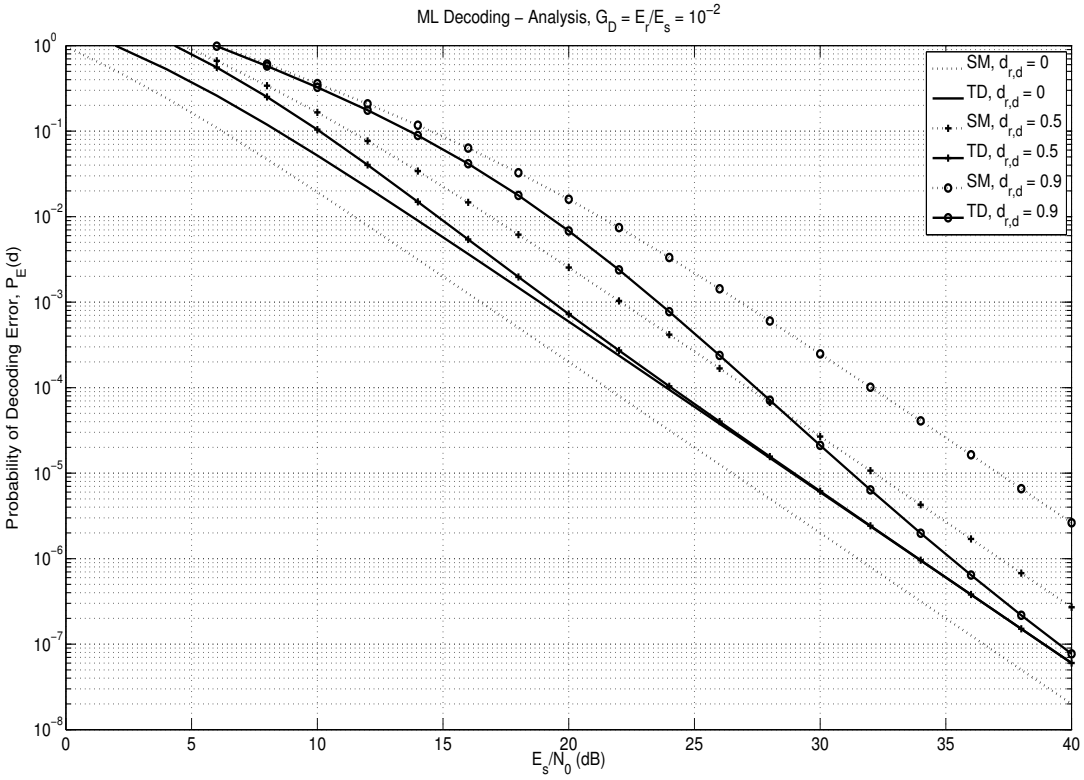

Figure 3.10 Decoding error probability versus source transmit energy E_s/N_0 at several relay location

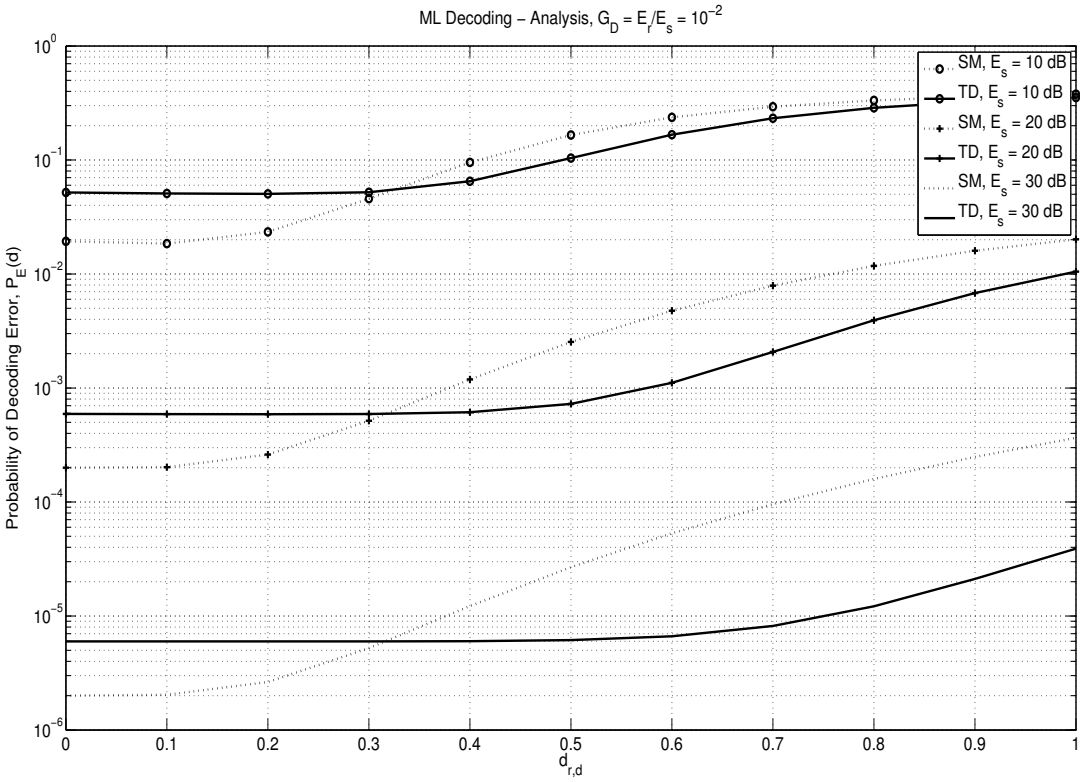

Figure 3.11 Decoding error probability versus relay location $d_{r,d}$ for fixed source transmit energy E_s/N_0

CHAPTER 4. ACHIEVABLE RATE AND RELIABILITY-RATE TRADEOFF

In this chapter, we consider random linear coding in noisy multiple-access relay channel where each relay is equipped with multiple antennas and sends the network coded information to the destination using three MIMO transmission modes: spatial multiplexing (SM), transmit diversity (TD), and Golden code (GC). SM mode allows to send more coded bits than TD mode, thereby increasing the Hamming distance at the cost of sacrificing the diversity gain, and vice versa. We derive the probability of decoding error with the maximum likelihood decoding at the destination and determine the fundamental tradeoff among rate, reliability, and MIMO mode. The tradeoff provides a complete view on the reliability-rate tradeoff for each MIMO mode at any given SNR, and shows how the energy and node density can be traded in achieving a given reliability-rate pair.

4.1 Introduction

We consider a multiple-access relay channel (MARC) where multiple sources communicate with a single destination with the help of multiple relays. Examples of such scenarios include next-generation cellular systems such as those envisaged in the 802.16m standard, hybrid wireless LAN/WAN networks, and sensor and ad hoc networks where cooperation between the sources is either undesirable or not possible, but one can use relays to aid communication between multiple sources and the destination.

In [86], Kim investigated the tradeoff between reliability and rate as a function of node density and SNR, and showed how the energy and node density can be traded in achieving a given reliability-rate pair in single antenna case. We extend the work of [86] to the case

of multiple antennas at the relay and destination nodes. Each relay independently generates parity bits using random linear coding rule and forwards to the destination after space-time encoding. We consider spatial multiplexing (SM), transmit diversity (TD) using Alamouti code, and Golden code (GC) [53] as space-time codes. SM mode allows to send more parity bits than TD mode, thereby increasing the Hamming distance at the cost of sacrificing the diversity gain, and vice versa. We derive the probability of decoding error with the maximum likelihood decoding at the destination and investigate the effect of MIMO transmission mode of relay nodes on the probability of decoding error at the destination. The inherent tradeoff between the Hamming distance gain offered by SM mode and the diversity gain offered by TD mode has been investigated in point-to-point communication systems [54], [55]. We investigate the effect of MIMO transmission mode of relay nodes on the probability of decoding error at the destination in multiple access relay network with random linear network coding.

The remainder part of this chapter is organized as follows. System model is described in Section II. The union bound on the probability of decoding error is derived in Section III, and the asymptotic analysis is performed in Section IV. Section V presents numerical results and Section VI concludes the chapter.

4.2 System Model

We consider a multiple access relay network in which K sources send packets to a common destination with the assistance of R relays, as illustrated in Fig. 4.1. We assume each node has multiple antennas and denote the number of antennas to be n_S, n_R, n_D for source, relay and the destination, respectively. For simplicity of the presentation, we consider the case of $(n_S, n_R) = (1, 2)$ but the analysis in this paper can be extended to a general combination of (n_S, n_R). By this constraint, the channel model classifies into two classes. First, we have a SIMO channel between source to relay and between source to destination. For SIMO channel, the receiver use maximum ratio combining (MRC) as receive diversity. Second, we have MIMO channel between relay to destination where the relay use the three transmission modes: Spatial Multiplexing (SM), Alamouti Coding as Transmit diversity (TD) and Golden Code (GC) [53].

The communication protocol consist of two-phase transmission. In the first phase, each K

source transmits a packet $\mathbf{u}_i$ over the orthogonal channel

$$\mathbf{u}_i = (u_{1,i}, u_{2,i}, \cdots, u_{n,i})^T, \quad u_{m,i} \in \{0, 1\} \tag{4.1}$$

and the subscript i denotes the i-th source. Due to the broadcast nature of the wireless medium, each relay may also overhear the packets $\mathbf{u}_1, \mathbf{u}_2, \cdots, \mathbf{u}_K$. However, in practice, the relays may be far away from the sources so that the channels between sources and relays are subject to error. After decoding, each relay checks for errors using the cyclic redundancy check (CRC) code. In general, the number of correctly decoded packets at a relay is a random variable.

In the second phase, each relay stores the correctly decoded packets in a two-dimensional array. If we let S_j denote the set of indices for correctly decoded packets at the j-th relay, then the array size is $n \times |S_j|$, where $|S_j|$ denotes the number of elements in the set S_j. Then, each relay generates L parity bits for each row of the array and sends them to the destination, where L depends on the relay transmission mode. If the relay is equipped with two antennas, the following space-time matrix may be considered:

$$X_{SM} = \begin{bmatrix} v_{m,1} & v_{m,3} \\ v_{m,2} & v_{m,4} \end{bmatrix} \qquad \text{SM Mode} \tag{4.2}$$

$$X_{TD} = \begin{bmatrix} v_{m,1} & -v_{m,2}^* \\ v_{m,2} & v_{m,1}^* \end{bmatrix} \qquad \text{TD Mode} \tag{4.3}$$

$$X_{GC} = \frac{1}{\sqrt{5}} \begin{bmatrix} \alpha(v_{m,1} + v_{m,2}\theta) & \alpha(v_{m,3} + v_{m,4}\theta) \\ \bar{\alpha}i(v_{m,3} + v_{m,4}\bar{\theta}) & \bar{\alpha}(v_{m,1} + v_{m,2}\bar{\theta}) \end{bmatrix} \qquad \text{GC Mode} \tag{4.4}$$

where $L = 4$ for SM and GC modes and $L = 2$ for TD mode, $\theta = 1 - \bar{\theta} = (1 + \sqrt{5})/2$, $\alpha = 1 + \bar{\theta}i$, and $\bar{\alpha} = 1 + \theta i$. The destination, after collecting K message bits from K sources and $RL(= P)$ -parity bits from R relays, may construct a $(K + P, K)$ code whose m-th codeword $\mathbf{c}_m$ is given by

$$\mathbf{c}_m = (\underbrace{u_{m,1}, u_{m,2}, \cdots, u_{m,K}}_{\mathbf{u}_m}, \underbrace{v_{m,1}, v_{m,2}, \cdots, v_{m,P}}_{\mathbf{v}_m}) \tag{4.5}$$

where the parity vector $\mathbf{v}_m$ is given by

$$\begin{aligned}\mathbf{v}_m &= (v_{m,1}, v_{m,2}, \cdots, v_{m,P}) \\ &= (\underbrace{v_{m,1}, v_{m,2}, \cdots, v_{m,L}}_{1^{\text{st}}\text{ Relay}}, \underbrace{v_{m,L+1}, \cdots, v_{m,2L}}_{2^{\text{nd}}\text{ Relay}}, v_{m,2L+1}, \cdots, v_{m,RL})\end{aligned} \tag{4.6}$$

The k-th parity bit $v_{m,k} \in \{0,1\}$, $1 \le k \le P$ is generated by the following random linear combining rule

$$v_{m,k} = \sum_{i \in S_j} g_{k,i} u_{m,i}, \quad v_{m,k} \in \{0,1\} \tag{4.7}$$

where the network encoding coefficients $\{g_{j,i}\}$ are independently and randomly chosen from $\{0,1\}$ and the summation is mod-2 addition. The number of generated parity bit L is determined by the transmission mode at each relay. For MIMO channel with 2 transmit antennas, the relay transmit 2×2 space-time (ST) matrix X_{RD} as follows and the number of generated parity bits L are $L = 4$ for SM, GC mode and $L = 2$ for TD mode.

Then, the destination may construct $n \times (K+P)$ array by combining K column vectors from source nodes and P parity vectors from the relay nodes, as illustrated in Fig. 4.1. Due to the distributed nature of encoding at the relay nodes, the coding coefficients $\{g_{k,i}\}$ are transmitted to the destination as a packet hearer, so that it can decode the source packets.

We assume that the channel links are composed of large-scale path loss and small-scale quasi-static frequency non-selective Rayleigh fading and the channel gain h_{ij} is modeled by

$$h_{ij} = \sqrt{d_{ij}^{-\alpha}} \cdot g_{ij} \tag{4.8}$$

where d_{ij} denote the distance between node i and j , α is the path loss exponent and g_{ij} captures the channel fading characteristic due to the rich scattering environment. The Rayleigh fading g_{ij} is modeled as a Gaussian random variable with mean zero and variance 0.5 per dimension. The background noise W_{ij} is modeled by a Gaussian random variable with mean zero and variance $N_0/2$ per dimension. We assume that the bits of source and relay are transmitted using BPSK modulation with symbol energies E_s and E_r, respectively. Hence, the transmit energy E_b per information bit is given by $(KE_s + 4RE_r)/K$.

4.3 Probability of Decoding Error

In this section, we derive the union bound on the probability of decoding error with the maximum likelihood (ML) decoding at the destination, averaged over all possible encoding rules at the relays and compare the error probability of three transmission modes.

Let $\mathbf{c}_a = (u_{a,1}, \cdots, u_{a,K}, v_{a,1}, \cdots, v_{a,P})$ and $\mathbf{c}_b = (u_{b,1}, \cdots, u_{b,K}, v_{b,1}, \cdots, v_{b,P})$ be two distinct row codewords of length $K+P$ in Fig. 4.1, where $u_{a,i} \in \{0,1\}$ is the information bit from the i-th source and $v_{a,k} \in \{0,1\}$ is the k-th network coded parity bit from the relay. Let $d_{s,i}$ denote the distance between the i-th source and the destination, and $d_{r,j}$ be the distance between the j-th relay and the destination. Then, the conditional pairwise error probability with the maximum likelihood (ML) of each transmission mode for a given distance vector $\mathbf{d} = \{d_{s,1}, \cdots, d_{s,K}, d_{r,1}, \cdots, d_{r,R}\}$ is given by [1]

$$\begin{aligned} Pr\left(\mathbf{c}_a \to \mathbf{c}_b|\mathbf{d}\right)_{SM,GC} &\leq \frac{1}{2}\prod_{i=1}^{K}\left[\frac{1}{1+d_{s,i}^{-\alpha}|x_{a,i}-x_{b,i}|^2/(4N_0)}\right]^{n_D} \\ &\quad \cdot \prod_{j=1}^{R}\left[\frac{1}{1+d_{r,j}^{-\alpha}\lambda_1/(4N_0)} \cdot \frac{1}{1+d_{r,j}^{-\alpha}\lambda_2/(4N_0)}\right]^{n_D} \\ Pr\left(\mathbf{c}_a \to \mathbf{c}_b|\mathbf{d}\right)_{TD} &\leq \frac{1}{2}\prod_{i=1}^{K}\left[\frac{1}{1+d_{s,i}^{-\alpha}|x_{a,i}-x_{b,i}|^2/(4N_0)}\right]^{n_D} \\ &\quad \cdot \prod_{j=1}^{R}\left[\frac{1}{1+d_{r,j}^{-\alpha}\left[|y_{a,1}-y_{b,1}|^2+|y_{a,2}-y_{b,2}|^2\right]/(4N_0)}\right]^{2n_D} \end{aligned} \tag{4.9}$$

where $x_{a,i} = (-1)^{u_{a,i}}\sqrt{E_s}$ and $y_{a,k} = (-1)^{v_{a,k}}\sqrt{E_r}$ are BPSK constellations corresponding to the parity bits $u_{a,i}$ and $v_{a,k}$, respectively. λ_1, λ_2 are the eigenvalues of $\Delta X_{RD} \cdot \Delta X_{RD}^H$ where $\Delta X_{RD} = X_{RD,a} - X_{RD,b}$ and $X_{RD,m}$ is the space-time matrix for corresponding transmission mode given by (4.2)-(4.4). The factor 1/2 follows from the exponential approximation to Q-function ($Q(x) \leq e^{-x^2/2}/2$ for $x \geq 0$). Then, the union bound on the probability of decoding error, conditioned on the distance vector $\mathbf{d}$ and the network encoding rule $\mathbf{c}_a$ and $\mathbf{c}_b$, is given by

$$P_E\left(\mathbf{c}_a, \mathbf{c}_b, \mathbf{d}\right) \leq \sum_{\mathbf{c}_b \neq \mathbf{c}_a} P_E\left(\mathbf{c}_a \to \mathbf{c}_b|\mathbf{d}\right) \tag{4.10}$$

[1] The first term on the right hand side of (4.9) is derived in [56] for n_D branch MRC and the second term on the right hand side of (4.9) is derived in [57] for $n_R \times n_D$ MIMO.

Without loss of generality, assume $u_{a,i} = 1$ for all i. Suppose that the weight of $(u_{b,1}, u_{b,2}, \cdots, u_{b,K})$ is W, i.e. $w_H(\mathbf{u}_a \oplus \mathbf{u}_b) = w_H(u_{a,1} \oplus u_{b,1}, \cdots, u_{a,K} \oplus u_{b,K}) = K - W$. Then, the first term on the right hand side of (4.9) is given by

$$\prod_{i=1}^{K} \left[\frac{1}{1 + d_{s,i}^{-\alpha} |x_{a,i} - x_{b,i}|^2/(4N_0)} \right]^{n_D} = \prod_{i=1}^{K-W} \left[\frac{1}{1 + d_{s,(i)}^{-\alpha} \gamma_s} \right]^{n_D} \tag{4.11}$$

where $d_{s,(i)}$ is the distance between (i)-th source and the destination for which $x_{a,(i)} \neq x_{b,(i)}$ and $\gamma_s = E_s/N_0$ is the transmit signal-to-noise ratio for the source symbol. Similarly, the second term on the right hand side of (4.9) for TD mode can be expressed as

$$\prod_{j=1}^{R} \left[\frac{1}{1 + d_{r,j}^{-\alpha} (\sum_{l=1}^{2} |y_{a,l} - y_{b,l}|^2)/(4N_0)} \right]^{2n_D} = \prod_{j=1}^{R} \left[\frac{1}{1 + \sum_{l=1}^{2} (v_{a,l} \oplus v_{b,l}) d_{r,j}^{-\alpha} \gamma_r} \right]^{2n_D} \tag{4.12}$$

where $\gamma_r = E_r/N_0$ is the transmit signal-to-noise ratio for the relay symbol.

Since, given $W = w$, there are $\binom{K}{w}$ vectors $(u_{b,1}, u_{b,2}, \cdots, u_{b,K})$ whose weight is w, it follows from (4.9)-(4.12) that the union bound in (4.10) is given by

$$\begin{aligned}
P_E(\mathbf{v}_a, \mathbf{v}_b, \mathbf{d})_{SM,GC} &\leq \frac{1}{2} \sum_{w=0}^{K-1} \binom{K}{w} \prod_{i=1}^{K-w} \left[\frac{1}{1 + d_{s,(i)}^{-\alpha} \gamma_s} \right]^{n_D} \\
&\quad \cdot \prod_{j=1}^{R} \left[\frac{1}{1 + d_{r,j}^{-\alpha} \lambda_1/(4N_0)} \cdot \frac{1}{1 + d_{r,j}^{-\alpha} \lambda_2/(4N_0)} \right]^{n_D} \\
P_E(\mathbf{v}_a, \mathbf{v}_b, \mathbf{d})_{TD} &\leq \frac{1}{2} \sum_{w=0}^{K-1} \binom{K}{w} \prod_{i=1}^{K-w} \left[\frac{1}{1 + d_{s,(i)}^{-\alpha} \gamma_s} \right]^{n_D} \\
&\quad \cdot \prod_{j=1}^{R} \left[\frac{1}{1 + \sum_{l=1}^{2} (v_{a,l} \oplus v_{b,l}) d_{r,j}^{-\alpha} \gamma_r} \right]^{2n_D}
\end{aligned} \tag{4.13}$$

where the eigenvalues λ_1, λ_2 are functions of $(v_{a,l} \oplus v_{b,l})$ as shown in Table 4.1.

In Lemma 1 of [86], it is shown that the probability mass function of $(v_{a,l} \oplus v_{b,l})$ is given by

$$Pr(v_{a,l} \oplus v_{b,l} = 1 | W, S_j) = Pr(v_{a,l} \oplus v_{b,l} = 0 | W, S_j) = \frac{1}{2} \tag{4.14}$$

when $u_{a,i} = 1$ for all i. Although the uniformness of $(v_{a,l} \oplus v_{b,l})$ is proved for the special case when all one codeword is transmitted, we used Monte Carlo simulation to show that even if we transmit a random codeword with arbitrary weight $w_H(\mathbf{u}_a)$, the decoding error probability is still virtually identical. Fig. 4.7 shows the probability of decoding error $P_E(\mathbf{d})$ versus E_b/N_0 for codewords with different Hamming weight. The dotted line corresponds to the case when

all one codeword $w_H(\mathbf{u}_a) = K$ is transmitted and the solid line with circle marker is the case when $u_{a,i} \in \{0, 1\}$ is randomly chosen between 0 and 1. We note that two curves has virtually identical error probability.

Then, we average (4.14) over S_j as follows.

$$Pr(v_{a,l} \oplus v_{b,l}|W) = \sum_{|S_j|=0}^{K} P(|S_j|) Pr(v_{a,l} \oplus v_{b,l}|W, S_j) = \frac{1}{2} \tag{4.15}$$

Since the random linear network coding (4.7) is performed independently, the probability of each network encoding rule are uniform as follows.

$$\begin{aligned} P\left(\mathbf{v}_a \oplus \mathbf{v}_b|W\right) &= P\left(v_{a,1} \oplus v_{b,1}, v_{a,2} \oplus v_{b,2}, \cdots, v_{a,P} \oplus v_{b,P}|W\right) \\ &= P\left(v_{a,1} \oplus v_{b,1}|W\right) P\left(v_{a,2} \oplus v_{b,2}|W\right) \cdots P\left(v_{a,P} \oplus v_{b,P}|W\right) \\ &= \left(\frac{1}{2}\right)^P = \left(\frac{1}{2^L}\right)^R, \quad P = RL \end{aligned} \tag{4.16}$$

Averaging the probability of decoding error in (4.13) over the network encoding rule $\mathbf{v}_a, \mathbf{v}_b$ using (4.16) yields

$$\begin{aligned} P_E(\mathbf{d})_{SM,GC} \;\leq\; & \frac{1}{2} \sum_{w=0}^{K-1} \binom{K}{w} \prod_{i=1}^{K-w} \left[\frac{1}{1 + d_{s,(i)}^{-\alpha} \gamma_s}\right]^{n_D} \\ & \cdot \prod_{j=1}^{R} \left[\frac{1}{2^4} \sum_{\substack{v_{a,l} \oplus v_{b,l} \\ l=1,\cdots,4}} \left[\frac{1}{1 + d_{r,j}^{-\alpha} \lambda_1/(4N_0)} \cdot \frac{1}{1 + d_{r,j}^{-\alpha} \lambda_2/(4N_0)}\right]^{n_D}\right] \end{aligned} \tag{4.17}$$

$$\begin{aligned} P_E(\mathbf{d})_{TD} \;\leq\; & \frac{1}{2} \sum_{w=0}^{K-1} \binom{K}{w} \prod_{i=1}^{K-w} \left[\frac{1}{1 + d_{s,(i)}^{-\alpha} \gamma_s}\right]^{n_D} \\ & \cdot \prod_{j=1}^{R} \left[\frac{1}{2^2} \sum_{\substack{v_{a,l} \oplus v_{b,l} \\ l=1,2}} \left[\frac{1}{1 + \sum_{l=1}^{2} (v_{a,l} \oplus v_{b,l}) d_{r,j}^{-\alpha} \gamma_r}\right]^{2n_D}\right] \end{aligned} \tag{4.18}$$

For TD mode, there are 4 available combination of $(v_{a,1} \oplus v_{b,1}, v_{a,2} \oplus v_{b,2})$; $(00, 01, 10, 11)$. By applying each case into the second part on the right hand side of (4.17), we obtain

$$\frac{1}{2^2} \sum_{\substack{v_{a,l} \oplus v_{b,l} \\ l=1,2}} \left[\frac{1}{1 + \sum_{l=1}^{2} (v_{a,l} \oplus v_{b,l}) d_{r,j}^{-\alpha} \gamma_r}\right]^{2n_D} = \frac{1}{2^2} \left[1 + \frac{2}{(1 + d_{r,j}^{-\alpha} \gamma_r)^{2n_D}} + \frac{1}{(1 + 2d_{r,j}^{-\alpha} \gamma_r)^{2n_D}}\right] \tag{4.19}$$

for TD mode. For SM and GC mode, the eigenvalues of $\Delta X_{RD} \cdot \Delta X_{RD}^H$ should be evaluated for all possible combination of $v_{a,l} \oplus v_{b,l}$, $l = 1, \cdots, 4$. We derived the eigenvalues for each transmission mode in Table 4.1 [2] and substituted these values into the second part on the right hand side of (4.17) to obtain

$$\begin{aligned}
&\frac{1}{2^4} \sum_{\substack{v_{a,l} \oplus v_{b,l} \\ l=1,\cdots,4}} \left[\frac{1}{1 + d_{r,j}^{-\alpha} \lambda_1/(4N_0)} \cdot \frac{1}{1 + d_{r,j}^{-\alpha} \lambda_2/(4N_0)} \right]^{n_D} \\
&= \frac{1}{2^4} \left[1 + \frac{4}{(1 + d_{r,j}^{-\alpha} \gamma_r)^{n_D}} + \frac{4}{(1 + 2d_{r,j}^{-\alpha} \gamma_r)^{n_D}} + \frac{2}{(1 + d_{r,j}^{-\alpha} \gamma_r)^{2n_D}} \right. \\
&\left. + \frac{4}{\left[(1 + (6 - 2\sqrt{5}) d_{r,j}^{-\alpha} \gamma_r/4)(1 + (6 + 2\sqrt{5}) d_{r,j}^{-\alpha} \gamma_r/4) \right]^{n_D}} + \frac{1}{(1 + 4d_{r,j}^{-\alpha} \gamma_r)^{n_D}} \right]
\end{aligned} \tag{4.20}$$

for SM mode. Then, the union bound of decoding error probability is given by

$$\begin{aligned}
P_E(\mathbf{d})_{SM} \leq \frac{1}{2} \sum_{w=0}^{K-1} \binom{K}{w} \prod_{i=1}^{K-w} \left[\frac{1}{1 + d_{s,(i)}^{-\alpha} \gamma_s} \right]^{n_D} \\
\cdot \prod_{j=1}^{R} \frac{1}{2^4} \left[1 + \frac{4}{(1 + d_{r,j}^{-\alpha} \gamma_r)^{n_D}} + \frac{4}{(1 + 2d_{r,j}^{-\alpha} \gamma_r)^{n_D}} + \frac{2}{(1 + d_{r,j}^{-\alpha} \gamma_r)^{2n_D}} \right. \\
\left. + \frac{4}{\left[(1 + (6 - 2\sqrt{5}) d_{r,j}^{-\alpha} \gamma_r/4)(1 + (6 + 2\sqrt{5}) d_{r,j}^{-\alpha} \gamma_r/4) \right]^{n_D}} + \frac{1}{(1 + 4d_{r,j}^{-\alpha} \gamma_r)^{n_D}} \right] \\
P_E(\mathbf{d})_{TD} \leq \frac{1}{2} \sum_{w=0}^{K-1} \binom{K}{w} \prod_{i=1}^{K-w} \left[\frac{1}{1 + d_{s,(i)}^{-\alpha} \gamma_s} \right]^{n_D} \cdot \prod_{j=1}^{R} \frac{1}{2^2} \left[1 + \frac{2}{(1 + d_{r,j}^{-\alpha} \gamma_r)^{2n_D}} + \frac{1}{(1 + 2d_{r,j}^{-\alpha} \gamma_r)^{2n_D}} \right]
\end{aligned} \tag{4.21}$$

The corresponding union bound for GC mode can be obtained similarly.

4.4 Asymptotic analysis and reliability-rate tradeoff

In this section we provide asymptotic analysis and compare the tradeoff between communication reliability and achievable rate for each transmission mode. To simplify the formulation, we assume that all source nodes are located at distance $d_{s,i} = 1$ from the destination and each relay nodes utilize power control to compensate the path loss between j-th relay to destination channel, such that the received SNR at the destination is $d_{r,j}^{-\alpha} \gamma_{r,j} = \gamma_r$ for all j. We denote the

[2] Table 4.1 is evaluated in Appendix D.

first part on the right hand side of (4.21) as $g_{n_D}(\gamma_s)$

$$g_{n_D}(\gamma_s) = \left[\frac{1}{1+\gamma_s}\right]^{n_D} \tag{4.22}$$

and the second part on the right hand side of (4.21) as $g_{SM}(\gamma_r)$ for SM mode

$$\begin{aligned} g_{SM}(\gamma_r) = \Bigg[&\frac{4}{(1+\gamma_r)^{n_D}} + \frac{4}{(1+2\gamma_r)^{n_D}} + \frac{2}{(1+\gamma_r)^{2n_D}} \\ &+ \frac{4}{\left[(1+(6-2\sqrt{5})\gamma_r/4)(1+(6+2\sqrt{5})\gamma_r/4)\right]^{n_D}} + \frac{1}{(1+4\gamma_r)^{n_D}}\Bigg] \end{aligned} \tag{4.23}$$

and $g_{TD}(\gamma_r)$ for TD mode as follows.

$$g_{TD}(\gamma_r) = \left[\frac{2}{(1+\gamma_r)^{2n_D}} + \frac{1}{(1+2\gamma_r)^{2n_D}}\right] \tag{4.24}$$

$g_{GC}(\gamma_r)$ for GC mode is provided in Appendix E. We note that $(g_{n_D}(\gamma), g_{SM}(\gamma), g_{GC}(\gamma), g_{TD}(\gamma))$ are all decreasing functions of γ and converge to zero as $\gamma \to \infty$.

$$\lim_{\gamma\to\infty} g_{n_D}(\gamma) = \lim_{\gamma\to\infty} g_{SM}(\gamma) = \lim_{\gamma\to\infty} g_{GC}(\gamma) = \lim_{\gamma\to\infty} g_{TD}(\gamma) = 0 \tag{4.25}$$

Substituting $(g_{n_D}(\gamma), g_{SM}(\gamma), g_{GC}(\gamma), g_{TD}(\gamma))$ in (4.21) yields

$$\begin{aligned} P_E(\mathbf{d})_{SM} &\le \frac{1}{2}\sum_{w=0}^{K-1}\binom{K}{w} g_{n_D}^{K-w}(\gamma_s)\left[\frac{1}{2^4}\left(1+g_{SM}(\gamma_r)\right)\right]^R \\ P_E(\mathbf{d})_{GC} &\le \frac{1}{2}\sum_{w=0}^{K-1}\binom{K}{w} g_{n_D}^{K-w}(\gamma_s)\left[\frac{1}{2^4}\left(1+g_{GC}(\gamma_r)\right)\right]^R \\ P_E(\mathbf{d})_{TD} &\le \frac{1}{2}\sum_{w=0}^{K-1}\binom{K}{w} g_{n_D}^{K-w}(\gamma_s)\left[\frac{1}{2^2}\left(1+g_{TD}(\gamma_r)\right)\right]^R. \end{aligned} \tag{4.26}$$

The decoding error probability (4.26) indicate the following two aspects. First, as $\gamma_s, \gamma_r \to \infty$, the parity part of (4.26) converge to the constant term $(1/2^L)^R$ and the average codeword error probability achieve diversity order n_D for all three transmission modes as follows.

$$\begin{aligned} P_E(\mathbf{d}) &\doteq \frac{1}{2}\sum_{w=0}^{K-1}\binom{K}{w}\prod_{i=1}^{K-w}\left[\frac{1}{1+\gamma_s}\right]^{n_D}\cdot\left(\frac{1}{2^L}\right)^R \\ &\doteq \frac{K}{2^{RL+1}}\left[\frac{1}{1+\gamma_s}\right]^{n_D} \doteq \gamma_s^{-n_D} \end{aligned} \tag{4.27}$$

Second, the decoding error probability of each transmission mode has the following inequality.

$$P_E(\mathbf{d})_{GC} \le P_E(\mathbf{d})_{SM} \le P_E(\mathbf{d})_{TD} \tag{4.28}$$

where GC mode delivers the lowest error probability and TD mode provides the highest error probability. The decoding error probability of SM mode is slightly larger than that of GC mode at low SNR, however, at high SNR, two transmission mode provides virtually identical decoding error probability. The difference between error probability of SM and that of TD mode at high SNR is

$$\begin{aligned}\lim_{\gamma_s,\gamma_r\to\infty}(P_E(\mathbf{d})_{\mathrm{TD}}-P_E(\mathbf{d})_{\mathrm{SM}}) &= \lim_{\gamma_s,\gamma_r\to\infty}\frac{1}{2}\sum_{w=0}^{K-1}\binom{K}{w}\prod_{i=1}^{K-w}\left[\frac{1}{1+\gamma_s}\right]^{n_D}\left[\frac{1}{2^{2R}}-\frac{1}{2^{4R}}\right] \\ &= \frac{1}{2}\sum_{w=0}^{K-1}\binom{K}{w}\prod_{i=1}^{K-w}\left[\frac{1}{1+\gamma_s}\right]^{n_D}\cdot\left[\frac{2^{2R}-1}{2^{4R}}\right].\end{aligned} \tag{4.29}$$

The performance advantage of GC over SM mode results from the fact that space-time matrix X_{RD} for GC mode always guaranty rank 2 for any combination of $v_{a,l}\oplus v_{b,l}$, $l=1,\cdots,4$, whereas X_{RD} for SM mode has rank 2 for only a particular combination of $v_{a,l}\oplus v_{b,l}$ as shown in Table 4.1. Thus, we have the following inequalities

$$g_{GC}(\gamma_r)\le g_{SM}(\gamma_r) \iff P_E(\mathbf{d})_{GC}\le P_E(\mathbf{d})_{SM} \tag{4.30}$$

as illustrated in Fig. **??**. The error probability gap between GC and SM mode is

$$\lim_{\gamma_r\to\infty}(P_E(\mathbf{d})_{\mathrm{GC}}-P_E(\mathbf{d})_{\mathrm{SM}}) = \lim_{\gamma_r\to\infty}\frac{1}{2}\sum_{w=0}^{K-1}\binom{K}{w}\prod_{i=1}^{K-w}\left[\frac{1}{1+\gamma_s}\right]^{n_D}\left[\frac{1}{2^{4R}}-\frac{1}{2^{4R}}\right]=0. \tag{4.31}$$

where the performance disadvantage of TD comparing to that of SM and GC mode results from the constant term $1/2^L$ in (4.26). Even though TD provides higher diversity order than SM mode, $1/2^L$ is the dominating factor of the error probability, such that the transmission mode with higher L always have a smaller decoding error probability. The constant term $1/2^L$ corresponds to the probability of choosing an encoding scheme which generates same parity vector for two distinct codeword $\mathbf{c}_a$ and $\mathbf{c}_b$ which has the highest error probability. Since this worst case event occurs with probability $1/2^L$, choosing a transmission mode with larger L is more effective than choosing a mode with higher diversity order. Based on this observation, we propose optimal mode selection scheme.

- **Optimal Mode Selection**

  Optimal mode selection scheme for MIMO-MARC with random linear network coding is to choose a transmission mode which generates more parity bits.

From (4.26), we obtain

$$\begin{aligned} P_E(\mathbf{d})_{SM} &\leq \frac{1}{2}\sum_{w=0}^{K-1}\binom{K}{w} g_{n_D}^{K-w}(\gamma_s)\left[\frac{1}{2^L}\left(1+g_{SM}(\gamma_r)\right)\right]^R, \quad L=4 \\ &= \frac{1}{2}\left[\left(1+g_{n_D}(\gamma_s)\right)^K - 1\right]\cdot\left[\frac{1}{2^L}\left(1+g_{SM}(\gamma_r)\right)\right]^R \\ &\leq \frac{1}{2}\left(1+g_{n_D}(\gamma_s)\right)^K\left[\frac{1+g_{SM}(\gamma_r)}{2^L}\right]^R \\ &\leq 2^{-K\cdot E_{SM}(K,R)} \end{aligned} \tag{4.32}$$

where

$$E_{SM}(K,R) = \log_2\left[\frac{\left\{2^L/\left(1+g_{SM}(\gamma_r)\right)\right\}^{R/K}}{1+g_{n_D}(\gamma_s)}\right]\Bigg|_{L=4} \tag{4.33}$$

is the *error exponent* or *reliability function* of SM mode. Similarly, we obtain the error exponent of GC and TD mode as follows.

$$\begin{aligned} E_{GC}(K,R) &= \log_2\left[\frac{\left\{2^L/\left(1+g_{GC}(\gamma_r)\right)\right\}^{R/K}}{1+g_{n_D}(\gamma_s)}\right]\Bigg|_{L=4} \\ E_{TD}(K,R) &= \log_2\left[\frac{\left\{2^L/\left(1+g_{TD}(\gamma_r)\right)\right\}^{R/K}}{1+g_{n_D}(\gamma_s)}\right]\Bigg|_{L=2} \end{aligned} \tag{4.34}$$

The error exponent indicate that the probability of decoding error decays exponentially with the number of source nodes K and the decaying factor depends on the error exponent. As the rate $K/(K+R)$ increases (or R/K decreases), the error exponent $E(K,R)$ decays linearly with R/K or inverse linearly with rate $K/(K+R)$ The inverse proportion between error exponent $E(K,R)$ and the rate $K/(K+R)$ is commonly known as the fundamental tradeoff between communication reliability and information rate. We note that the mode with larger L has a higher error exponent $E(K,R)$ as illustrated in Fig. 4.8.

As $K, R \to \infty$ while the rate $K/(K+R)$ is held constant, the probability of decoding error can be made arbitrarily small if $E(K,R) > 0$ or equivalently

$$\begin{aligned} \frac{K}{K+R}\Big|_{SM} &< \left[1+\frac{\log_2(1+g_{n_D}(\gamma_s))}{\log_2\left(2^4/(1+g_{SM}(\gamma_r))\right)}\right]^{-1} \\ \frac{K}{K+R}\Big|_{GC} &< \left[1+\frac{\log_2(1+g_{n_D}(\gamma_s))}{\log_2\left(2^4/(1+g_{GC}(\gamma_r))\right)}\right]^{-1} \\ \frac{K}{K+R}\Big|_{TD} &< \left[1+\frac{\log_2(1+g_{n_D}(\gamma_s))}{\log_2\left(2^2/(1+g_{TD}(\gamma_r))\right)}\right]^{-1} \end{aligned} \tag{4.35}$$

The right hand side of (4.35) is called the *achievable rate* in symbols per channel use.

4.5 Numerical Results

In this section we provide numerical results. Fig. 4.2 compares the probability of decoding error $P_E(\mathbf{d})$ obtained from simulation and the union bound in (4.21). The SNR gap between union bound (solid line) and simulation result (dotted line) is about 3 dB at $P_E(\bar{d}) = 10^{-3}$ which is caused by Q-function approximation. This gap can be removed by using tighter bound as follows.

$$\frac{Q(\sqrt{x+y})}{Q(\sqrt{x})} \leq e^{-y/2}, x, y \geq 0 \tag{4.36}$$

Both numerical and simulation shows that TD mode has the highest error probability, whereas SM, GC has virtually identical decoding error probability for $d_{RD} = 0.5$.

Fig. 4.3 shows the probability of decoding error $P_E(\mathbf{d})$ versus E_b/N_0 for different number of receive antennas n_D at the destination. We can see that the red curves with single antenna has diversity order 1, whereas the blue curves with two antennas has diversity order 2 as we analyzed in (4.27).

Fig. 4.4 shows the probability of decoding error $P_E(\mathbf{d})$ versus relay location $d_{r,D}$ when there is a single relay. We find that the error probability of TD mode is larger than that of SM mode and the gap $(P_E(\mathbf{d})_{TD} - P_E(\mathbf{d})_{SM})$ for high SNR is calculated in (4.29). The error probability of GC mode is smaller than that of SM mode when the received SNR at the destination is small ($d_{r,D}$ is large). However, as the received SNR increases ($d_{r,D}$ decreases), the error probability of GC and SM mode becomes virtually identical as we shown in (4.30), (4.31).

Fig. 4.5 shows the probability of decoding error $P_E(\mathbf{d})$ versus E_b/N_0 for 4 different mode selection scenarios when 10 source nodes are assisted by 9 relay nodes. We assume that all relay node use GC mode for case 1, SM mode for case 2 and TD mode for case 3. For case 4, we assume 3 of the relays use SM mode, 3 of the relays use TD mode and the remaining 3 relays use GC mode. The figure shows that using GC mode exclusively provide dominant SNR advantage. At target $P_E(d) = 10^{-8}$, the SNR loss between case 1 and case 2 is 0.3 dB, case 1 and case 4 is 1.2 dB, and case 1 and case 3 is 14.8 dB.

Fig. 4.6 shows the probability of decoding error $P_E(\mathbf{d})$ versus E_b/N_0 for different number of relay nodes R. We can see that the error probability decreases by increasing R and the

decreasing rate $(P_E(\mathbf{d})|_{R=R_0} - P_E(\mathbf{d})|_{R=R_0+1})$ of adding one additional relay is given by

$$\begin{aligned}
&\lim_{\gamma_r\to\infty} \left(P_E(\mathbf{d})|_{R=R_0} - P_E(\mathbf{d})|_{R=R_0+1}\right) \\
&= \lim_{\gamma_r\to\infty} \frac{1}{2}\sum_{w=0}^{K-1}\binom{K}{w}\prod_{i=1}^{K-w}\left[\frac{1}{1+d_{s,(i)}^{-\alpha}\gamma_s}\right]^{n_D}\left[\frac{1}{2^{LR_0}} - \frac{1}{2^{L(R_0+1)}}\right] \\
&= \frac{1}{2}\sum_{w=0}^{K-1}\binom{K}{w}\prod_{i=1}^{K-w}\left[\frac{1}{1+d_{s,(i)}^{-\alpha}\gamma_s}\right]^{n_D}\cdot\frac{1}{2^{LR_0}}\left(1-\frac{1}{2^L}\right)
\end{aligned} \tag{4.37}$$

and this rate diminishes by increasing the number of relays.

Fig. 4.8 shows the error exponent $E(K,R)$ for each transmission mode versus rate $K/(K+r)$. We can see that error exponent of GC and SM is higher than that of TD mode. The achievable rate $K/(K+R)$ are 0.9789 for GC, 0.9780 for SM and 0.9609 for TD mode, which are evaluated by using (4.35).

4.6 Conclusion

We considered randomized linear network coding over multiple antenna multiple access relay channel where multiple sources communicate with a common destination with the help of multiple relays. We assume internode channels are noisy and subject to channel errors. We derived the average probability of decoding error with maximum likelihood decoding at the destination, averaged over all possible encoding rules at the relays. We compared the decoding error probability for each transmission mode to find the optimal mode selection scheme for MARC with random linear network coding. We provided asymptotic analysis of the error probability and examine the *reliability-rate* tradeoff for each transmission mode. The insight provided by the analysis would be of great importance for understanding the fundamental tradeoffs of random network coding in MIMO multiple-access relay networks.

Table 4.1 Eigenvalues of $\Delta X_{RD} \cdot \Delta X_{RD}^{H}$ for SM and GC mode

$v_{a,l} \oplus v_{b,l}$	SM Mode		GC Mode	
$l = (1,2,3,4)$	λ_1	λ_2	λ_1	λ_2
0 0 0 0	0	0	0	0
0 0 0 1	$4E_r$	0	$\frac{4\theta E_r}{\sqrt{5}}$	$\frac{-4\bar{\theta} E_r}{\sqrt{5}}$
0 0 1 0	$4E_r$	0	$\frac{4\theta E_r}{\sqrt{5}}$	$\frac{-4\bar{\theta} E_r}{\sqrt{5}}$
0 1 0 0	$4E_r$	0	$\frac{4\theta E_r}{\sqrt{5}}$	$\frac{-4\bar{\theta} E_r}{\sqrt{5}}$
1 0 0 0	$4E_r$	0	$\frac{4\theta E_r}{\sqrt{5}}$	$\frac{-4\bar{\theta} E_r}{\sqrt{5}}$
0 0 1 1	$8E_r$	0	$\frac{4(1+2\theta) E_r}{\sqrt{5}}$	$\frac{-4(1+2\bar{\theta}) E_r}{\sqrt{5}}$
0 1 0 1	$8E_r$	0	$\frac{4(\sqrt{5}+\sqrt{3}) E_r}{\sqrt{5}}$	$\frac{4(\sqrt{5}-\sqrt{3}) E_r}{\sqrt{5}}$
1 0 0 1	$4E_r$	$4E_r$	$\frac{4(\sqrt{5}+\sqrt{3}) E_r}{\sqrt{5}}$	$\frac{4(\sqrt{5}-\sqrt{3}) E_r}{\sqrt{5}}$
0 1 1 0	$4E_r$	$4E_r$	$\frac{4(\sqrt{5}+\sqrt{3}) E_r}{\sqrt{5}}$	$\frac{4(\sqrt{5}-\sqrt{3}) E_r}{\sqrt{5}}$
1 0 1 0	$8E_r$	0	$\frac{4(\sqrt{5}+\sqrt{3}) E_r}{\sqrt{5}}$	$\frac{4(\sqrt{5}-\sqrt{3}) E_r}{\sqrt{5}}$
1 1 0 0	$8E_r$	0	$\frac{4(1+2\theta) E_r}{\sqrt{5}}$	$\frac{-4(1+2\bar{\theta}) E_r}{\sqrt{5}}$
1 1 1 0	$(6+2\sqrt{5}) E_r$	$(6-2\sqrt{5}) E_r$	$\left(6+\sqrt{\frac{148}{5}}\right) E_r$	$\left(6+\sqrt{\frac{148}{5}}\right) E_r$
1 1 0 1	$(6+2\sqrt{5}) E_r$	$(6-2\sqrt{5}) E_r$	$\left(6+\sqrt{\frac{148}{5}}\right) E_r$	$\left(6+\sqrt{\frac{148}{5}}\right) E_r$
1 0 1 1	$(6+2\sqrt{5}) E_r$	$(6-2\sqrt{5}) E_r$	$\left(6+\sqrt{\frac{148}{5}}\right) E_r$	$\left(6+\sqrt{\frac{148}{5}}\right) E_r$
0 1 1 1	$(6+2\sqrt{5}) E_r$	$(6-2\sqrt{5}) E_r$	$\left(6+\sqrt{\frac{148}{5}}\right) E_r$	$\left(6+\sqrt{\frac{148}{5}}\right) E_r$
1 1 1 1	$16E_r$	0	$\frac{4(2\sqrt{5}+3\sqrt{2}) E_r}{\sqrt{5}}$	$\frac{4(2\sqrt{5}-3\sqrt{2}) E_r}{\sqrt{5}}$

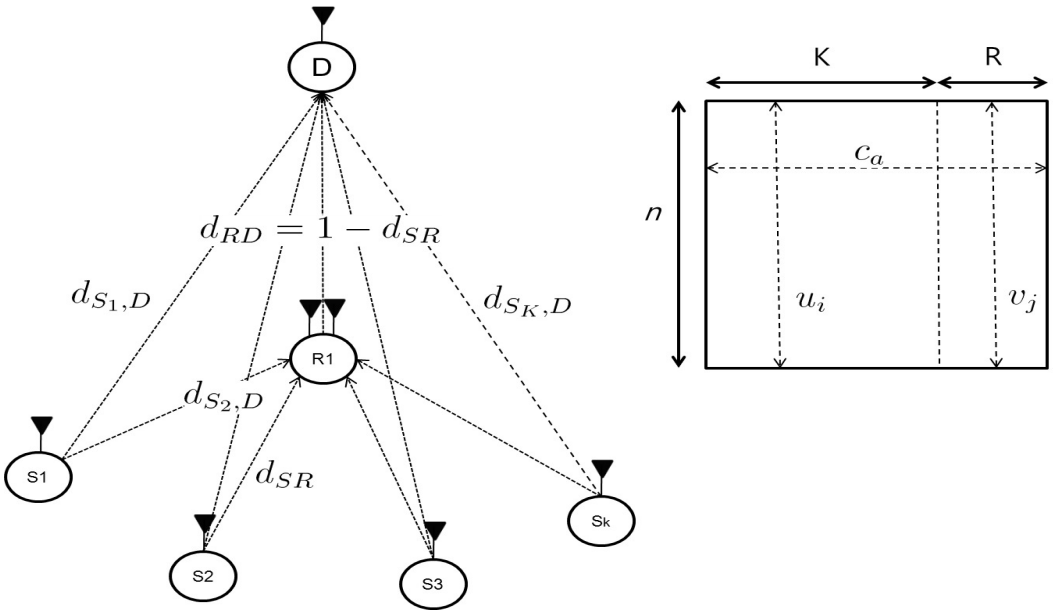

Figure 4.1 Symmetric Multiple Access Relay Channel

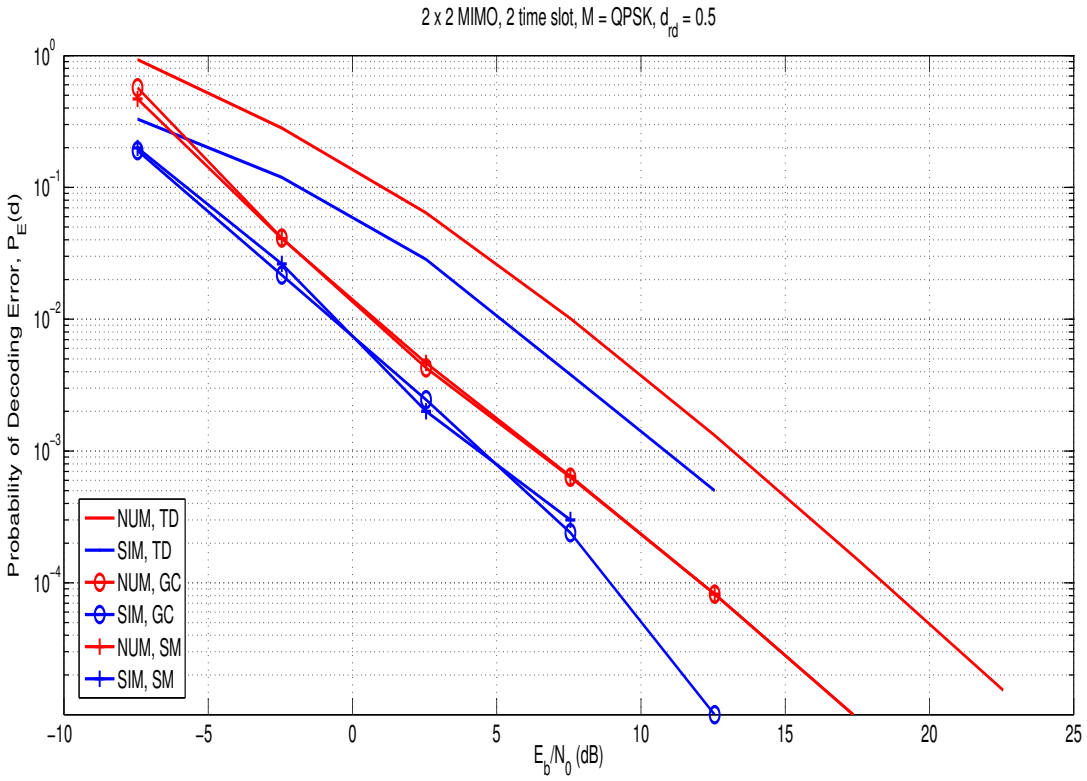

Figure 4.2 Probability of decoding error P_E versus E_b/N_0, simulation versus union bound: $K = 5$, $R = 1$, $\alpha = 4$, $\gamma_s = \gamma_r$, $d_{r,D} = 0.5$, $n_D = 2$

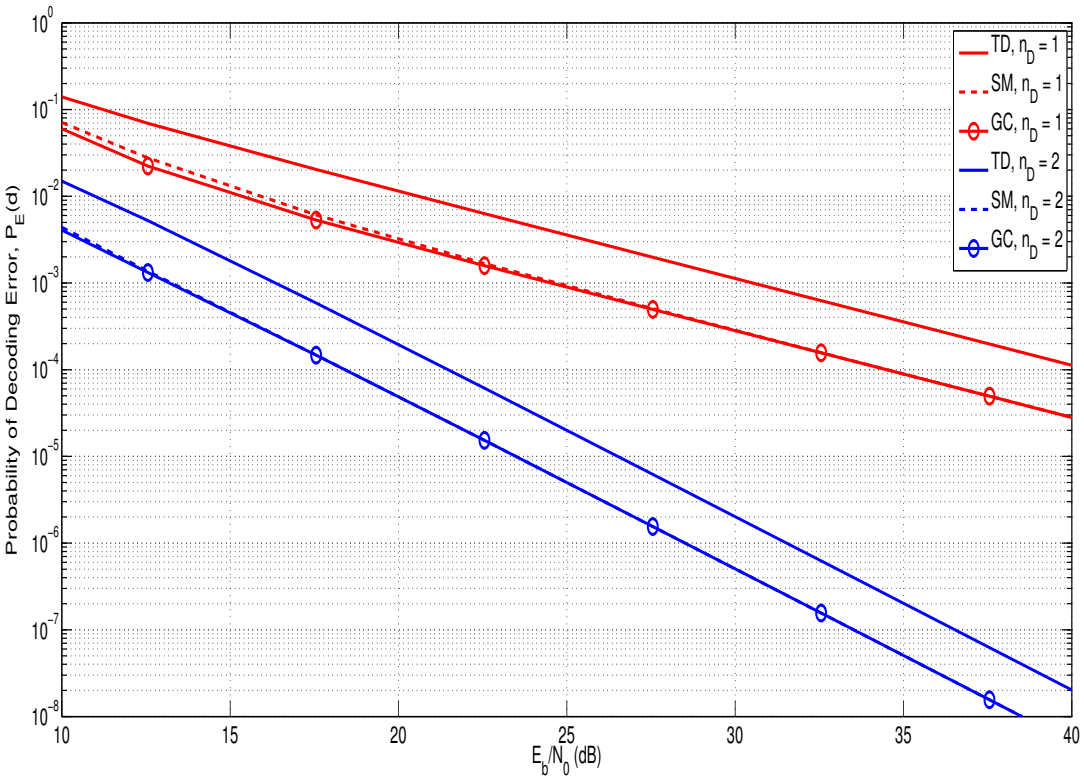

Figure 4.3 Probability of decoding error P_E versus E_b/N_0 for different number of receive antennas n_D at the destination: $K = 5$, $R = 1$, $\alpha = 4$, $\gamma_s = \gamma_r$, $d_{r,D} = 0.5$

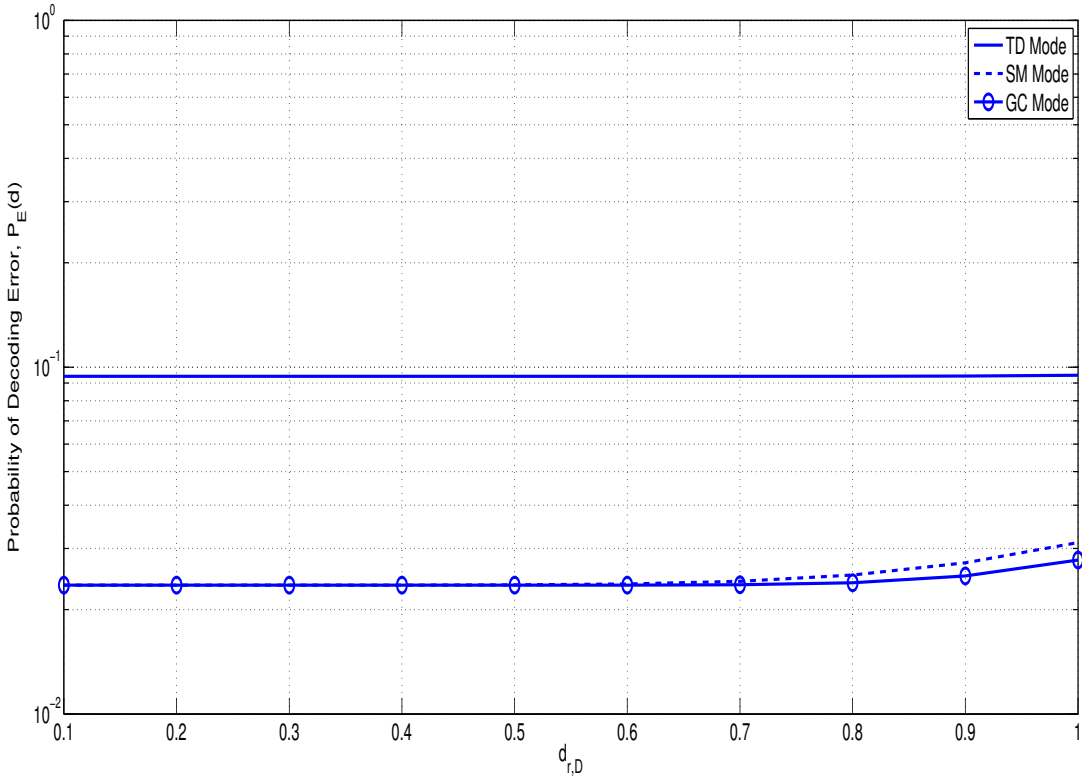

Figure 4.4 Probability of decoding error P_E versus relay location $d_{r,D}$: $K = 5$, $R = 1$, $\alpha = 4$, $\gamma_s = \gamma_r = 5$ dB, $n_D = 2$

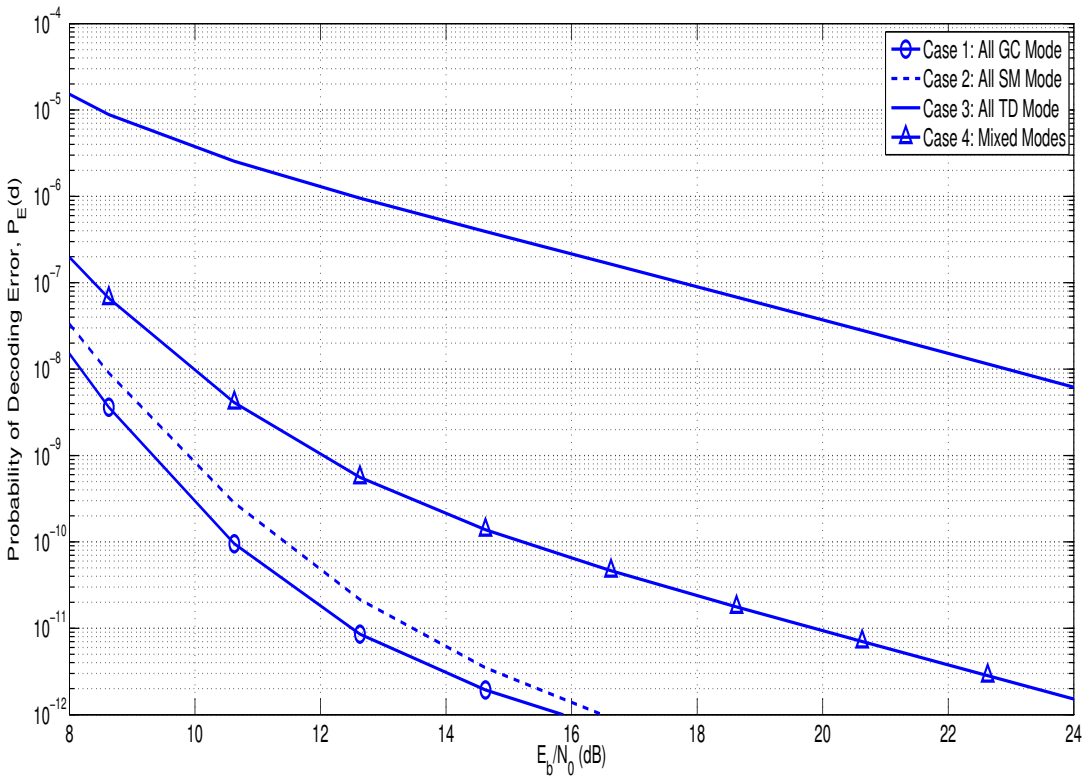

Figure 4.5 Probability of decoding error P_E versus E_b/N_0 for 4 different mode selection scenarios: $K = 10$, $R = 9$, $\alpha = 4$, $\gamma_s = \gamma_r$, $n_D = 2$, $d_{r,D} = 1$

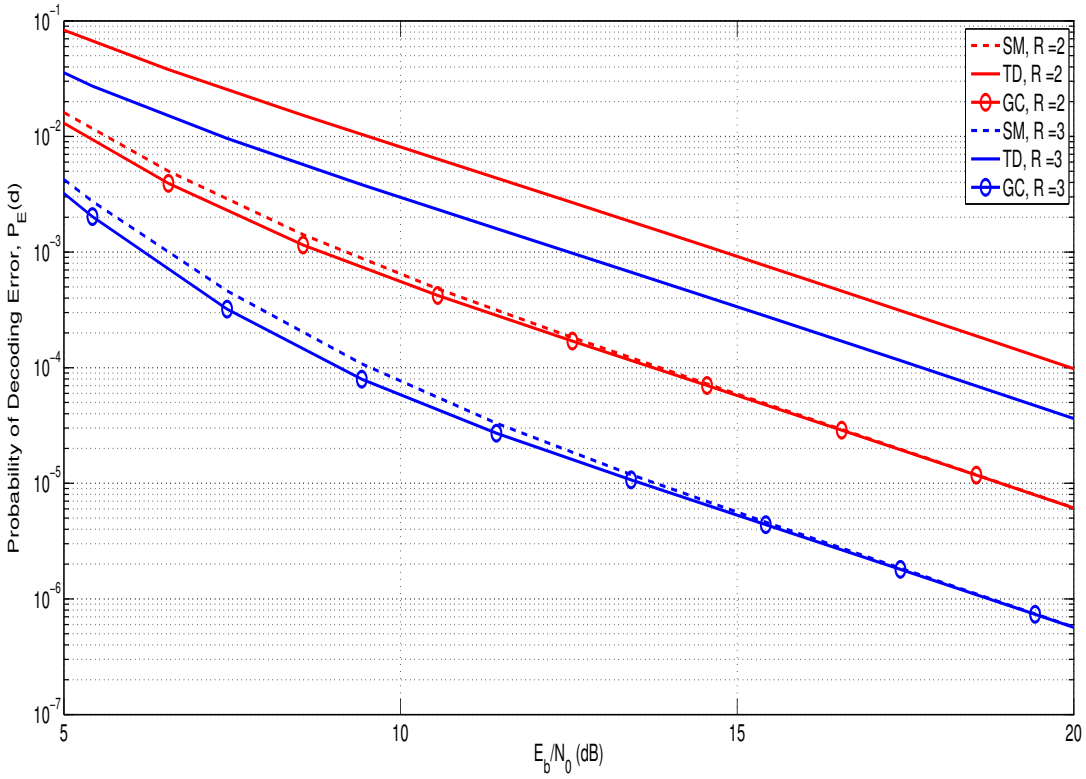

Figure 4.6 Probability of decoding error P_E versus E_b/N_0 for different number of relay nodes R: $K = 10$, $\alpha = 4$, $\gamma_s = \gamma_r$, $n_D = 2$, $d_{r,D} = 1$

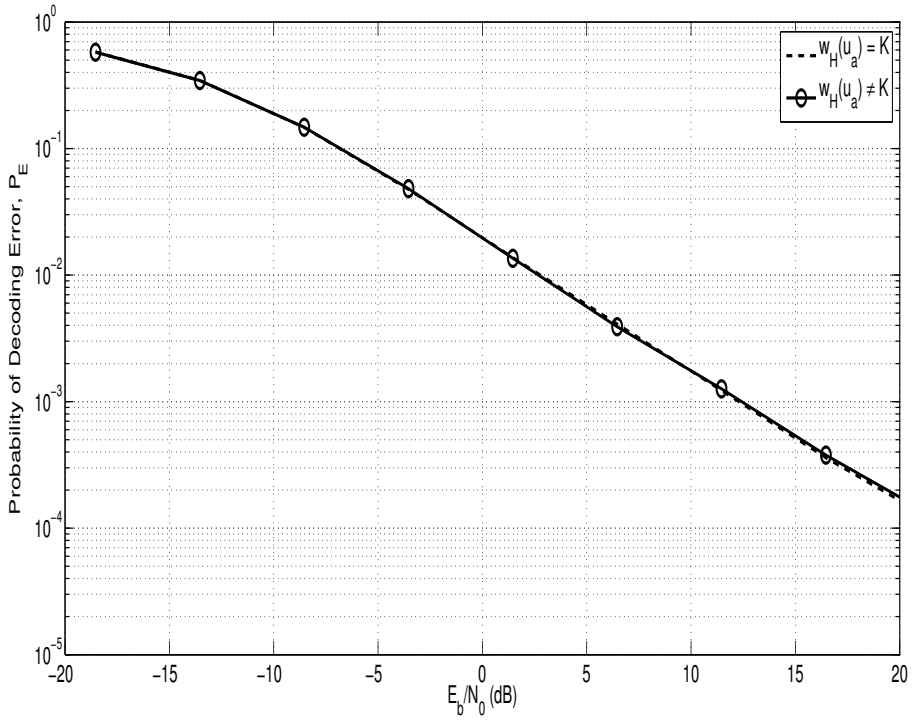

Figure 4.7 Probability of decoding error P_E versus E_b/N_0 for codewords with different Hamming weight: $K = 5$, $R = 2$, $\alpha = 4$, $\gamma_s = \gamma_r$, $n_D = n_R = 1$

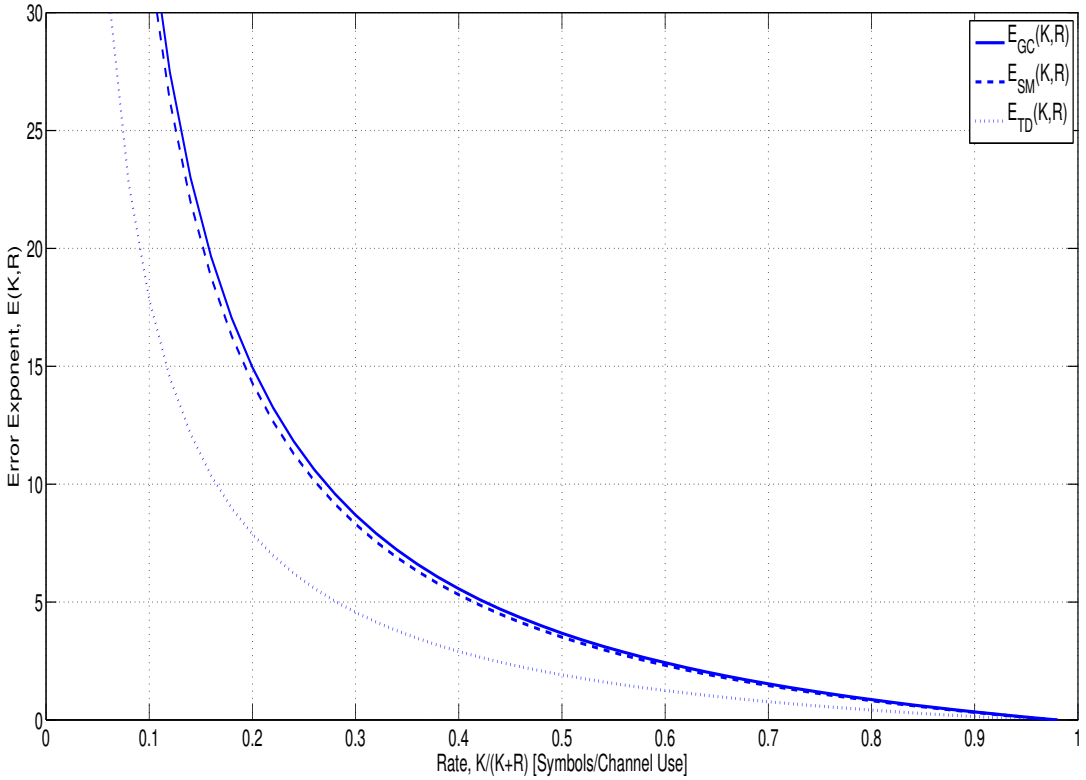

Figure 4.8 Error exponent $E(K,R)$ versus rate $K/(K+R)$: $\alpha = 4$, $\gamma_s = \gamma_r = 5$ dB, $n_D = 2$

CHAPTER 5. INTERFERENCE CANCELLATION IN MULTI-USER MIMO SYSTEMS

In this chapter, we analyze log-likelihood-ratio (LLR) ordered successive interference cancellation (SIC) scheme in multi-user, multi-mode, multi-input multi-output (MIMO) systems where each user may choose between two operation modes: spatial multiplexing or beamforming. The main idea is to detect and cancel the user signal in order of LLR which provides *a posteriori* information about the reliability of detection. The simulation results indicate that LLR-ordered SIC provides $1 \sim 3$dB gain over the conventional SNR-ordered SIC in multiuser MIMO system and the gain increases with increasing number of users. The impact of the knowledge of transmit mode at the receiver and the knowledge of the optimum transmit mode at the transmitter is analyzed in different SIC schemes.

5.1 Introduction

Recently, there has been considerable research in exploiting the space dimension through transmit diversity, space-time coding, and spatial multiplexing that employ multiple transmit and/or receive antennas [58]. Spatial multiplexing enables a high data rate, whereas diversity enables a high reliability. In multi-user environment, receiver antenna arrays have long been recognized as an effective technique for mitigating co-channel interference (CCI) [59]. The value of CCI mitigation is that it enables a better frequency reuse and hence improves the spectrum efficiency. That is, different users may simultaneously transmit in the same frequency band.

One popular method to mitigate CCI is successive interference cancellation (SIC) which is composed of three parts: nulling, cancelling, and ordering. The conventional SIC detects the user signal that provides the maximum signal-to-noise ratio (SNR) and cancels the correspond-

ing user from the received signal, updates the channel matrix, and repeats this process until all user signals are detected [60]. In reference [61], a new ordering technique based on the log-likelihood ratio (LLR) is proposed in single user case. The difference between LLR ordering and SNR ordering is that the former uses *a posteriori* information about the reliability of detection, thereby minimizes the effect of error propagation. Use of this additional *a posteriori* information is known to provide a significant SNR gain over the conventional SNR based ordering. In this paper, we extend the analysis to *multi-mode, multi-user* MIMO case, where each user may choose to use either spatial multiplexing (SM) or beamforming (BF) for transmission. Mode selection between SM and transmit diversity in point-to-point (single user) communication has been discussed in [62]. We investigate the impact of the knowledge of transmit mode at the receiver and the knowledge of transmit mode at the transmitter in different SIC schemes.

This chapter is organized as follows. Section II describes the system model. Section III describes LLR-ordered SIC, SNR-ordered SIC, and computational complexity analysis. Section IV presents an adaptive operation mode selection methodology. Section V presents the simulation results, and Section VI contains concluding remarks.

5.2 System model

We consider a synchronous multi-access communication system in which K users send independent messages to a common receiver (e.g. uplink cellular). The system block diagram is shown in Figure 5.1. Each user, equipped with n_t antennas, transmits simultaneously over the same frequency band to a common receiver equipped with n_r receive antennas. The channel matrix for user k is denoted by H_k which is an $n_r \times n_t$ matrix with each element modeled by a complex Gaussian random variable with mean zero and variance 0.5 per dimension, and the overall channel matrix is denoted by $H = [H_1, H_2, \cdots, H_K]$.

The received signal is then given by

$$Y = \sum_{k=1}^{K} H_k X_k + W \tag{5.1}$$

where X_k is an $n_t \times 1$ matrix representing the transmitted signal of user k and W is a $n_r \times 1$ matrix representing the complex Gaussian noise with each component having mean zero and

variance $N_0/2$ per dimension.

We assume that the receiver knows the channel matrix H, but user k knows H_k only. We assume that $K/2$ users (randomly selected) are in SM mode and the remaining $K/2$ users are in BF mode for data transmission. In Section IV, we will consider the case where the receiver informs each transmitter of appropriate mode of operation to further reduce the probability of error. In SM mode different symbols are transmitted through different antenna, whereas in BF mode the same symbol is transmitted through different antenna with different weightings. We assume that users in SM mode use M-ary modulation and those in BF mode use M^{n_t}-ary modulation to maintain the same transmission rate of $n_t \times \log_2 M$ bits per symbol time. We assume that the mode of operation of each user is known at the receiver, which can be indicated in the packet header.

Since K users transmit simultaneously, each user experiences $n_T - n_t$ interfering signals, where $n_T = K \times n_t$. We assume that there are $n_r (\geq n_T - n_t + 1)$ receive antennas to suppress $n_T - n_t$ interfering signals. If we let $\Lambda(k) = [H_1, H_2, \cdots, H_{k-1}, H_{k+1}, \cdots, H_K]$ and $\mathcal{N}$ be the null space of $\Lambda(k)$, then $dim(\mathcal{N}) + rank[\Lambda(k)] = n_r$ [63]. Since $rank[\Lambda(k)] \leq n_T - n_t$, we obtain $dim(\mathcal{N}) \geq n_r - n_T + n_t$. Hence, we can find a set of orthonormal matrix $V_k = [v_1^T, v_2^T, \cdots, v_{n_r - n_T + n_t}^T]^T$ for user k, where each component v_i is an $n_r \times 1$ column vector, that satisfies the following two properties:

$$V_k (V_k)^H = I_{n_r - n_T + n_t} \tag{5.2}$$

$$V_k H = V_k H_k. \tag{5.3}$$

Multiplying V_k to both sides of (5.1) yields

$$Z_k = V_k Y = V_k H_k X_k + V_k W \tag{5.4}$$

where the equality follows from (5.3). Thus, all users in the set $\{1, 2, \cdots, k-1, k+1, \cdots, K\}$ are suppressed and only the signal from user k remains. Since V_k is unitary and W is circular symmetric, the distributions of W and $V_k W$ are the same, but their dimensions can be different.

Then, the maximum likelihood (ML) estimate of X_k for users in SM mode after user sepa-

ration is given by

$$\hat{X}_k = \arg\min_{\underline{s}_m} ||Z_k - V_k H_k \underline{s}_m||^2. \tag{5.5}$$

where $\underline{s}_m$ is an $n_t \times 1$ matrix representing the transmitted vector. Beamforming exploits only the dominant mode of the channel, so the transmitter performs the singular value decomposition ($H_k = U_1 \Lambda U_2^H$) on the channel matrix which is assumed to be known at the transmitter for users in BF mode. Let $\sigma_{\max}$ be the maximum of singular values $\lambda_1, \lambda_2, ..., \lambda_r$ of H_k, where r is the rank of H_k, and i^* be the argument of $\max\{\lambda_i\}$. Let u_{1,i^*} and u_{2,i^*} be the i^*th column of U_1 and U_2, respectively. Then the transmitted vector X_k for users in BF mode is $u_{2,i^*} s_m$, where s_m is the transmitted symbol [64]. Multiplying $u_{1,i^*}^H N$, where $N = H_k((V_k H_k)^H (V_k H_k))^{-1}(V_k H_k)^H$ is the nulling vector, to (5.4) yields

$$Z_k^{'} = u_{1,i^*}^H N \cdot Z_k = \sigma_{\max} s_m + W^{'}. \tag{5.6}$$

The noise term in (5.6) is a complex Gaussian with mean zero and variance $N_0 \cdot ||u_{1,i^*}^H N||^2$. Hence, the ML estimate of X_k for users in BF mode is given by

$$\hat{X}_k = \arg\min_{s_m} |Z_k^{'} - \sigma_{\max} s_m|^2. \tag{5.7}$$

After detecting X_k, the estimate of X_k, $\hat{X}_k$, is canceled from Y to yield

$$Y^{(1)} = Y - H_k \widehat{X}_k. \tag{5.8}$$

Then, we update the channel matrix $H^{(1)} = [H_1, H_2, \cdots, H_{k-1}, H_{k+1}, \cdots, H_K]$ and the corresponding null space.

5.3 Successive Interference Cancellation Ordering

In this section, we describe SIC ordering methods, assuming that the receiver is informed of the transmitter's mode of operation.

5.3.1 LLR-based Ordering

The conditional error probability given Z_k in SM mode (or $Z_k^{'}$ in BF mode) is given by [61]

$$P(\hat{X}_k \neq X_k | Z_k) = 1 - \frac{1}{\sum_m e^{-\Lambda_{k,m}}} \tag{5.9}$$

where

$$\begin{aligned}\Lambda_{k,m} &= \ln \frac{p(X_k = \hat{X}_k|Z_k)}{p(X_k = \underline{s}_m|Z_k)} \\ &= \frac{||Z_k - V_k H_k \underline{s}_m||^2 - ||Z_k - V_k H_k \hat{X}_k||^2}{N_0}\end{aligned} \tag{5.10}$$

is the pairwise LLR. Similarly, in BF mode

$$\Lambda_{k,m} = \frac{|Z_k' - \sigma_{\max} s_m|^2 - |Z_k' - \sigma_{\max} \hat{X}_k|^2}{N_0 N'} \tag{5.11}$$

where $N' = ||u_{1,i^*}^H N||^2$. The LLR-based SIC ordering is to detect and cancel in order of minimizing $P(\hat{X}_k \neq X_k|Z_k)$ or equivalently minimizing $\sum_m e^{-\Lambda_{k,m}}$. This approach, utilizing *a posteriori* information Z_k in SM mode (or Z_k' in BF mode), can reduce the effect of error propagation.

5.3.2 SNR-based Ordering

The SNR-ordered SIC is to detect and cancel in order of minimizing $P(\hat{X}_k \neq X_k)$. It follows from (5.4) that the average probability of error in SM mode is bounded by

$$P(\hat{X}_k \neq X_k) \leq \sum_{\underline{x}_j \neq \underline{x}_i} Q\Big(\frac{||V_k H_k(\underline{x}_i - \underline{x}_j)||}{\sqrt{2N_0}}\Big) \tag{5.12}$$

$$\leq (M^{n_t} - 1) Q\Big(\frac{d_{\min}(V_k H_k)}{\sqrt{2N_0}}\Big) \tag{5.13}$$

where $d_{\min}(V_k H_k) = \min_{\underline{x}_i \neq \underline{x}_j} ||V_k H_k(\underline{x}_i - \underline{x}_j)||$. Similarly, in BF mode, the average probability of error is bounded by (5.13) with $d_{\min}(V_k H_k)$ replaced by $d_{\min}(\sigma_{\max})/\sqrt{N'} = \min_{x_i \neq x_j} |\sigma_{\max}(x_i - x_j)|/\sqrt{N'}$. Therefore, the SNR-ordered SIC is to detect and cancel users in order of maximizing $d_{\min}(V_k H_k)$ in SM mode or $d_{\min}(\sigma_{\max})/\sqrt{N'}$ in BF mode.

5.3.3 Computational Complexity Analysis

The computational complexities of the LLR-ordered SIC, the SNR-ordered SIC, and the maximum-likelihood (ML) detection are compared in Table 5.1. The main computation in SIC is the determination of the null space V_k for all users. The computational complexity in calculating V_k is $O(n_r n_t^2 K^2)$. This follows from the fact that the computational complexity of

Gram-Schmidt orthogonalization of $m \times n$ matrix is $O(mn^2)$ [65] and that the channel matrix H is $n_r \times Kn_t$. Since V_k needs to be calculated for all K users and iterated K times for successive cancellation, the overall complexity of the SNR-based SIC is on the order of $O(n_r n_t^2 K^4)$. For the LLR-ordered SIC, ordering needs to be recalculated for each symbol interval because *a posteriori* information Z_k changes for each symbol interval. So, if the channel changes every L symbol intervals, then the LLR-ordered SIC is about L times more complex than the SNR-ordered SIC. For ML detection of $\min_{\{X_k\}} ||Y - \sum_{k=1}^{K} H_k X_k||^2$, the computational complexity in calculating $\sum_{k=1}^{K} H_k X_k$ is of order $O(n_r n_t K)$ and the number of comparisons involved in finding the minimum is on the order of $O(M^{n_t K})$, yielding the overall complexity of $O(n_r n_t K M^{n_t K} L)$.

5.4 Adaptive Transmit Mode Selection

In this section, we consider the case where the receiver determines an appropriate mode of operation for each user based on the channel matrix H (obtained by using pilot symbols from each user) and informs it to all users such that they can adapt their mode of operation. The required amount of feedback information is 1 bit per user when each user is allowed to choose either SM or BF mode at a time. We assume that this information is sent to each user without error.

The mode selection criterion is as follows. It is shown in (5.13) that the union bound on $P(\hat{X}_k \neq X_k)$ is determined by a single parameter: $d_{\min}(V_k H_k)$ for the SM mode and $d_{\min}(\sigma_{\max})/\sqrt{N'}$ for the BF mode. Hence, the receiver computes $d_{\min}(V_k H_k)$ and $d_{\min}(\sigma_{\max})/\sqrt{N'}$ and chooses the SM mode if $d_{\min}(V_k H_k) \geq d_{\min}(\sigma_{\max})/\sqrt{N'}$, and, otherwise, chooses the BF mode for user k.

If the channel changes every L symbol intervals, the mode selection will be updated once every L symbol intervals. Computational complexity of $d_{\min}(V_k H_k)$ and $d_{\min}(\sigma_{\max})/\sqrt{N'}$ grows linearly only with K. Hence, it can be ignored compared to the computational complexity of SIC.

5.5 Simulation Results

In this section, we present the numerical results obtained by performing Monte Carlo simulation with MATLAB. Figure 5.3 shows the average bit error rate (BER) versus the bit SNR per receive antenna for several number of users and receive antennas. Each user has two transmit antennas. The simulation result shows that the power gain that the LLR-ordered SIC provides over the SNR-ordered SIC is more significant with larger number of users: the power gain is 1.18dB for two users, 2.40dB for four users and 2.92dB for six users.

Figure 5.4 is a plot of the average BER versus bit SNR per receive antenna when the number of receive antenna is fixed. Each user has two transmit antennas and the receiver has eight receive antennas. Similar observation can be made as in Fig. 5.3. The power gains are 0.44dB with two users and 2.50dB with four users.

Figure 5.5 is a plot of the average BER versus bit SNR per receive antenna with several detection methods. Each user has two transmit antennas and the receiver has eight receive antennas. The simulation result shows that the SNR loss of LLR-ordered SIC against ML detection is 4dB, and the SNR gain against the SNR-ordered SIC is 2.5dB at BER $= 10^{-3}$. However, the computational complexity of the ML detection grows with $K \cdot M^{n_t K}$ whereas that of LLR-ordered SIC grows with K^4 only. Also, shown in the figure is the average BER with SNR-ordered SIC without knowing the transmit mode of operation of each user (denoted by Sub SNR-SIC), in which case the cancellation order is determined based on the SNR given by $\|V_k H_k X_k\|^2 / E[\|V_k W\|^2]$, which follows from (5.4). We find that the knowledge of transmit mode at the receiver, that requires 1 bit transmission from each transmitter to the receiver, can significantly improve the performance.

Figure 5.7 is a plot of the average BER versus bit SNR per receive antenna for several values of L with the SNR-SIC scheme, where L is the number of symbols for which the channel state remains constant. We find that the SNR gain that the adaptive mode selection provides over the random mode section grows with L: the SNR gains at BER of 10^{-3} are 1.70dB and 4.22dB for $L = 5$ and $L = 20$, respectively. This is because the random mode selection requires the user to remain in the selected mode for at least L symbol intervals even though it is not

optimal. This makes a larger performance loss against the optimal mode selection with larger L (slower fading channel).

Figure 5.6 is a plot of the average BER versus bit SNR per receive antenna with random and adaptive mode selection. Each user has two transmit antennas and the receiver has eight receive antennas. The simulation result shows that the adaptive selection provides a SNR gain of 1.2dB against the random selection at BER = 10^{-3} at the cost of sending 1 bit of feedback information on the optimum mode of operation for each user by the receiver. The SNR gain from the adaptive mode selection is even more significant in Sub SNR-SIC case where the receiver does not utilize the transmit mode information in SIC ordering. It is interesting to note that knowing the transmit mode at the receiver (SNR-SIC (random)) is more helpful in reducing the BER than knowing the optimum transmit mode at the transmitter (Sub SNR-SIC (adaptive)). The former requires each transmitter to send 1 bit of information (SM,BF) to the receiver, while the latter requires the receiver to send 1 bit of information (SM,BF) to each transmitter. In both cases the amount of information exchanges is identical.

5.6 Conclusion

In this chapter, we proposed a new detection ordering for successive interference cancellation in a multi-user, multi-mode MIMO system, where each user may simultaneously transmit in either spatial multiplexing or beamforming mode to a common receiver. The receiver decides the order of detection based on the LLR, which provides *a posteriori* information on reliability of detection. The proposed approach, exploiting this additional information, can provide a SNR gain of $1 \sim 3$dB over the conventional SNR-ordered successive interference cancellation and the SNR gain is more significant with increasing number of users. We provided computational complexity analysis of the considered detection methods. We also presented an adaptive mode selection scheme which provides $1 \sim 2$dB SNR gain against the random mode selection scheme. The impact of the knowledge of transmit mode at the receiver and that of the knowledge of the optimum transmit mode at the transmitter has been analyzed in different SIC schemes.

Table 5.1 Comparison of Computational complexities

Computational complexity	
LLR-ordered SIC	$O\left(n_r n_t^2 K^4 L\right)$
SNR-ordered SIC	$O\left(n_r n_t^2 K^4\right)$
ML detection	$O\left(n_r n_t K L M^{n_r K}\right)$

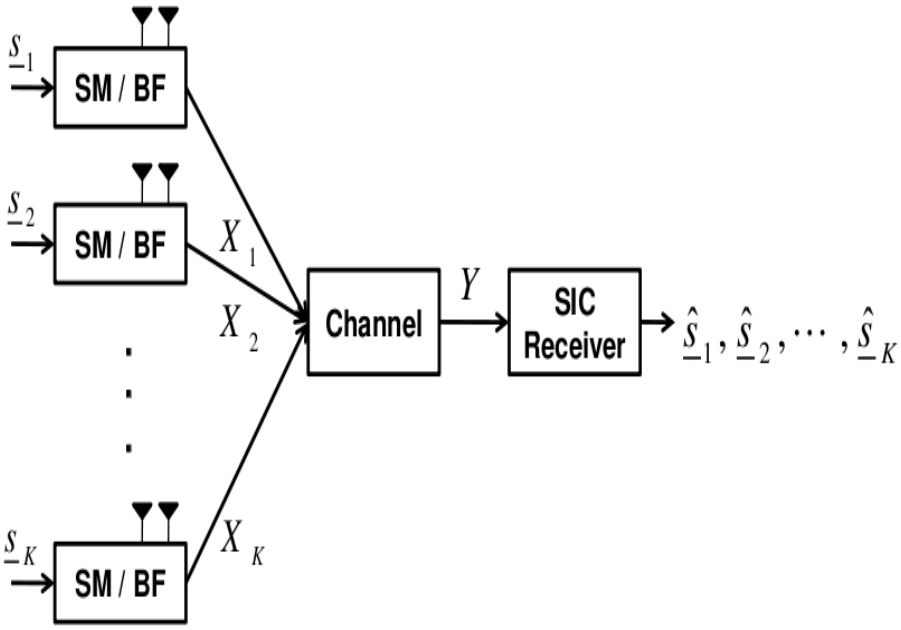

Figure 5.1 Multi-user, multi-mode MIMO System.

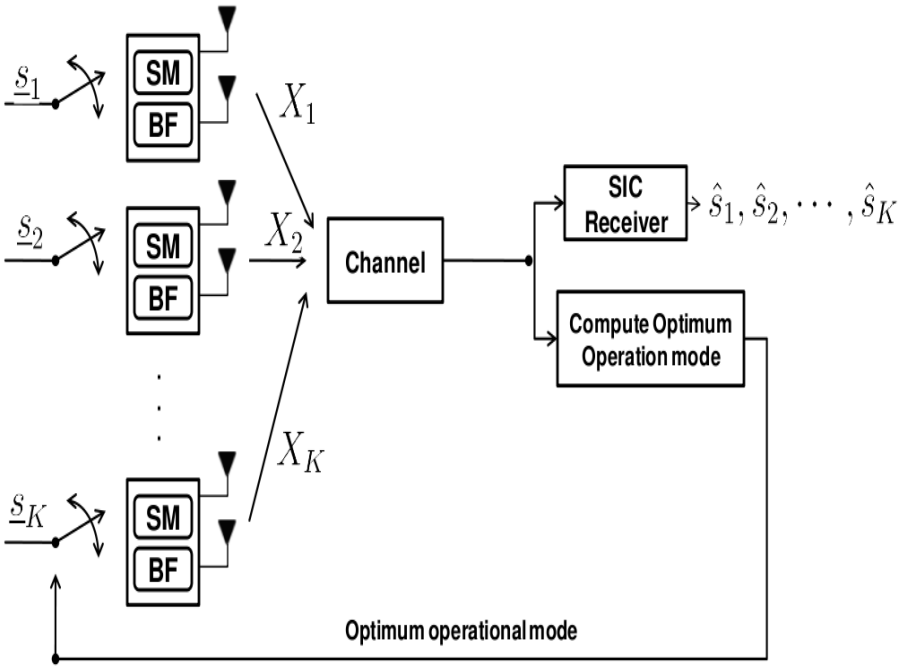

Figure 5.2 Multi-user MIMO System with adaptive transmit mode selection.

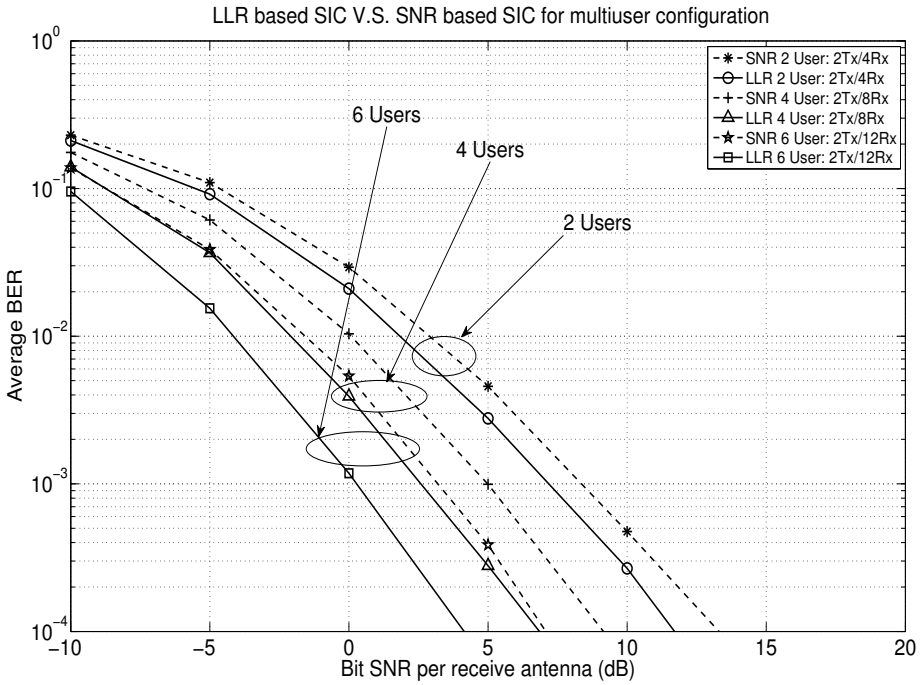

Figure 5.3 Average BER versus bit SNR per receive antenna for different number of users, $M = 2$.

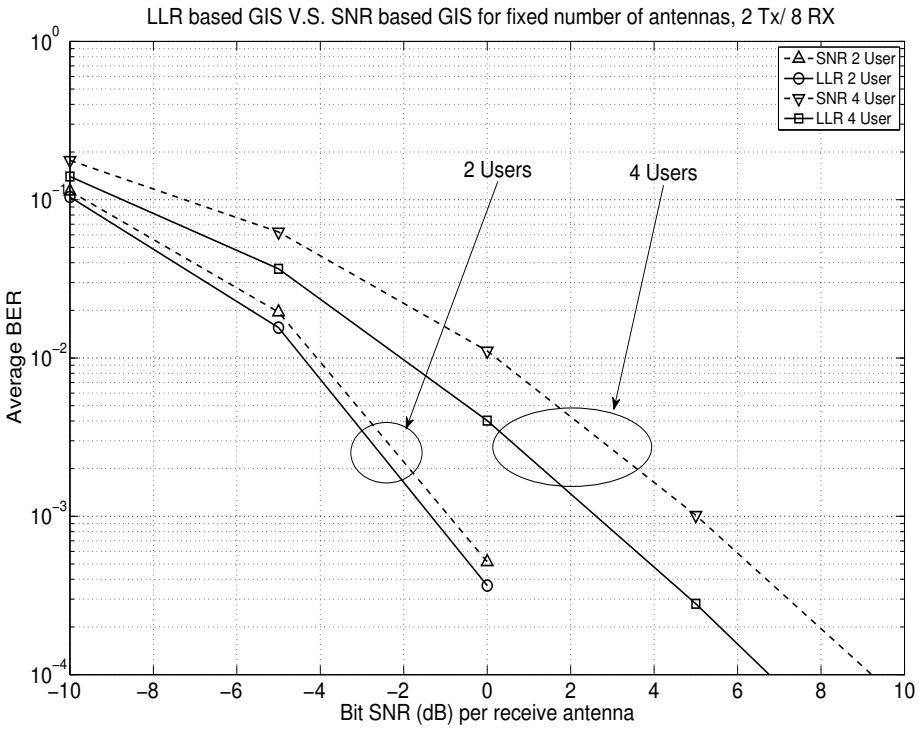

Figure 5.4 Average BER versus Bit SNR for fixed number of antennas, $n_t = 2$, $n_r = 8$, $M = 2$.

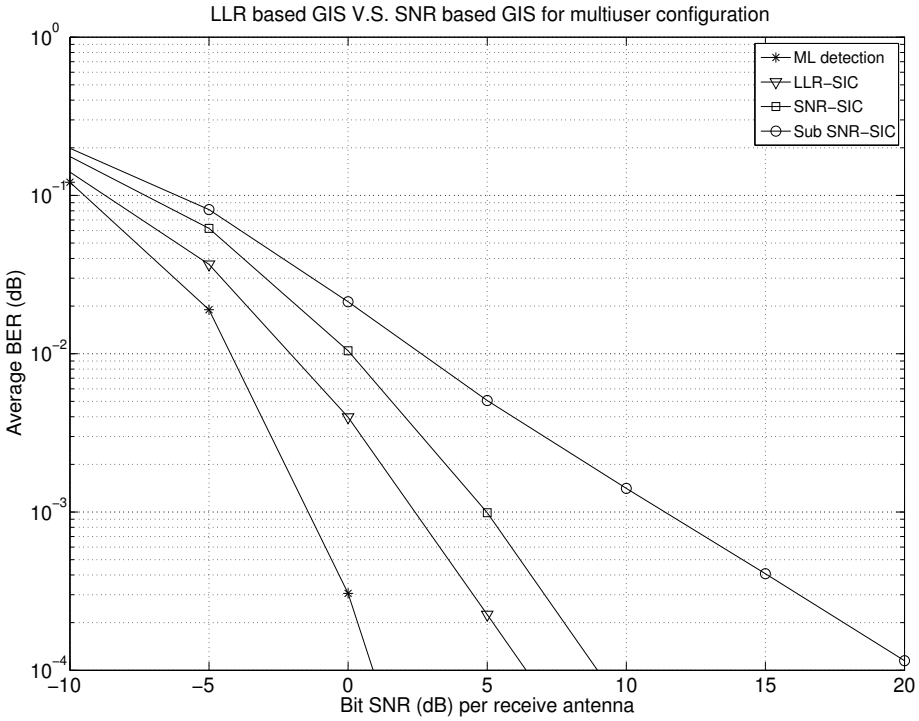

Figure 5.5 Average BER versus received bit SNR with ML detection method, $n_t = 2$, $n_r = 8$, $M = 2$, $K = 4$.

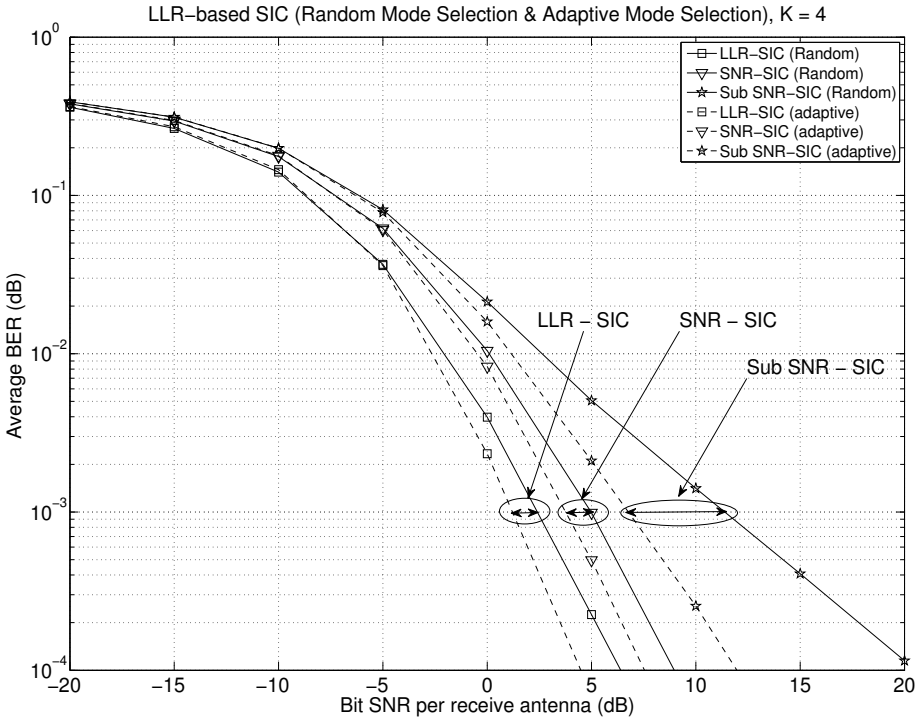

Figure 5.6 Average BER versus received bit SNR for different mode selection methods, $n_t = 2$, $n_r = 8$, $M = 2$, $K = 4$, $L = 4$.

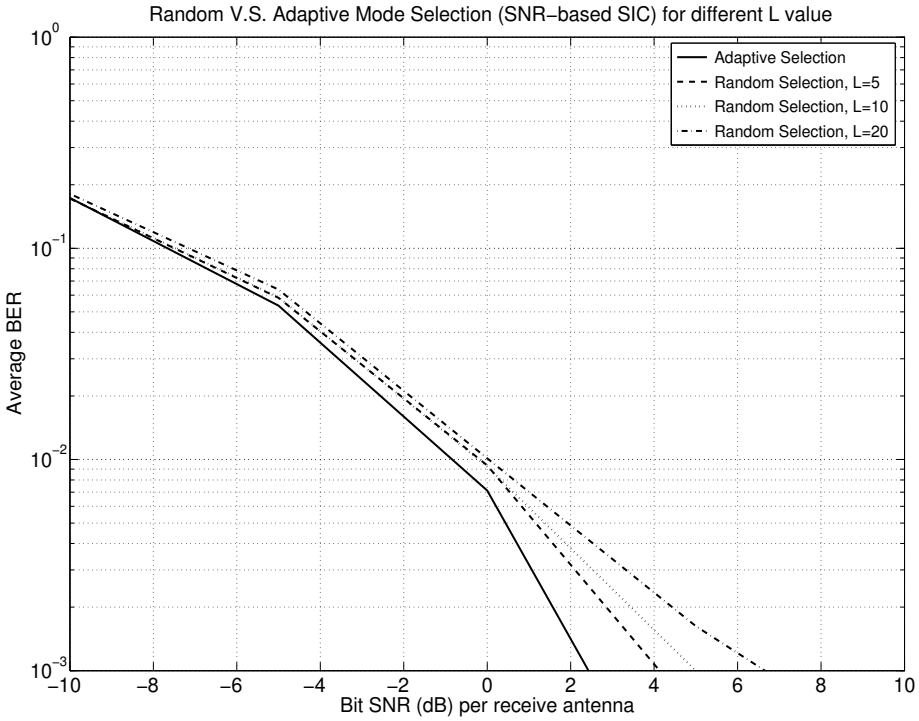

Figure 5.7 Average BER versus received bit SNR for different L values, $n_t = 2$, $n_r = 8$, $M = 2$, $K = 4$.

CHAPTER 6. INTERFERENCE CANCELLATION USING SINGLE RADIO FREQUENCY CHAIN

In this chapter, we present a new architecture for multi-antenna receivers that cancel the co-channel interference (CCI) using a single radio frequency (RF) and baseband (BB) chain, while still achieving nearly the same bit error rate that can be provided by the conventional receiver requiring multiple RF/BB chains. The proposed receiver architecture enables multiple transmitter-receiver pairs to simultaneously communicate in the same frequency band without additional bandwidth, thereby increasing the spectral efficiency or capacity, with significantly reduced receiver complexity and power consumption.

6.1 Introduction

The use of antenna arrays has long been recognized as an effective technique for mitigating co-channel interference (CCI) [66]. The value of CCI mitigation in wireless networks is that it enables to provide a better frequency reuse and hence improves spectrum efficiency. That is, different signals can be simultaneously transmitted in the same frequency band.

If there are K users, each equipped with one antenna, transmitting simultaneously in the same frequency band, the receiver needs at least K antennas to completely cancel $K-1$ interferers and detect the desired signal [66]. This implies that for each CCI source, we need one antenna at the receiver to cancel it. The use of multiple antennas at the receiver requires a radio frequency (RF) chain (low noise amplifier, mixer, and A/D converter) and baseband (BB) chain (matched filter and analog-to-digital converter) for each antenna element, limiting its application to the case of small K and N_T due to a considerable power consumption and chip size for each additional RF/BB chain.

Antenna selection techniques can reduce the need for multiple RF/BB chains. In [67], a soft antenna selection approach that uses a joint RF/BB design is introduced to reduce the number of RF chains. [68] spreads each antenna signals using orthogonal codes and combines them in the analog domain. The combined RF signal is fed to a shared RF/BB chain and digital matched filters are used to recover each signal. However, the use of orthogonal codes expands the bandwidth, which incurs additional power dissipation that grows almost linearly to the bandwidth. [68] also explored the use of non-orthogonal codes to reduce the bandwidth at the cost of performance loss. [69] halves the number of A/D converters in a dual-antenna receiver using complex filtering, but the application is limited to two antennas and is inherently incapable of sharing RF/BB chains.

In this chapter we present a new architecture for multi-antenna receivers that cancel the CCI using a *single* RF/BB chain, while still achieving nearly the same bit error rate that can be provided by the conventional receiver architecture that requires multiple RF/BB chains. The basic idea is to perform the CCI cancellation in the RF domain and then down convert the processed information to the baseband to detect the desired user's data. The proposed receiver architecture enables multiple transmitter-receiver pairs to simultaneously communicate in the same frequency band without additional bandwidth, thereby increasing the spectral efficiency or capacity, with significantly reduced receiver complexity and power consumption. The proposed approach does not involve an antenna selection which loses information that comes through non-selected antennas, thereby suffers from a certain performance loss. Instead, it utilizes all available information that comes through all antennas and processes them at the RF level to reduce the number of RF/BB chains to one.

In Section II, we describe the system model. In Sections III and IV, we describe the conventional receiver architecture and the proposed receiver architecture, respectively. In Section V we present simulation results. In Section VI, concluding remarks are provided.

6.2 System Model

We consider a network of K transmitter-receiver pairs communicating simultaneously in the same frequency band, where each transmitter (Tx) is equipped with one antenna element

and each receiver (Rx) with N_R antenna elements (see Figure 6.1). Extension to N_T antennas per transmitter is straightforward. Example scenarios include wireless ad-hoc networks or peer-to-peer communications in the same frequency band. The channel is assumed to be frequency nonselective and slowly fading, and the fading processes, $\mathbf{h}_1$ and $\mathbf{h}_2$, are assumed to be statistically independent. The signal is corrupted by zero-mean white Gaussian noise. The noise processes are assumed to be statistically independent, with identical autocorrelation functions. Thus, the received RF signal vector, $\tilde{\mathbf{y}}(t) = [\tilde{y}_1(t), \cdots, \tilde{y}_{N_R}(t)]^T$, is given by

$$\tilde{\mathbf{y}}(t) = Re\left\{\left(\sum_{k=1}^{K} \mathbf{h}_k x_k(t) + \mathbf{n}(t)\right) e^{j2\pi f_c t}\right\} \tag{6.1}$$

where $\mathbf{h}_k = [h_{k,1} \cdots, h_{k,N_R}]^T$ denotes the complex channel gain for the k-th transmitter, $x_k(t)$ denotes the low-pass equivalent signal of the k-th transmitter, $\mathbf{n}(t) = [n_1(t), \cdots, n_{N_R}(t)]^T$ denotes the low-pass equivalent complex white Gaussian noise at the receiver, and f_c denotes the carrier frequency. We assume that $h_{k,l}$ and $h_{k,m}$ are independent for $l \neq m$ and $E[|h_{k,l}|^2] = 1$ for all k, l. We assume that the noise $n_i(t)$, $i = 1, 2, \cdots, N_R$ has mean zero and variance N_0.

6.3 Conventional Receiver Architecture

The conventional receiver architecture for detecting the signal of the j-th transmitter is shown in Figure 6.2. The received RF signals are down converted into baseband and then CCI is cancelled in the baseband (BB). If K transmitters, each equipped with one antenna, transmit simultaneously in the same frequency band, then the number of RF/BB chains at the receiver needs to be at least K to completely cancel $K-1$ interferers. For large K, the complexity of the conventional receiver architecture can be prohibitive.

For simplicity of analysis, let us assume that $K = 2, N_T = 1$, and $N_R = 2$. The analysis can be easily extended to arbitrary values of K, N_T, and N_R. The received RF signals can be expressed in the form

$$\tilde{y}_1(t) = Re\{\bar{y}_1(t)e^{j2\pi f_c t}\} \tag{6.2}$$

$$\tilde{y}_2(t) = Re\{\bar{y}_2(t)e^{j2\pi f_c t}\} \tag{6.3}$$

where

$$\bar{y}_1(t) = h_{11}x_1(t) + h_{21}x_2(t) + n_1(t) \tag{6.4}$$

$$\bar{y}_2(t) = h_{12}x_1(t) + h_{22}x_2(t) + n_2(t) \tag{6.5}$$

are the BB signal. The corresponding matched filter outputs are

$$\bar{y}_1 = h_{11}s_1 + h_{21}s_2 + \bar{n}_1 \tag{6.6}$$

$$\bar{y}_2 = h_{12}s_1 + h_{22}s_2 + \bar{n}_2 \tag{6.7}$$

where s_1 and s_2 are the transmitted data of Tx 1 and Tx 2, respectively, and $\bar{n}_j$ is the BB chain output of $n_j(t)$, $j = 1, 2$.

6.3.1 Zero-Forcing Detector

Let

$$H = \begin{bmatrix} h_{11} & h_{21} \\ h_{12} & h_{22} \end{bmatrix} \tag{6.8}$$

be the channel matrix. Then the zero-forcing (ZF) matrix

$$\begin{aligned} W_{ZF} &= (H^H H)^{-1} H^H \\ &= \begin{bmatrix} w_{11} & w_{21} \\ w_{12} & w_{22} \end{bmatrix} \end{aligned} \tag{6.9}$$

makes $WH = I$ [70]. Applying W_{ZF} to the BB chain outputs

$$\begin{aligned} \bar{\mathbf{y}} &= [\bar{y}_1 \bar{y}_2]^T \\ &= H[s_1 s_2]^T + [\bar{n}_1 \bar{n}_2]^T \end{aligned} \tag{6.10}$$

yields

$$\begin{bmatrix} z_1 \\ z_2 \end{bmatrix} = \begin{bmatrix} s_1 \\ s_2 \end{bmatrix} + W_{ZF} \begin{bmatrix} \bar{n}_1 \\ \bar{n}_2 \end{bmatrix} \tag{6.11}$$

which follows from the property $W_{ZF}H = I$. The ZF detector completely eliminates CCI at the expense of noise enhancement.

6.3.2 MMSE Detector

The minimum mean square error (MMSE) detector [70], balancing CCI mitigation with noise enhancement, calculates MMSE matrix

$$\begin{aligned} W_{MMSE} &= (H^H H + I_K/\gamma)^{-1} H^H \\ &= \begin{bmatrix} w'_{11} & w'_{21} \\ w'_{12} & w'_{22} \end{bmatrix} \end{aligned} \tag{6.12}$$

where $\gamma = \mathrm{E}[|x_1(t)|^2]/\mathrm{E}[|n_i(t)|^2]$ is the signal-to-noise ratio per transmit antenna, and applies W_{MMSE} to $\bar{y}$ to yield

$$\begin{aligned} \begin{bmatrix} z_1 \\ z_2 \end{bmatrix} &= W_{MMSE}\ \bar{y} \\ &= W_{MMSE} H \begin{bmatrix} s_1 \\ s_2 \end{bmatrix} + W_{MMSE} \begin{bmatrix} \bar{n}_1 \\ \bar{n}_2 \end{bmatrix} \end{aligned} \tag{6.13}$$

6.4 Proposed Receiver Architecture

The block diagram of the proposed receiver architecture is shown in Figure 6.3, where the RF weighting block for the k-th receive antenna for detecting the signal of the j-th user is shown in Figure 6.4. Each weighting block needs two real multiplications and one *fixed* delay unit. The proposed architecture requires only one RF/BB chain, thereby significantly reducing the hardware complexity, power consumption, and size. In what follows we show that the BB chain output z_j in Fig. 6.3 is nearly identical to that of the conventional receiver shown in Fig. 6.2, hence providing nearly an identical performance.

Without loss of generality, consider the ZF receiver that detects the data of Tx1. The RF weighting block 11 (first block) in Fig. 6.3, which is shown in more detail in Fig. 6.4, produces

$$\begin{aligned} y_{11}(t) &= w_{11,R}\tilde{y}_1(t) + w_{11,I}\tilde{y}_1(t-\tau) \\ &= Re\{[w_{11,R}\bar{y}_1(t) + w_{11,I}\bar{y}_1(t-\tau)e^{-j2\pi f_c \tau}] \cdot e^{j2\pi f_c t}\} \end{aligned} \tag{6.14}$$

where $w_{11,R} = Re\{w_{11}\}$ and $w_{11,I} = Im\{w_{11}\}$. If the time delay τ is chosen to be

$$\tau = 3/(4f_c) \tag{6.15}$$

then we obtain $e^{-j2\pi f_c \tau} = j$ and

$$x_i(t-\tau) \simeq x_i(t) \tag{6.16}$$

$$n_i(t-\tau) \simeq n_i(t), \quad i = 1, 2 \tag{6.17}$$

for large enough f_c. The accuracy of the approximation in (6.16) for the rectangular pulse shaping and the raised-cosine pulse shaping and that in (6.17) for a low-pass, wide sense stationary noise with a flat power spectral density are provided in Appendix F. Substituting (6.17) in (6.14) yields

$$y_{11}(t) \simeq Re\{w_{11}\bar{y}_1(t)e^{j2\pi f_c t}\}. \tag{6.18}$$

Similarly,

$$y_{21}(t) \simeq Re\{w_{21}\bar{y}_2(t)e^{j2\pi f_c t}\}. \tag{6.19}$$

Adding $y_{11}(t)$ and $y_{21}(t)$ yields

$$\begin{aligned} y_1(t) &= y_{11}(t) + y_{21}(t) \qquad (6.20)\\ &\simeq Re\{[\underbrace{(w_{11}h_{11} + w_{21}h_{12})}_{=1}x_1(t) \\ &\quad + \underbrace{(w_{11}h_{21} + w_{21}h_{22})}_{=0}x_2(t) \\ &\quad + w_{11}n_1(t) + w_{21}n_2(t)]e^{j2\pi f_c t}\} \\ &= Re\{[x_1(t) + w_{11}n_1(t) + w_{21}n_2(t)]e^{j2\pi f_c t}\} \qquad (6.21) \end{aligned}$$

where the last equality follows from the property $WH = I$. After passing $y_1(t)$ through the RF/BB chain, we obtain

$$z_1 \simeq s_1 + w_{11}\bar{n}_1 + w_{21}\bar{n}_2. \tag{6.22}$$

Similarly, adding $y_{12}(t)$ and $y_{22}(t)$ and passing the sum $y_{12}(t) + y_{22}(t)$ through the RF/BB chain yields

$$z_2 \simeq s_2 + w_{12}\bar{n}_1 + w_{22}\bar{n}_2. \tag{6.23}$$

Comparison of (6.11),(6.22), and (6.23) indicates that the proposed receiver that uses a single RF/BB chain produces nearly the same output as the conventional receiver (Fig. 6.2) that requires multiple RF/BB chains.

The accuracy of the approximations in (6.22) and (6.23) is discussed in Appendix G. It is also shown in Appendix G that the ratio between the signal-to-interference-plus-noise ratio (SINR) of the conventional receiver and that of the proposed receiver for the rectangular pulse shaping is given by

$$\frac{\mathrm{SINR_c}}{\mathrm{SINR_p}} = 1 + \frac{4}{3}\frac{|\tau|\gamma}{T} + \frac{1}{6}(\pi\tau W)^2 \tag{6.24}$$

where $\gamma = E[|x_1(t)|^2]/E[|n_i(t)|^2]$ is the signal-to-noise ratio per receive antenna and T is the symbol duration. In (6.24), the second term on the right hand side is due to the inaccuracy of (6.16) and the third term is due to the inaccuracy of (6.17). For practical values of f_c and T, the ratio is very close to 1. For example, when f_c is 1GHz and the symbol duration T is 10^{-6} second, corresponding to the symbol rate of 1M symbols per second, $\frac{1}{3}(\pi\tau W)^2 = 1.85\text{x}10^{-6}$ and $|\tau|/T = 7.5\text{x}10^{-4}$, which are both negligibly small compared to 1. It is shown in Appendix A that the accuracy of the approximation in (6.16) is even higher for the raised-cosine pulse shaping. The enhanced accuracy of the approximation makes the ratio in (6.24) even closer to one.

6.5 Channel Estimation Issue

Both receiver architectures require knowledge of the channel gains, $\{h_{ij}\}$. For the proposed receiver architecture, they can be obtained by multiplexing the antenna elements to the RF chain during the training period. That is, the RF chain is connected to the first antenna element during the first part of the training sequence, then to the second antenna element during the next part, and so on. Thus, we need a few more training symbols and extra training time, not more RF chains. Especially in high data rate applications, those additional training bits decrease the spectral efficiency in a negligible way.

Following the channel estimation model for MIMO systems in [71; 72], the noisy channel estimate with the maximum likelihood (ML) channel estimation can be modeled as [73]

$$\hat{H} = H + e\Omega, \tag{6.25}$$

where $\hat{H}$ is the estimated channel matrix, H is the true channel matrix, and $e\Omega$ is the estimation error that is uncorrelated with H. The entries of Ω are i.i.d zero-mean complex Gaussian with

unit variance [71; 72] and e is the measure of channel estimation accuracy. As e gets smaller, the estimation is more accurate and vice versa. The correlation coefficient between $\hat{H}$ and H is given by [73].

$$\begin{aligned}\rho_{ij} &= \frac{e[h_{ij}\hat{h}_{ij}^*]}{\sqrt{e[|h_{ij}|^2] \cdot e[|\hat{h}_{ij}|^2]}} \\ &= \frac{1}{\sqrt{1+e^2}}\end{aligned} \tag{6.26}$$

where h_{ij} and $\hat{h}_{ij}$ represent the (i,j) component of H and $\hat{H}$, respectively. The normalized mean square error (NMSE) of the channel estimation is given by [73]

$$\begin{aligned}NMSE &= \frac{E[|h_{ij}-\hat{h}_{ij}|^2]}{E[|h_{ij}|^2]} \\ &= e^2.\end{aligned} \tag{6.27}$$

6.6 Simulation Results

In this section we present simulation results for the case of rectangular pulse shaping. Fig. 6.5 compares the bit error rate (BER) of the conventional receiver with that of the proposed receiver for the case of $K = 2$, $N_R = 2$, $N_T = 1$, and BPSK modulation. We find that both receivers provide nearly identical BER for $T \geq 10^{-6}$, i.e. for bit rate less than 1Mbps and that for $T = 10^{-5}$ both receivers provide exactly identical BER. For the raised-cosine pulse shaping, the analysis in Appendix A shows that the BER of the proposed receiver is even closer to that of the conventional receiver.

Fig. 6.6 shows that the difference in BER between the proposed receiver and the conventional receiver is even smaller when the number of transmitter-receiver pairs, hence the number of receive antennas, is larger ($K = 4$, $N_R = 4$, $N_T = 1$). We find that both receivers provide nearly identical BER for $T \geq 10^{-7}$, i.e. for bit rate less than 10Mbps. Figs. 6.5 and 6.6 show that the proposed receiver architecture provides nearly the same BER that can be provided by the conventional receiver that requires multiple RF/BB chains.

Fig. 6.7 shows the BER when the number of RF chains is smaller than that of users K and the MMSE nulling matrix in (6.12) is applied. For the conventional receiver with $N_R = 4$, the SNR-based antenna selection technique [74; 75] is applied in choosing 2 antenna elements out

of 4 antenna elements and passing the RF signals to 2 RF chains. Also, shown in the figure is the BER for the conventional receiver with $N_R = 2$. We can see a significant performance degradation for the conventional receiver architecture when the number of RF chains is smaller than that of users, even though it requires one more RF chain than the proposed receiver architecture.

Fig. 6.8 shows the effect of the channel estimation error on the average BER for different value of normalized root mean square error e. For both conventional and proposed receiver architecture, the BER performance is sensitive to the channel estimation error and degrades significantly as e increases.

6.7 Conclusion

We proposed a new receiver architecture that enables to detect the desired signal in the presence of co-channel interference with a single RF/BB chain, while still providing nearly the same bit error rate that can be provided by the conventional receiver that requires multiple RF/BB chains. Reduction of the number of RF/BB chains leads to a reduction of hardware complexity and power consumption at the receiver. The proposed receiver architecture enables multiple transmitter-receiver pairs to simultaneously communicate in the same frequency band without additional bandwidth, thereby increasing the spectral efficiency or capacity, with significantly reduced receiver complexity and power consumption.

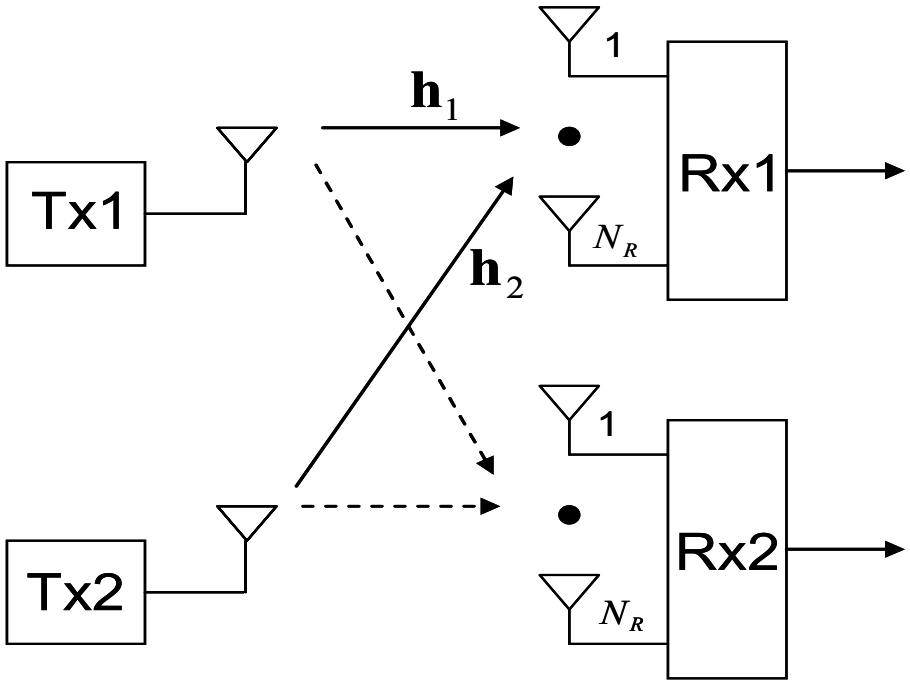

Figure 6.1 System model for $K = 2$.

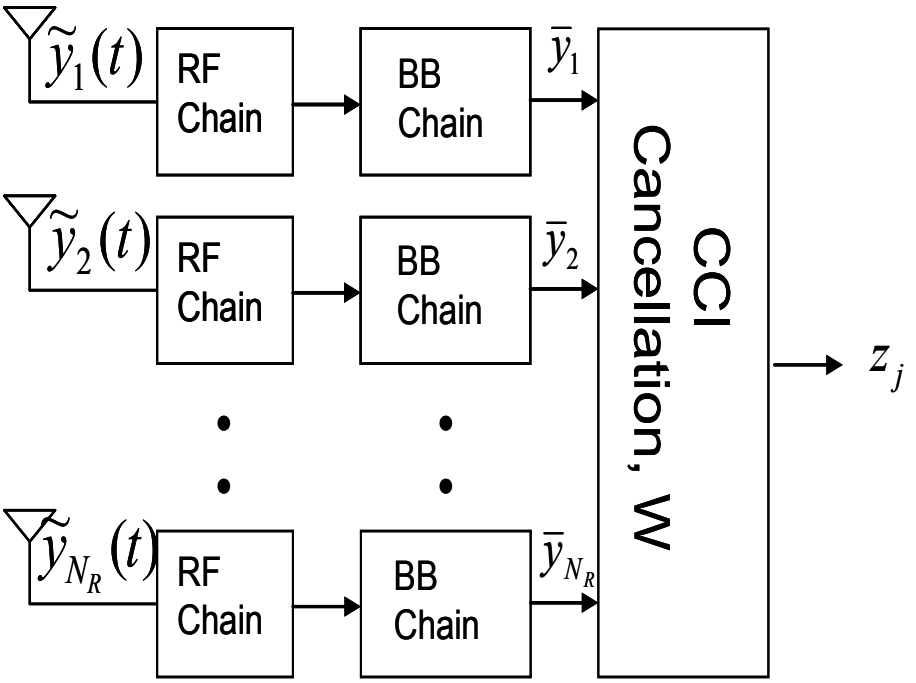

Figure 6.2 Conventional receiver architecture.

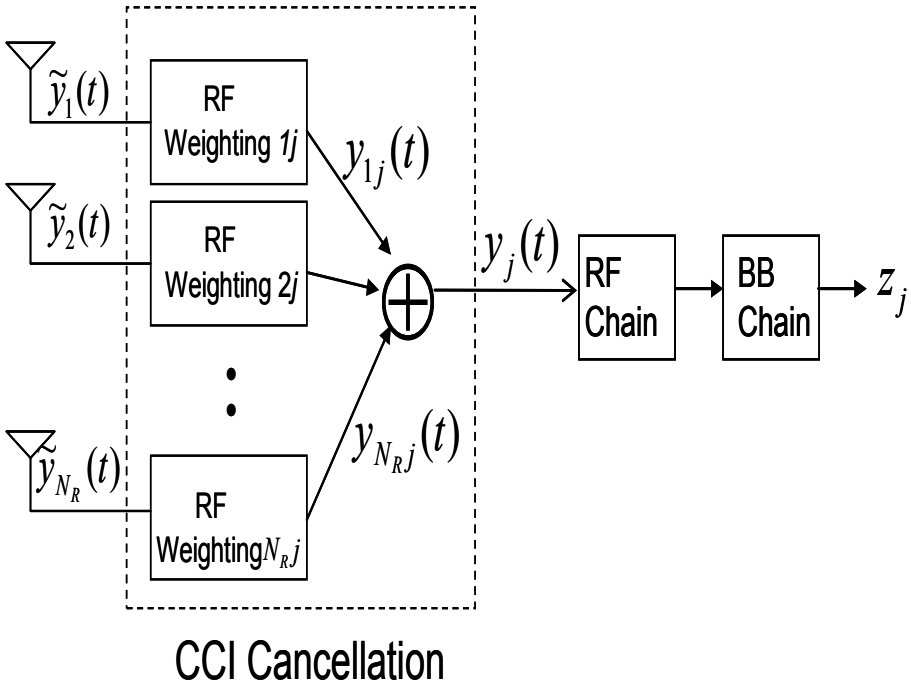

Figure 6.3 Proposed receiver architecture for detecting the signal of the j-th user.

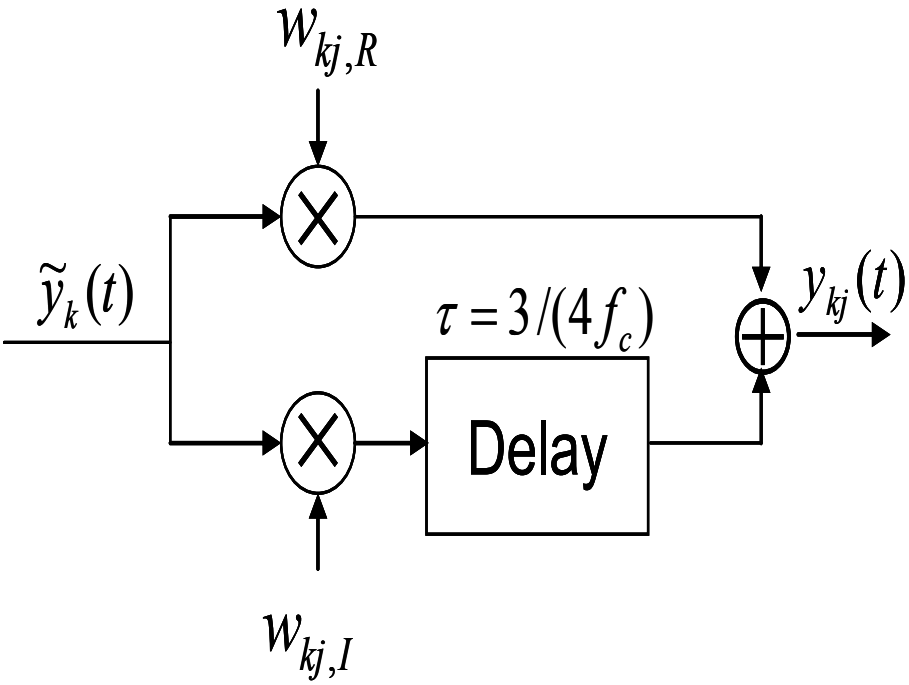

Figure 6.4 RF weighting block kj for the k-th receive antenna for detecting the j-th transmitter signal.

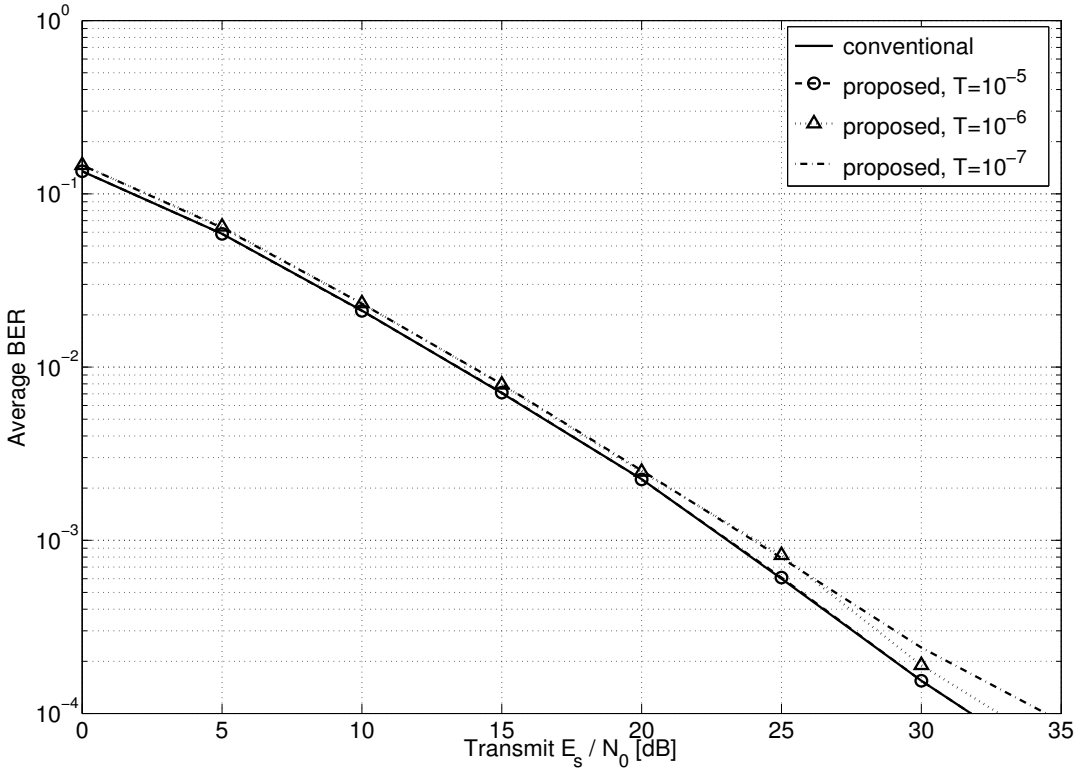

Figure 6.5 Bit error rate of the conventional receiver and the proposed receiver for different values of T, rectangular pulse shaping, f_c=1GHz, $K = N_R = 2$, $N_T = 1$.

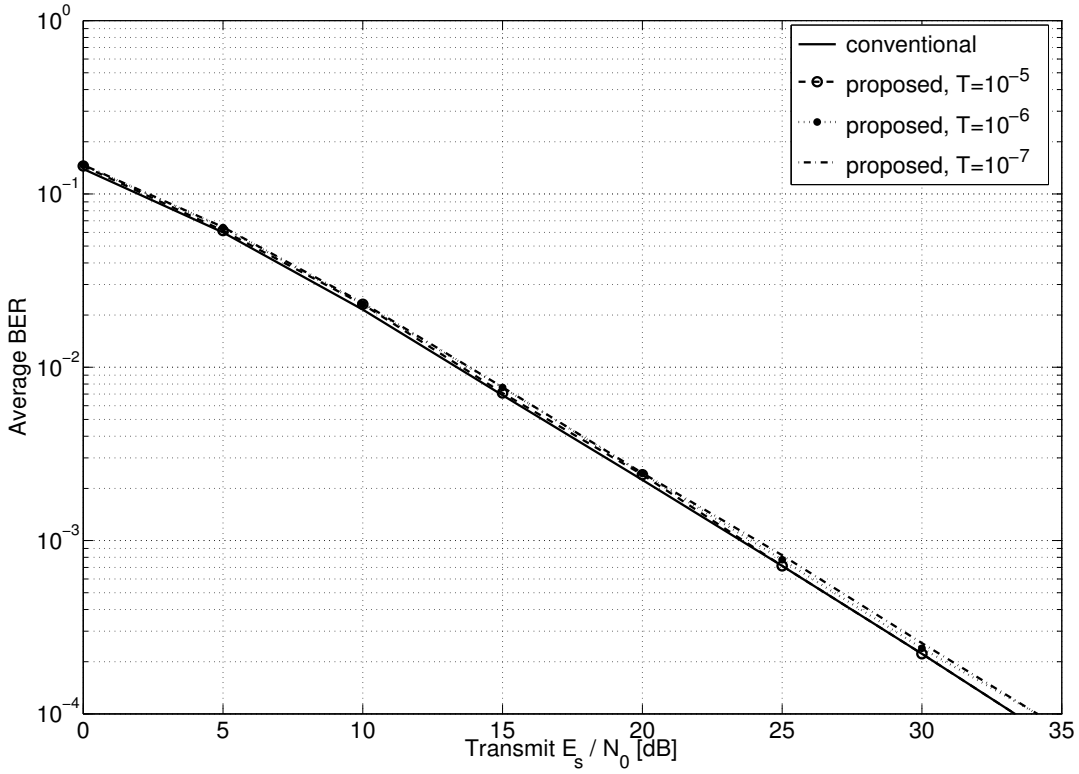

Figure 6.6 Bit error rate of the conventional receiver and the proposed receiver for different values of T, rectangular pulse shaping, f_c=1GHz, $K = N_R = 4$, $N_T = 1$.

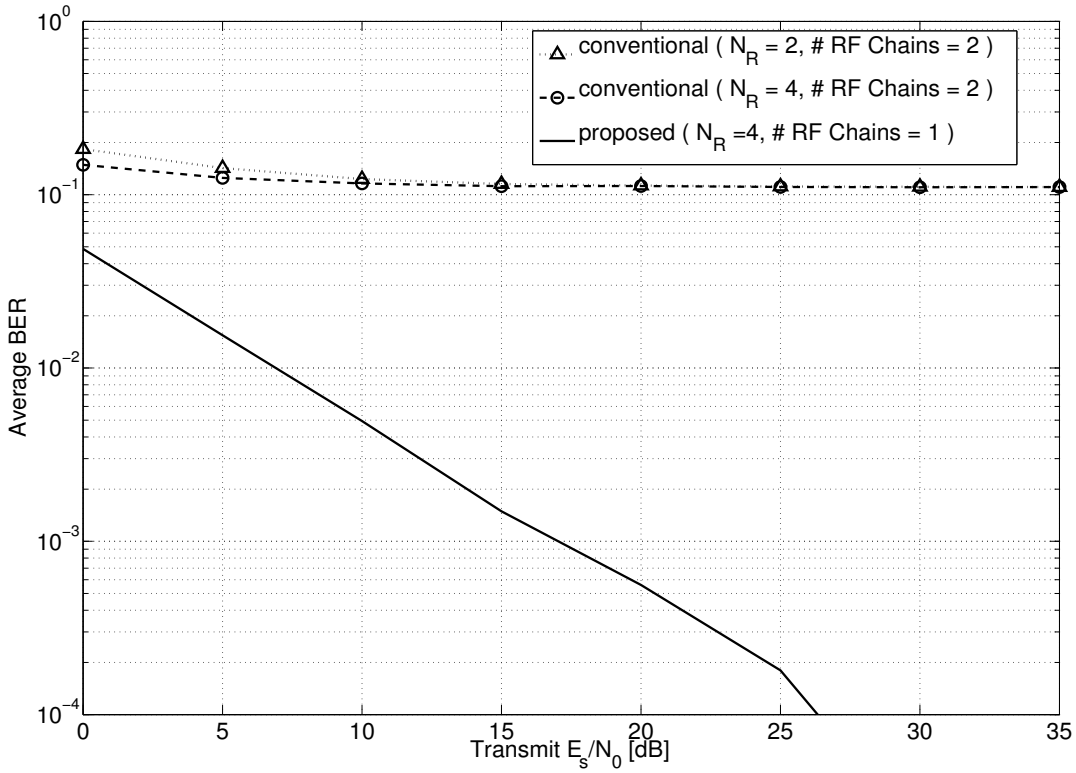

Figure 6.7 Bit error rate of the conventional receiver and the proposed receiver for different values of N_R and RF Chains, rectangular pulse shaping, , f_c=1GHz, $K = 4$, $N_T = 1$, $T = 10^{-7}$.

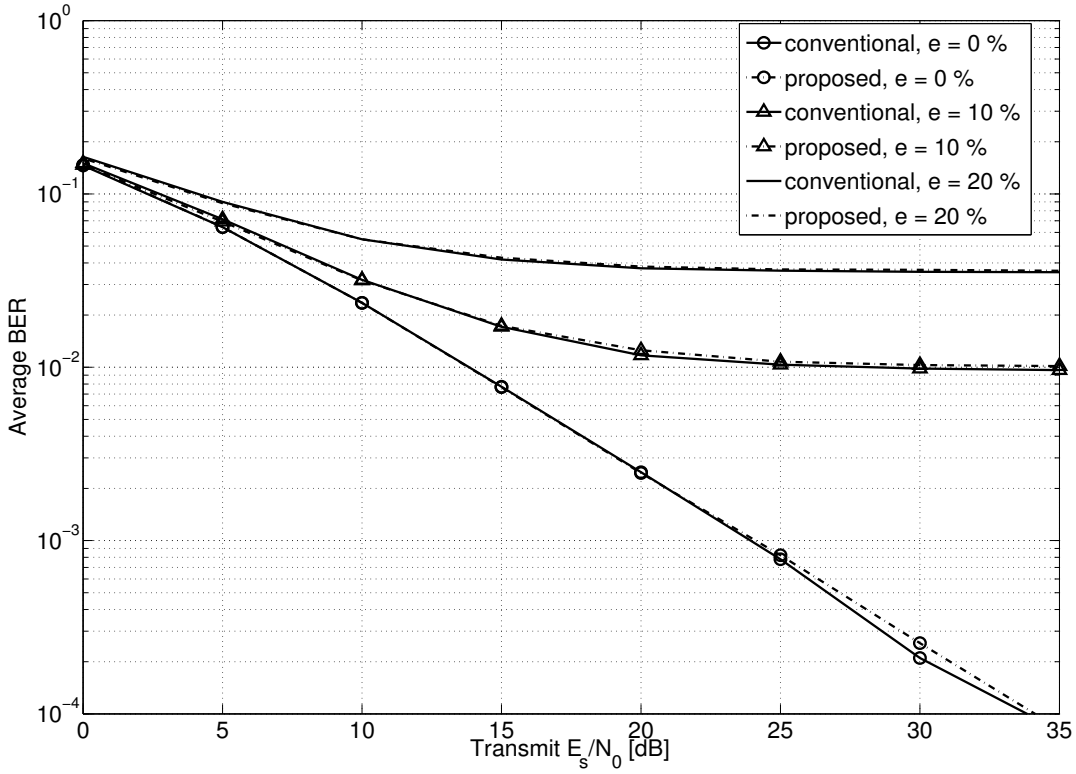

Figure 6.8 Bit error rate of the conventional receiver and the proposed receiver for different values of e, rectangular pulse shaping, f_c=1GHz, $K = N_R = 4$, $N_T = 1$, $T = 10^{-7}$.

CHAPTER 7. CONCLUSION

In chapter 3, we considered a multiple access relay network where each source transmits a channel coded packet, the relay decodes the transmitted packet, generates network coded packet, and re-transmits it. We assumed multiple antennas at the relay and considered two MIMO transmission modes at the relay; spatial multiplexing (SM) and beamforming as transmit diversity (TD). We applied different network coding schemes depending on the MIMO transmission modes. We derived the outage probability with the maximum likelihood decoding at the destination, and investigated the effect of MIMO transmission modes at the relay, coding rate from each source, relay locations, and different network coding schemes on the outage probability. We proposed an optimal MIMO mode selection sheme which depends on channel coding from the source, network coding at the relay, and MIMO transmission modes.

This thesis also investigates the fundamental tradeoff between achievable rate and reliability of multiple access relay network with multiple antennas. We considered three MIMO transmission modes, spatial multiplexing (SM), Alamouti coding as transmit diversity (TD), and Golden Coding, and random linear network coding at the relay. We derived the union bound on the average decoding error probability with maximum likelihood decoding at the destination. We found that TD mode provides the highest error probability, and SM and GC modes provide virtually identical probability of decoding error.

Chapter 5 proposed a new detection ordering for successive interference cancellation in a multi-user, multi-mode MIMO system, where each user may simultaneously transmit in either spatial multiplexing or beamforming mode to a common receiver. The receiver decides the order of detection based on the LLR, which provides *a posteriori* information on reliability of detection. The proposed approach, exploiting this additional information, can provide a SNR gain of $1 \sim 3$dB over the conventional SNR-ordered successive interference cancellation and

the SNR gain is more significant with increasing number of users. We provided computational complexity analysis of the considered detection methods. We also presented an adaptive mode selection scheme which provides $1 \sim 2$dB SNR gain against the random mode selection scheme. The impact of the knowledge of transmit mode at the receiver and that of the knowledge of the optimum transmit mode at the transmitter has been analyzed in different SIC schemes.

Chapter 6 proposed a new receiver architecture that enables to detect the desired signal in the presence of co-channel interference with a single RF/BB chain, while still providing nearly the same bit error rate that can be provided by the conventional receiver that requires multiple RF/BB chains. Reduction of the number of RF/BB chains leads to a reduction of hardware complexity and power consumption at the receiver. The proposed receiver architecture enables multiple transmitter-receiver pairs to simultaneously communicate in the same frequency band without additional bandwidth, thereby increasing the spectral efficiency or capacity, with significantly reduced receiver complexity and power consumption.

APPENDIX A. LINK OUTAGE PROBABILITY OF SM MODE

In this appendix, we prove (3.10) the outage probability between $R \to D$ link when SM mode is used. In SM mode, independent symbols are transmitted through different antennas and the received signal at the destination is given by (3.6). Since each antenna transmit equal amount of information bit for a given time, the data rate R_i between i-th antenna and the destination is identical for all antennas ($R_1 = R_2 = R$).

First, we find the capacity region for each outage events. We define three error events E_{1j}, E_{i1}, E_{ij} where

$$\begin{aligned} E_{1,\bar{2}} &= \{p_1 \text{ is correctly decoded, } p_2 \text{ is in outage}\} \\ E_{\bar{1},2} &= \{p_1 \text{ is in outage, } p_2 \text{ is correctly decoded}\} \\ E_{\bar{1},\bar{2}} &= \{p_1 \text{ and } p_2 \text{ are both in outage}\}. \end{aligned} \tag{A.1}$$

Then the event $\overline{p_1}$ that p_1 is in outage is given by

$$\overline{p_1} = E_{\bar{1},2} \cup E_{\bar{1},\bar{2}} \tag{A.2}$$

and the event $\overline{p_1} \cdot \overline{p_2}$ that both p_1 and p_2 are in outage is given by

$$\overline{p_1} \cdot \overline{p_2} = E_{\bar{1},\bar{2}} \tag{A.3}$$

Using the steps in [95], the error events E_{1j}, E_{i1}, E_{ij} can be upper bounded as follow

$$\begin{aligned} P(E_{\bar{1},2}) &\leq 2^{nR_1} 2^{-n(\ \mathrm{I}(p_1:y_r|p_2)-3\epsilon\ )} \\ P(E_{1,\bar{2}}) &\leq 2^{nR_2} 2^{-n(\ \mathrm{I}(p_2:y_r|p_1)-3\epsilon\ )} \\ P(E_{\bar{1},\bar{2}}) &\leq 2^{n(R_1+R_2)} 2^{-n(\ \mathrm{I}(p_1,p_2:y_r)-4\epsilon\ )} \end{aligned} \tag{A.4}$$

Hence, $\overline{p_1}$ occurs if and only if $R_1 > \mathrm{I}(p_1 : y_r|p_2)$ or $(R_1 + R_2) > \mathrm{I}(p_1, p_2 : y_r)$ and $\overline{p_1} \cdot \overline{p_2}$ occurs iff $(R_1 + R_2) > \mathrm{I}(p_1, p_2 : y_r)$.

Second, the outage probability for $\overline{p_1}$ and $\overline{p_1} \cdot \overline{p_2}$ can be derived as follows

$$\begin{aligned} P(\overline{p_1}) &= P(R > \mathrm{I}(p_1 : y_{dr}|p_2) \text{ or } 2R > \mathrm{I}(p_1, p_2 : y_{dr})) \\ &= P\left(\log_2\left(1+\gamma_{r_1}\right) < R \text{or} \quad \log_2\left(1+\gamma_{r_1}+\gamma_{r_2}\right) < 2R\right) \\ &= P\left(\gamma_{r_1} < 2^R - 1 \text{ or } \left(\gamma_{r_1}+\gamma_{r_2}\right) < 2^{2R}-1\right) \end{aligned} \tag{A.5}$$

where $\gamma_{r_i} = |g_i|^2 E_r/N_0$ and $R_1 = R_2 = R$ is applied into the first equality. For Rayleigh fading, γ_{r_i} becomes exponential random variable with the following probability distribution

$$f(\gamma_{r_i}) = \frac{1}{\gamma_r}\exp\left(-\frac{\gamma_{r_i}}{\gamma_r}\right), \quad \gamma_{r,i} \geq 0 \tag{A.6}$$

where $\gamma_r = \mathrm{E}[|g_i|^2 E_r/N_0] = d_{rd}^{-\alpha} E_r/N_0$. Hence,

$$\begin{aligned} P(\overline{p_1}) &= \int_0^{2^R-1}\int_{2^R-1-\gamma_{r_1}}^{\infty} f(\gamma_{r_2})f(\gamma_{r_1})d\gamma_{r_2}d\gamma_{r_1} \\ &\quad + \int_0^{2^{2R}-1}\int_0^{2^{2R}-1-\gamma_{r_1}} f(\gamma_{r_2})f(\gamma_{r_1})d\gamma_{r_2}d\gamma_{r_1} \\ &= 1 - \left(1+\frac{2^{2R}-2^R}{\gamma_r}\right)\exp\left(-\frac{2^{2R}-1}{\gamma_r}\right) \end{aligned} \tag{A.7}$$

Similarly,

$$\begin{aligned} P(\overline{p_1}\cdot\overline{p_2}) &= P\left(\log_2\left(1+\frac{|g_1|^2E_r}{N_0}+\frac{|g_2|^2E_r}{N_0}\right) < 2R\right) \\ &= P\left(\left(\gamma_{r_1}+\gamma_{r_2}\right) < 2^{2R}-1\right) \\ &= \int_0^{2^{2R}-1}\int_0^{2^{2R}-1-\gamma_{r_1}} f(\gamma_{r_2})f(\gamma_{r_1})d\gamma_{r_2}d\gamma_{r_1} \\ &= 1 - \left(1+\frac{2^{2R}-1}{\gamma_r}\right)\exp\left(-\frac{2^{2R}-1}{\gamma_r}\right) \end{aligned} \tag{A.8}$$

This completes the proof.

APPENDIX B. GENERALIZATION TO K SOURCES

In this appendix, we prove the first equality in (3.19) using mathematical induction. For $K = 2$, the last term in (3.19) is

$$\begin{aligned} P\left(\overline{x}_2 \cup \overline{p}_0\right) &= P\left(\overline{x}_2\right) + P\left(\overline{p}_0\right) - P\left(\overline{x}_2\right) P\left(\overline{p}_0\right) \\ &= p_{sd} + p_{TD} - p_{sd}p_{TD} \\ &= 1 - (1 - p_{TD})(1 - p_{sd}) \end{aligned} \tag{B.1}$$

where we denote $\overline{p}_0 \triangleq \{\mathrm{I}(p_0 : y_{dr}) < R_c\}$. Assume that the following statement holds for $K = n$.

$$P\left(\overline{x}_2^n \cup \overline{p}_0\right) = 1 - (1 - p_{TD})(1 - p_{sd})^{n-1} \tag{B.2}$$

Then for $K = n + 1$,

$$\begin{aligned} &P\left(\overline{x}_2^{n+1} \cup \overline{p}_0\right) = P\left(\overline{x}_2^n \cup \overline{x}_{n+1} \cup \overline{p}_0\right) \\ &= P\left(\overline{x}_2^n \cup \overline{p}_0\right) + P\left(\overline{x}_{n+1}\right)\left(1 - P\left(\overline{x}_2^n \cup \overline{p}_0\right)\right) \\ &= 1 - (1 - p_{TD})(1 - p_{sd})^{n-1} + p_{sd}(1 - p_{TD})(1 - p_{sd})^{n-1} \\ &= 1 - (1 - p_{TD})(1 - p_{sd})^n \end{aligned} \tag{B.3}$$

Thereby the statement (B.2) holds.

APPENDIX C. ERROR PROBABILITY FOR ERROR PATTERN $\mathbf{e}_i$

In this appendix, we present the codebook and derive the union bound of the decoding error probability for each error pattern $\mathbf{e}_i$, $i = 1, \cdots, 16$.

Table C.1 Codebook for Error Pattern $\mathbf{e}_1 = (e_1, e_2, e_3, e_4) = (0, 0, 0, 0)$

				SM		TD
x_1	x_2	x_3	x_4	$p_1 = x_1 \oplus x_2$	$p_2 = x_3 \oplus x_4$	$p_0 = x_1 \oplus x_2 \oplus x_3 \oplus x_4$
0	0	0	0	0	0	0
0	0	0	1	0	1	1
0	0	1	0	0	1	1
0	1	0	0	1	0	1
1	0	0	0	1	0	1
0	0	1	1	0	0	0
0	1	0	1	1	1	0
1	0	0	1	1	1	0
0	1	1	0	1	1	0
1	0	1	0	1	1	0
1	1	0	0	0	0	0
1	1	1	0	0	1	1
1	1	0	1	0	1	1
1	0	1	1	1	0	1
0	1	1	1	1	0	1
1	1	1	1	0	0	0

The decoding error probability for error pattern $\mathbf{e}_1 = (0, 0, 0, 0)$ is upper bounded by

$$\begin{aligned} P_E(\mathbf{e}_1)^{\mathrm{SM}} &\le 4\left(\frac{1}{1+\gamma_s}\right)\left(\frac{1}{1+\gamma_r}\right) + 2\left(\frac{1}{1+\gamma_s}\right)^2 + 4\left(\frac{1}{1+\gamma_s}\right)^2\left(\frac{1}{1+2\gamma_r}\right) \\ &\quad + 4\left(\frac{1}{1+\gamma_s}\right)^3\left(\frac{1}{1+\gamma_r}\right) + \left(\frac{1}{1+\gamma_s}\right)^4 \sim \frac{4}{\gamma_s\gamma_r} + \frac{2}{\gamma_s^2} \text{ as } \gamma_s, \gamma_r \to \infty \\ P_E(\mathbf{e}_1)^{\mathrm{TD}} &\le 4\left(\frac{1}{1+\gamma_s}\right)\left(\frac{1}{1+\gamma_r}\right)^2 + 6\left(\frac{1}{1+\gamma_s}\right)^2 \\ &\quad + 4\left(\frac{1}{1+\gamma_s}\right)^3\left(\frac{1}{1+\gamma_r}\right)^2 + \left(\frac{1}{1+\gamma_s}\right)^4 \sim \frac{4}{\gamma_s\gamma_r}^2 + \frac{6}{\gamma_s^2} \end{aligned} \tag{C.1}$$

Table C.2 Codebook for Error Pattern $\mathbf{e}_2 = (e_1, e_2, e_3, e_4) = (0, 0, 0, 1)$

				SM		TD
x_1	x_2	x_3	x_4	$p_1 = x_1 \oplus x_2$	$p_2 = x_3$	$p_0 = x_1 \oplus x_2 \oplus x_3$
0	0	0	0	0	0	0
0	0	0	1	0	0	0
0	0	1	0	0	1	1
0	1	0	0	1	0	1
1	0	0	0	1	0	1
0	0	1	1	0	1	1
0	1	0	1	1	0	1
1	0	0	1	1	0	1
0	1	1	0	1	1	0
1	0	1	0	1	1	0
1	1	0	0	0	0	0
1	1	1	0	0	1	1
1	1	0	1	0	0	0
1	0	1	1	1	1	0
0	1	1	1	1	1	0
1	1	1	1	0	1	1

The decoding error probability for error pattern $\mathbf{e}_2 = (0, 0, 0, 1)$ is upper bounded by

$$\begin{aligned}
P_E(\mathbf{e}_2)^{\mathrm{SM}} \leq & \left(\frac{1}{1+\gamma_s}\right) + 3\left(\frac{1}{1+\gamma_s}\right)\left(\frac{1}{1+\gamma_r}\right) + 3\left(\frac{1}{1+\gamma_s}\right)^2\left(\frac{1}{1+\gamma_r}\right) \\
& + 2\left(\frac{1}{1+\gamma_s}\right)^2\left(\frac{1}{1+2\gamma_r}\right) + \left(\frac{1}{1+\gamma_s}\right)^2 + \left(\frac{1}{1+\gamma_s}\right)^3\left(\frac{1}{1+\gamma_r}\right) \\
& + \left(\frac{1}{1+\gamma_s}\right)^3 + 2\left(\frac{1}{1+\gamma_s}\right)^3\left(\frac{1}{1+2\gamma_r}\right) + \left(\frac{1}{1+\gamma_s}\right)^4\left(\frac{1}{1+\gamma_r}\right) \\
& \sim \frac{1}{\gamma_s} \text{ as } \gamma_s, \gamma_r \to \infty \qquad \text{(C.2)} \\
P_E(\mathbf{e}_2)^{\mathrm{TD}} \leq & \left(\frac{1}{1+\gamma_s}\right) + 3\left(\frac{1}{1+\gamma_s}\right)\left(\frac{1}{1+\gamma_r}\right)^2 + 3\left(\frac{1}{1+\gamma_s}\right)^2\left(\frac{1}{1+\gamma_r}\right)^2 \\
& + 3\left(\frac{1}{1+\gamma_s}\right)^2 + \left(\frac{1}{1+\gamma_s}\right)^3\left(\frac{1}{1+\gamma_r}\right)^2 + 3\left(\frac{1}{1+\gamma_s}\right)^3 \\
& + \left(\frac{1}{1+\gamma_s}\right)^4\left(\frac{1}{1+\gamma_r}\right)^2 \sim \frac{1}{\gamma_s}
\end{aligned}$$

where the error event $\mathbf{e}_2$ occurs with the following probability

$$P(\mathbf{e}_2) = P(e_1 = 0)P(e_2 = 0)P(e_3 = 0)P(e_4 = 1) = p_{e,r4}\prod_{i=1}^{3}(1 - p_{e,ri}) \qquad \text{(C.3)}$$

Table C.3 Codebook for Error Pattern $\mathbf{e}_3 = (e_1, e_2, e_3, e_4) = (0, 0, 1, 0)$

				SM		TD
x_1	x_2	x_3	x_4	$p_1 = x_1 \oplus x_2$	$p_2 = x_4$	$p_0 = x_1 \oplus x_2 \oplus x_4$
0	0	0	0	0	0	0
0	0	0	1	0	1	1
0	0	1	0	0	0	0
0	1	0	0	1	0	1
1	0	0	0	1	0	1
0	0	1	1	0	1	1
0	1	0	1	1	1	0
1	0	0	1	1	1	0
0	1	1	0	1	0	1
1	0	1	0	1	0	1
1	1	0	0	0	0	0
1	1	1	0	0	0	0
1	1	0	1	0	1	1
1	0	1	1	1	1	0
0	1	1	1	1	1	0
1	1	1	1	0	1	1

The decoding error probability for error pattern $\mathbf{e}_3 = (0, 0, 1, 0)$ is upper bounded by

$$\begin{aligned}
P_E(\mathbf{e}_3)^{\mathrm{SM}} \leq & \left(\frac{1}{1+\gamma_s}\right) + 3\left(\frac{1}{1+\gamma_s}\right)\left(\frac{1}{1+\gamma_r}\right) + 3\left(\frac{1}{1+\gamma_s}\right)^2\left(\frac{1}{1+\gamma_r}\right) \\
& + 2\left(\frac{1}{1+\gamma_s}\right)^2\left(\frac{1}{1+2\gamma_r}\right) + \left(\frac{1}{1+\gamma_s}\right)^2 + \left(\frac{1}{1+\gamma_s}\right)^3\left(\frac{1}{1+\gamma_r}\right) \\
& + \left(\frac{1}{1+\gamma_s}\right)^3 + 2\left(\frac{1}{1+\gamma_s}\right)^3\left(\frac{1}{1+2\gamma_r}\right) + \left(\frac{1}{1+\gamma_s}\right)^4\left(\frac{1}{1+\gamma_r}\right) \\
& \sim \frac{1}{\gamma_s} \text{ as } \gamma_s, \gamma_r \to \infty \qquad \text{(C.4)} \\
P_E(\mathbf{e}_3)^{\mathrm{TD}} \leq & \left(\frac{1}{1+\gamma_s}\right) + 3\left(\frac{1}{1+\gamma_s}\right)\left(\frac{1}{1+\gamma_r}\right)^2 + 3\left(\frac{1}{1+\gamma_s}\right)^2\left(\frac{1}{1+\gamma_r}\right)^2 \\
& + 3\left(\frac{1}{1+\gamma_s}\right)^2 + \left(\frac{1}{1+\gamma_s}\right)^3\left(\frac{1}{1+\gamma_r}\right)^2 + 3\left(\frac{1}{1+\gamma_s}\right)^3 \\
& + \left(\frac{1}{1+\gamma_s}\right)^4\left(\frac{1}{1+\gamma_r}\right)^2 \sim \frac{1}{\gamma_s}
\end{aligned}$$

where the error event $\mathbf{e}_3$ occurs with probability

$$\begin{aligned}
P(\mathbf{e}_3) &= P(e_1 = 0)P(e_2 = 0)P(e_3 = 1)P(e_4 = 0) \\
&= (1 - p_{e,r1})(1 - p_{e,r2})p_{e,r3}(1 - p_{e,r4})
\end{aligned} \qquad \text{(C.5)}$$

Table C.4 Codebook for Error Pattern $\mathbf{e}_4 = (e_1, e_2, e_3, e_4) = (0, 1, 0, 0)$

				SM		TD
x_1	x_2	x_3	x_4	$p_1 = x_1$	$p_2 = x_3 \oplus x_4$	$p_0 = x_1 \oplus x_3 \oplus x_4$
0	0	0	0	0	0	0
0	0	0	1	0	1	1
0	0	1	0	0	1	1
0	1	0	0	0	0	0
1	0	0	0	1	0	1
0	0	1	1	0	0	0
0	1	0	1	0	1	1
1	0	0	1	1	1	0
0	1	1	0	0	1	1
1	0	1	0	1	1	0
1	1	0	0	1	0	1
1	1	1	0	1	1	0
1	1	0	1	1	1	0
1	0	1	1	1	0	1
0	1	1	1	0	0	0
1	1	1	1	1	0	1

The decoding error probability for error pattern $\mathbf{e}_4 = (0, 1, 0, 0)$ is upper bounded by

$$\begin{aligned}
P_E(\mathbf{e}_4)^{\text{SM}} \leq & \left(\frac{1}{1+\gamma_s}\right) + 3\left(\frac{1}{1+\gamma_s}\right)\left(\frac{1}{1+\gamma_r}\right) + 3\left(\frac{1}{1+\gamma_s}\right)^2\left(\frac{1}{1+\gamma_r}\right) \\
& + 2\left(\frac{1}{1+\gamma_s}\right)^2\left(\frac{1}{1+2\gamma_r}\right) + \left(\frac{1}{1+\gamma_s}\right)^2 + \left(\frac{1}{1+\gamma_s}\right)^3\left(\frac{1}{1+\gamma_r}\right) \\
& + \left(\frac{1}{1+\gamma_s}\right)^3 + 2\left(\frac{1}{1+\gamma_s}\right)^3\left(\frac{1}{1+2\gamma_r}\right) + \left(\frac{1}{1+\gamma_s}\right)^4\left(\frac{1}{1+\gamma_r}\right) \\
& \sim \frac{1}{\gamma_s} \text{ as } \gamma_s, \gamma_r \to \infty \qquad \text{(C.6)} \\
P_E(\mathbf{e}_4)^{\text{TD}} \leq & \left(\frac{1}{1+\gamma_s}\right) + 3\left(\frac{1}{1+\gamma_s}\right)\left(\frac{1}{1+\gamma_r}\right)^2 + 3\left(\frac{1}{1+\gamma_s}\right)^2\left(\frac{1}{1+\gamma_r}\right)^2 \\
& + 3\left(\frac{1}{1+\gamma_s}\right)^2 + \left(\frac{1}{1+\gamma_s}\right)^3\left(\frac{1}{1+\gamma_r}\right)^2 + 3\left(\frac{1}{1+\gamma_s}\right)^3 \\
& + \left(\frac{1}{1+\gamma_s}\right)^4\left(\frac{1}{1+\gamma_r}\right)^2 \sim \frac{1}{\gamma_s}
\end{aligned}$$

where the error event $\mathbf{e}_4$ occurs with the following probability

$$\begin{aligned}
P(\mathbf{e}_4) &= P(e_1 = 0)P(e_2 = 1)P(e_3 = 0)P(e_4 = 0) \\
&= (1 - p_{e,r1})p_{e,r2}(1 - p_{e,r3})(1 - p_{e,r4})
\end{aligned} \qquad \text{(C.7)}$$

Table C.5 Codebook for Error Pattern $\mathbf{e}_5 = (e_1, e_2, e_3, e_4) = (1, 0, 0, 0)$

				SM		TD
x_1	x_2	x_3	x_4	$p_1 = x_2$	$p_2 = x_3 \oplus x_4$	$p_0 = x_2 \oplus x_3 \oplus x_4$
0	0	0	0	0	0	0
0	0	0	1	0	1	1
0	0	1	0	0	1	1
0	1	0	0	1	0	1
1	0	0	0	0	0	0
0	0	1	1	0	0	0
0	1	0	1	1	1	0
1	0	0	1	0	1	1
0	1	1	0	1	1	0
1	0	1	0	0	1	1
1	1	0	0	1	0	1
1	1	1	0	1	1	0
1	1	0	1	1	1	0
1	0	1	1	0	0	0
0	1	1	1	1	0	1
1	1	1	1	1	0	1

The decoding error probability for error pattern $\mathbf{e}_5 = (1, 0, 0, 0)$ is upper bounded by

$$\begin{aligned} P_E(\mathbf{e}_5)^{\mathrm{SM}} \leq & \left(\frac{1}{1+\gamma_s}\right) + 3\left(\frac{1}{1+\gamma_s}\right)\left(\frac{1}{1+\gamma_r}\right) + 3\left(\frac{1}{1+\gamma_s}\right)^2\left(\frac{1}{1+\gamma_r}\right) \\ & + 2\left(\frac{1}{1+\gamma_s}\right)^2\left(\frac{1}{1+2\gamma_r}\right) + \left(\frac{1}{1+\gamma_s}\right)^2 + \left(\frac{1}{1+\gamma_s}\right)^3\left(\frac{1}{1+\gamma_r}\right) \\ & + \left(\frac{1}{1+\gamma_s}\right)^3 + 2\left(\frac{1}{1+\gamma_s}\right)^3\left(\frac{1}{1+2\gamma_r}\right) + \left(\frac{1}{1+\gamma_s}\right)^4\left(\frac{1}{1+\gamma_r}\right) \\ & \sim \frac{1}{\gamma_s} \text{ as } \gamma_s, \gamma_r \to \infty \end{aligned} \tag{C.8}$$

$$\begin{aligned} P_E(\mathbf{e}_5)^{\mathrm{TD}} \leq & \left(\frac{1}{1+\gamma_s}\right) + 3\left(\frac{1}{1+\gamma_s}\right)\left(\frac{1}{1+\gamma_r}\right)^2 + 3\left(\frac{1}{1+\gamma_s}\right)^2\left(\frac{1}{1+\gamma_r}\right)^2 \\ & + 3\left(\frac{1}{1+\gamma_s}\right)^2 + \left(\frac{1}{1+\gamma_s}\right)^3\left(\frac{1}{1+\gamma_r}\right)^2 + 3\left(\frac{1}{1+\gamma_s}\right)^3 \\ & + \left(\frac{1}{1+\gamma_s}\right)^4\left(\frac{1}{1+\gamma_r}\right)^2 \sim \frac{1}{\gamma_s} \end{aligned}$$

where the error event $\mathbf{e}_5$ occurs with the following probability

$$\begin{aligned} P(\mathbf{e}_5) &= P(e_1 = 1)P(e_2 = 0)P(e_3 = 0)P(e_4 = 0) \\ &= p_{e,r1}\prod_{i=2}^{4}(1 - p_{e,ri}) \end{aligned} \tag{C.9}$$

Table C.6 Codebook for Error Pattern $\mathbf{e}_6 = (e_1, e_2, e_3, e_4) = (0, 0, 1, 1)$

				SM		TD
x_1	x_2	x_3	x_4	$p_1 = x_1 \oplus x_2$	$p_2 = x_1 \oplus x_2$	$p_0 = x_1 \oplus x_2$
0	0	0	0	0	0	0
0	0	0	1	0	0	0
0	0	1	0	0	0	0
0	1	0	0	1	1	1
1	0	0	0	1	1	1
0	0	1	1	0	0	0
0	1	0	1	1	1	1
1	0	0	1	1	1	1
0	1	1	0	1	1	1
1	0	1	0	1	1	1
1	1	0	0	0	0	0
1	1	1	0	0	0	0
1	1	0	1	0	0	0
1	0	1	1	1	1	1
0	1	1	1	1	1	1
1	1	1	1	0	0	0

The decoding error probability for error pattern $\mathbf{e}_6 = (0, 0, 1, 1)$ is upper bounded by

$$\begin{aligned} P_E(\mathbf{e}_6)^{\mathrm{SM}} &\le 2\left(\frac{1}{1+\gamma_s}\right) + 2\left(\frac{1}{1+\gamma_s}\right)\left(\frac{1}{1+2\gamma_r}\right) + 2\left(\frac{1}{1+\gamma_s}\right)^2 \\ &\quad + 4\left(\frac{1}{1+\gamma_s}\right)^2\left(\frac{1}{1+2\gamma_r}\right) + 2\left(\frac{1}{1+\gamma_s}\right)^3 + 2\left(\frac{1}{1+\gamma_s}\right)^3\left(\frac{1}{1+2\gamma_r}\right) \\ &\quad + \left(\frac{1}{1+\gamma_s}\right)^4 \sim \frac{2}{\gamma_s} \text{ as } \gamma_s, \gamma_r \to \infty \\ P_E(\mathbf{e}_6)^{\mathrm{TD}} &\le 2\left(\frac{1}{1+\gamma_s}\right) + 2\left(\frac{1}{1+\gamma_s}\right)\left(\frac{1}{1+\gamma_r}\right)^2 + 2\left(\frac{1}{1+\gamma_s}\right)^2 \\ &\quad + 4\left(\frac{1}{1+\gamma_s}\right)^2\left(\frac{1}{1+\gamma_r}\right)^2 + 2\left(\frac{1}{1+\gamma_s}\right)^3 + 2\left(\frac{1}{1+\gamma_s}\right)^3\left(\frac{1}{1+\gamma_r}\right)^2 \\ &\quad + \left(\frac{1}{1+\gamma_s}\right)^4 \sim \frac{2}{\gamma_s} \end{aligned} \tag{C.10}$$

where the error event $\mathbf{e}_6$ occurs with the following probability

$$\begin{aligned} P(\mathbf{e}_6) &= P(e_1 = 0)P(e_2 = 0)P(e_3 = 1)P(e_4 = 1) \\ &= \prod_{i=1}^{2}(1 - p_{e,ri}) \prod_{j=3}^{4} p_{e,rj} \end{aligned} \tag{C.11}$$

Table C.7 Codebook for Error Pattern $\mathbf{e}_7 = (e_1, e_2, e_3, e_4) = (0, 1, 0, 1)$

				SM		TD
x_1	x_2	x_3	x_4	$p_1 = x_1$	$p_2 = x_3$	$p_0 = x_1 \oplus x_3$
0	0	0	0	0	0	0
0	0	0	1	0	0	0
0	0	1	0	0	1	1
0	1	0	0	0	0	0
1	0	0	0	1	0	1
0	0	1	1	0	1	1
0	1	0	1	0	0	0
1	0	0	1	1	0	1
0	1	1	0	0	1	1
1	0	1	0	1	1	0
1	1	0	0	1	0	1
1	1	1	0	1	1	0
1	1	0	1	1	0	1
1	0	1	1	1	1	0
0	1	1	1	0	1	1
1	1	1	1	1	1	0

The decoding error probability for error pattern $\mathbf{e}_7 = (0, 1, 0, 1)$ is upper bounded by

$$\begin{aligned}
P_E(\mathbf{e}_7)^{\mathrm{SM}} &\le 2\left(\frac{1}{1+\gamma_s}\right) + 2\left(\frac{1}{1+\gamma_s}\right)\left(\frac{1}{1+\gamma_r}\right) + \left(\frac{1}{1+\gamma_s}\right)^2 \\
&\quad + 4\left(\frac{1}{1+\gamma_s}\right)^2\left(\frac{1}{1+\gamma_r}\right) + \left(\frac{1}{1+\gamma_s}\right)^2\left(\frac{1}{1+2\gamma_r}\right) + 2\left(\frac{1}{1+\gamma_s}\right)^3\left(\frac{1}{1+\gamma_r}\right) \\
&\quad + 2\left(\frac{1}{1+\gamma_s}\right)^3\left(\frac{1}{1+2\gamma_r}\right) + \left(\frac{1}{1+\gamma_s}\right)^4\left(\frac{1}{1+2\gamma_r}\right) \\
&\quad \sim \frac{2}{\gamma_s} \text{ as } \gamma_s, \gamma_r \to \infty \\
P_E(\mathbf{e}_7)^{\mathrm{TD}} &\le 2\left(\frac{1}{1+\gamma_s}\right) + 2\left(\frac{1}{1+\gamma_s}\right)\left(\frac{1}{1+\gamma_r}\right)^2 + 2\left(\frac{1}{1+\gamma_s}\right)^2 \\
&\quad + 4\left(\frac{1}{1+\gamma_s}\right)^2\left(\frac{1}{1+\gamma_r}\right)^2 + 2\left(\frac{1}{1+\gamma_s}\right)^3 \\
&\quad + 2\left(\frac{1}{1+\gamma_s}\right)^3\left(\frac{1}{1+\gamma_r}\right)^2 + \left(\frac{1}{1+\gamma_s}\right)^4 \sim \frac{2}{\gamma_s}
\end{aligned} \tag{C.12}$$

where the error event $\mathbf{e}_7$ occurs with the following probability

$$\begin{aligned}
P(\mathbf{e}_7) &= P(e_1 = 0)P(e_2 = 1)P(e_3 = 0)P(e_4 = 1) \\
&= (1 - p_{e,r1})p_{e,r2}(1 - p_{e,r3})p_{e,r4}
\end{aligned} \tag{C.13}$$

Table C.8 Codebook for Error Pattern $\mathbf{e}_8 = (e_1, e_2, e_3, e_4) = (1, 0, 0, 1)$

				SM		TD
x_1	x_2	x_3	x_4	$p_1 = x_2$	$p_2 = x_3$	$p_0 = x_2 \oplus x_3$
0	0	0	0	0	0	0
0	0	0	1	0	0	0
0	0	1	0	0	1	1
0	1	0	0	1	0	1
1	0	0	0	0	0	0
0	0	1	1	0	1	1
0	1	0	1	1	0	1
1	0	0	1	0	0	0
0	1	1	0	1	1	0
1	0	1	0	0	1	1
1	1	0	0	1	0	1
1	1	1	0	1	1	0
1	1	0	1	1	0	1
1	0	1	1	0	1	1
0	1	1	1	1	1	0
1	1	1	1	1	1	0

The decoding error probability for error pattern $\mathbf{e}_8 = (1, 0, 0, 1)$ is upper bounded by

$$\begin{aligned}
P_E(\mathbf{e}_8)^{\mathrm{SM}} &\le 2\left(\frac{1}{1+\gamma_s}\right) + 2\left(\frac{1}{1+\gamma_s}\right)\left(\frac{1}{1+\gamma_r}\right) + \left(\frac{1}{1+\gamma_s}\right)^2 \\
&\quad + 4\left(\frac{1}{1+\gamma_s}\right)^2\left(\frac{1}{1+\gamma_r}\right) + \left(\frac{1}{1+\gamma_s}\right)^2\left(\frac{1}{1+2\gamma_r}\right) + 2\left(\frac{1}{1+\gamma_s}\right)^3\left(\frac{1}{1+\gamma_r}\right) \\
&\quad + 2\left(\frac{1}{1+\gamma_s}\right)^3\left(\frac{1}{1+2\gamma_r}\right) + \left(\frac{1}{1+\gamma_s}\right)^4\left(\frac{1}{1+2\gamma_r}\right) \\
&\quad \sim \frac{2}{\gamma_s} \text{ as } \gamma_s, \gamma_r \to \infty \\
P_E(\mathbf{e}_8)^{\mathrm{TD}} &\le 2\left(\frac{1}{1+\gamma_s}\right) + 2\left(\frac{1}{1+\gamma_s}\right)\left(\frac{1}{1+\gamma_r}\right)^2 + 2\left(\frac{1}{1+\gamma_s}\right)^2 \\
&\quad + 4\left(\frac{1}{1+\gamma_s}\right)^2\left(\frac{1}{1+\gamma_r}\right)^2 + 2\left(\frac{1}{1+\gamma_s}\right)^3 \\
&\quad + 2\left(\frac{1}{1+\gamma_s}\right)^3\left(\frac{1}{1+\gamma_r}\right)^2 + \left(\frac{1}{1+\gamma_s}\right)^4 \sim \frac{2}{\gamma_s}
\end{aligned} \tag{C.14}$$

where the error event $\mathbf{e}_8$ occurs with the following probability

$$\begin{aligned}
P(\mathbf{e}_8) &= P(e_1 = 1)P(e_2 = 0)P(e_3 = 0)P(e_4 = 1) \\
&= p_{e,r1}(1 - p_{e,r2})(1 - p_{e,r3})p_{e,r4}
\end{aligned} \tag{C.15}$$

Table C.9 Codebook for Error Pattern $\mathbf{e}_9 = (e_1, e_2, e_3, e_4) = (0, 1, 1, 0)$

				SM		TD
x_1	x_2	x_3	x_4	$p_1 = x_1$	$p_2 = x_4$	$p_0 = x_1 \oplus x_4$
0	0	0	0	0	0	0
0	0	0	1	0	1	1
0	0	1	0	0	0	0
0	1	0	0	0	0	0
1	0	0	0	1	0	1
0	0	1	1	0	1	1
0	1	0	1	0	1	1
1	0	0	1	1	1	0
0	1	1	0	0	0	0
1	0	1	0	1	0	1
1	1	0	0	1	0	1
1	1	1	0	1	0	1
1	1	0	1	1	1	0
1	0	1	1	1	1	0
0	1	1	1	0	1	1
1	1	1	1	1	1	0

The decoding error probability for error pattern $\mathbf{e}_9 = (0, 1, 1, 0)$ is upper bounded by

$$\begin{aligned}
P_E(\mathbf{e}_9)^{\mathrm{SM}} &\le 2\left(\frac{1}{1+\gamma_s}\right) + 2\left(\frac{1}{1+\gamma_s}\right)\left(\frac{1}{1+\gamma_r}\right) + \left(\frac{1}{1+\gamma_s}\right)^2 \\
&\quad + 4\left(\frac{1}{1+\gamma_s}\right)^2\left(\frac{1}{1+\gamma_r}\right) + \left(\frac{1}{1+\gamma_s}\right)^2\left(\frac{1}{1+2\gamma_r}\right) + 2\left(\frac{1}{1+\gamma_s}\right)^3\left(\frac{1}{1+\gamma_r}\right) \\
&\quad + 2\left(\frac{1}{1+\gamma_s}\right)^3\left(\frac{1}{1+2\gamma_r}\right) + \left(\frac{1}{1+\gamma_s}\right)^4\left(\frac{1}{1+2\gamma_r}\right) \\
&\quad \sim \frac{2}{\gamma_s} \text{ as } \gamma_s, \gamma_r \to \infty \\
P_E(\mathbf{e}_9)^{\mathrm{TD}} &\le 2\left(\frac{1}{1+\gamma_s}\right) + 2\left(\frac{1}{1+\gamma_s}\right)\left(\frac{1}{1+\gamma_r}\right)^2 + 2\left(\frac{1}{1+\gamma_s}\right)^2 \\
&\quad + 4\left(\frac{1}{1+\gamma_s}\right)^2\left(\frac{1}{1+\gamma_r}\right)^2 + 2\left(\frac{1}{1+\gamma_s}\right)^3 + 2\left(\frac{1}{1+\gamma_s}\right)^3\left(\frac{1}{1+\gamma_r}\right)^2 \\
&\quad + \left(\frac{1}{1+\gamma_s}\right)^4 \sim \frac{2}{\gamma_s}
\end{aligned} \tag{C.16}$$

where the error event $\mathbf{e}_9$ occurs with the following probability

$$\begin{aligned}
P(\mathbf{e}_9) &= P(e_1 = 0)P(e_2 = 1)P(e_3 = 1)P(e_4 = 0) \\
&= (1 - p_{e,r1}) \prod_{i=2}^{3} p_{e,ri} \; (1 - p_{e,r4})
\end{aligned} \tag{C.17}$$

Table C.10 Codebook for Error Pattern $\mathbf{e}_{10} = (e_1, e_2, e_3, e_4) = (1, 0, 1, 0)$

				SM		TD
x_1	x_2	x_3	x_4	$p_1 = x_2$	$p_2 = x_4$	$p_0 = x_2 \oplus x_4$
0	0	0	0	0	0	0
0	0	0	1	0	1	1
0	0	1	0	0	0	0
0	1	0	0	1	0	1
1	0	0	0	0	0	0
0	0	1	1	0	1	1
0	1	0	1	1	1	0
1	0	0	1	0	1	1
0	1	1	0	1	0	1
1	0	1	0	0	0	0
1	1	0	0	1	0	1
1	1	1	0	1	0	1
1	1	0	1	1	1	0
1	0	1	1	0	1	1
0	1	1	1	1	1	0
1	1	1	1	1	1	0

The decoding error probability for error pattern $\mathbf{e}_{10} = (1, 0, 1, 0)$ is upper bounded by

$$\begin{aligned}
P_E(\mathbf{e}_{10})^{\text{SM}} &\le 2\left(\frac{1}{1+\gamma_s}\right) + 2\left(\frac{1}{1+\gamma_s}\right)\left(\frac{1}{1+\gamma_r}\right) + \left(\frac{1}{1+\gamma_s}\right)^2 \\
&\quad + 4\left(\frac{1}{1+\gamma_s}\right)^2\left(\frac{1}{1+\gamma_r}\right) + \left(\frac{1}{1+\gamma_s}\right)^2\left(\frac{1}{1+2\gamma_r}\right) + 2\left(\frac{1}{1+\gamma_s}\right)^3\left(\frac{1}{1+\gamma_r}\right) \\
&\quad + 2\left(\frac{1}{1+\gamma_s}\right)^3\left(\frac{1}{1+2\gamma_r}\right) + \left(\frac{1}{1+\gamma_s}\right)^4\left(\frac{1}{1+2\gamma_r}\right) \\
&\quad \sim \frac{2}{\gamma_s} \text{ as } \gamma_s, \gamma_r \to \infty \\
P_E(\mathbf{e}_{10})^{\text{TD}} &\le 2\left(\frac{1}{1+\gamma_s}\right) + 2\left(\frac{1}{1+\gamma_s}\right)\left(\frac{1}{1+\gamma_r}\right)^2 + 2\left(\frac{1}{1+\gamma_s}\right)^2 \\
&\quad + 4\left(\frac{1}{1+\gamma_s}\right)^2\left(\frac{1}{1+\gamma_r}\right)^2 + 2\left(\frac{1}{1+\gamma_s}\right)^3 \\
&\quad + 2\left(\frac{1}{1+\gamma_s}\right)^3\left(\frac{1}{1+\gamma_r}\right)^2 + \left(\frac{1}{1+\gamma_s}\right)^4 \sim \frac{2}{\gamma_s}
\end{aligned} \tag{C.18}$$

where the error event $\mathbf{e}_{10}$ occurs with the following probability

$$\begin{aligned}
P(\mathbf{e}_{10}) &= P(e_1 = 1)P(e_2 = 0)P(e_3 = 1)P(e_4 = 0) \\
&= p_{e,r1}(1 - p_{e,r2})p_{e,r3}(1 - p_{e,r4})
\end{aligned} \tag{C.19}$$

Table C.11 Codebook for Error Pattern $\mathbf{e}_{11} = (e_1, e_2, e_3, e_4) = (1, 1, 0, 0)$

				SM		TD
x_1	x_2	x_3	x_4	$p_1 = x_3 \oplus x_4$	$p_2 = x_3 \oplus x_4$	$p_0 = x_3 \oplus x_4$
0	0	0	0	0	0	0
0	0	0	1	1	1	1
0	0	1	0	1	1	1
0	1	0	0	0	0	0
1	0	0	0	0	0	0
0	0	1	1	0	0	0
0	1	0	1	1	1	1
1	0	0	1	1	1	1
0	1	1	0	1	1	1
1	0	1	0	1	1	1
1	1	0	0	0	0	0
1	1	1	0	1	1	1
1	1	0	1	1	1	1
1	0	1	1	0	0	0
0	1	1	1	0	0	0
1	1	1	1	0	0	0

The decoding error probability for error pattern $\mathbf{e}_{11} = (1, 1, 0, 0)$ is upper bounded by

$$\begin{aligned} P_E(\mathbf{e}_{11})^{\text{SM}} &\le 2\left(\frac{1}{1+\gamma_s}\right) + 2\left(\frac{1}{1+\gamma_s}\right)\left(\frac{1}{1+2\gamma_r}\right) + 2\left(\frac{1}{1+\gamma_s}\right)^2 \\ &\quad + 4\left(\frac{1}{1+\gamma_s}\right)^2\left(\frac{1}{1+2\gamma_r}\right) + 2\left(\frac{1}{1+\gamma_s}\right)^3 + 2\left(\frac{1}{1+\gamma_s}\right)^3\left(\frac{1}{1+2\gamma_r}\right) \\ &\quad + \left(\frac{1}{1+\gamma_s}\right)^4 \sim \frac{2}{\gamma_s} \text{ as } \gamma_s, \gamma_r \to \infty \\ P_E(\mathbf{e}_{12})^{\text{TD}} &\le 2\left(\frac{1}{1+\gamma_s}\right) + 2\left(\frac{1}{1+\gamma_s}\right)\left(\frac{1}{1+\gamma_r}\right)^2 + 2\left(\frac{1}{1+\gamma_s}\right)^2 \\ &\quad + 4\left(\frac{1}{1+\gamma_s}\right)^2\left(\frac{1}{1+\gamma_r}\right)^2 + 2\left(\frac{1}{1+\gamma_s}\right)^3 + 2\left(\frac{1}{1+\gamma_s}\right)^3\left(\frac{1}{1+\gamma_r}\right)^2 \\ &\quad + \left(\frac{1}{1+\gamma_s}\right)^4 \sim \frac{2}{\gamma_s} \end{aligned} \tag{C.20}$$

where the error event $\mathbf{e}_{11}$ occurs with the following probability

$$\begin{aligned} P(\mathbf{e}_{11}) &= P(e_1 = 1)P(e_2 = 1)P(e_3 = 0)P(e_4 = 0) \\ &= p_{e,r1}p_{e,r2}(1 - p_{e,r3})(1 - p_{e,r4}) \end{aligned} \tag{C.21}$$

Table C.12 Codebook for Error Pattern $\mathbf{e}_{12} = (e_1, e_2, e_3, e_4) = (1, 1, 1, 0)$

				SM		TD
x_1	x_2	x_3	x_4	$p_1 = x_4$	$p_2 = x_4$	$p_0 = x_4$
0	0	0	0	0	0	0
0	0	0	1	1	1	1
0	0	1	0	0	0	0
0	1	0	0	0	0	0
1	0	0	0	0	0	0
0	0	1	1	1	1	1
0	1	0	1	1	1	1
1	0	0	1	1	1	1
0	1	1	0	0	0	0
1	0	1	0	0	0	0
1	1	0	0	0	0	0
1	1	1	0	0	0	0
1	1	0	1	1	1	1
1	0	1	1	1	1	1
0	1	1	1	1	1	1
1	1	1	1	1	1	1

The decoding error probability for error pattern $\mathbf{e}_{12} = (1, 1, 1, 0)$ is upper bounded by

$$\begin{aligned} P_E(\mathbf{e}_{12})^{\text{SM}} &\leq 3\left(\frac{1}{1+\gamma_s}\right) + \left(\frac{1}{1+\gamma_s}\right)\left(\frac{1}{1+2\gamma_r}\right) + 3\left(\frac{1}{1+\gamma_s}\right)^2 \\ &\quad + 3\left(\frac{1}{1+\gamma_s}\right)^2\left(\frac{1}{1+2\gamma_r}\right) + \left(\frac{1}{1+\gamma_s}\right)^3 + 3\left(\frac{1}{1+\gamma_s}\right)^3\left(\frac{1}{1+2\gamma_r}\right) \\ &\quad + \left(\frac{1}{1+\gamma_s}\right)^4\left(\frac{1}{1+2\gamma_r}\right) \sim \frac{3}{\gamma_s} \text{ as } \gamma_s, \gamma_r \to \infty \\ P_E(\mathbf{e}_{12})^{\text{TD}} &\leq 3\left(\frac{1}{1+\gamma_s}\right) + \left(\frac{1}{1+\gamma_s}\right)\left(\frac{1}{1+\gamma_r}\right)^2 + 3\left(\frac{1}{1+\gamma_s}\right)^2 \\ &\quad + 3\left(\frac{1}{1+\gamma_s}\right)^2\left(\frac{1}{1+\gamma_r}\right)^2 + \left(\frac{1}{1+\gamma_s}\right)^3 + 3\left(\frac{1}{1+\gamma_s}\right)^3\left(\frac{1}{1+\gamma_r}\right)^2 \\ &\quad + \left(\frac{1}{1+\gamma_s}\right)^4\left(\frac{1}{1+\gamma_r}\right)^2 \sim \frac{3}{\gamma_s} \end{aligned} \tag{C.22}$$

where the error event $\mathbf{e}_{12}$ occurs with the following probability

$$\begin{aligned} P(\mathbf{e}_{12}) &= P(e_1 = 1)P(e_2 = 1)P(e_3 = 1)P(e_4 = 0) \\ &= \prod_{i=1}^{3} p_{e,ri}\ (1 - p_{e,r4}) \end{aligned} \tag{C.23}$$

Table C.13 Codebook for Error Pattern $\mathbf{e}_{13} = (e_1, e_2, e_3, e_4) = (1, 1, 0, 1)$

				SM		TD
x_1	x_2	x_3	x_4	$p_1 = x_3$	$p_2 = x_3$	$p_0 = x_3$
0	0	0	0	0	0	0
0	0	0	1	0	0	0
0	0	1	0	1	1	1
0	1	0	0	0	0	0
1	0	0	0	0	0	0
0	0	1	1	1	1	1
0	1	0	1	0	0	0
1	0	0	1	0	0	0
0	1	1	0	1	1	1
1	0	1	0	1	1	1
1	1	0	0	0	0	0
1	1	1	0	1	1	1
1	1	0	1	0	0	0
1	0	1	1	1	1	1
0	1	1	1	1	1	1
1	1	1	1	1	1	1

The decoding error probability for error pattern $\mathbf{e}_{13} = (1, 1, 0, 1)$ is upper bounded by

$$\begin{aligned}
P_E(\mathbf{e}_{13})^{\text{SM}} &\le 3\left(\frac{1}{1+\gamma_s}\right) + \left(\frac{1}{1+\gamma_s}\right)\left(\frac{1}{1+2\gamma_r}\right) + 3\left(\frac{1}{1+\gamma_s}\right)^2 \\
&\quad + 3\left(\frac{1}{1+\gamma_s}\right)^2\left(\frac{1}{1+2\gamma_r}\right) + \left(\frac{1}{1+\gamma_s}\right)^3 + 3\left(\frac{1}{1+\gamma_s}\right)^3\left(\frac{1}{1+2\gamma_r}\right) \\
&\quad + \left(\frac{1}{1+\gamma_s}\right)^4\left(\frac{1}{1+2\gamma_r}\right) \sim \frac{3}{\gamma_s} \text{ as } \gamma_s, \gamma_r \to \infty \\
P_E(\mathbf{e}_{13})^{\text{TD}} &\le 3\left(\frac{1}{1+\gamma_s}\right) + \left(\frac{1}{1+\gamma_s}\right)\left(\frac{1}{1+\gamma_r}\right)^2 + 3\left(\frac{1}{1+\gamma_s}\right)^2 \\
&\quad + 3\left(\frac{1}{1+\gamma_s}\right)^2\left(\frac{1}{1+\gamma_r}\right)^2 + \left(\frac{1}{1+\gamma_s}\right)^3 + 3\left(\frac{1}{1+\gamma_s}\right)^3\left(\frac{1}{1+\gamma_r}\right)^2 \\
&\quad + \left(\frac{1}{1+\gamma_s}\right)^4\left(\frac{1}{1+\gamma_r}\right)^2 \sim \frac{3}{\gamma_s}
\end{aligned} \tag{C.24}$$

where the error event $\mathbf{e}_{13}$ occurs with the following probability

$$\begin{aligned}
P(\mathbf{e}_{13}) &= P(e_1 = 1)P(e_2 = 1)P(e_3 = 0)P(e_4 = 1) \\
&= p_{e,r1}p_{e,r2}(1 - p_{e,r3})p_{e,r4}
\end{aligned} \tag{C.25}$$

Table C.14 Codebook for Error Pattern $\mathbf{e}_{14} = (e_1, e_2, e_3, e_4) = (1, 0, 1, 1)$

				SM		TD
x_1	x_2	x_3	x_4	$p_1 = x_2$	$p_2 = x_2$	$p_0 = x_2$
0	0	0	0	0	0	0
0	0	0	1	0	0	0
0	0	1	0	0	0	0
0	1	0	0	1	1	1
1	0	0	0	0	0	0
0	0	1	1	0	0	0
0	1	0	1	1	1	1
1	0	0	1	0	0	0
0	1	1	0	1	1	1
1	0	1	0	0	0	0
1	1	0	0	1	1	1
1	1	1	0	1	1	1
1	1	0	1	1	1	1
1	0	1	1	0	0	0
0	1	1	1	1	1	1
1	1	1	1	1	1	1

The decoding error probability for error pattern $\mathbf{e}_{14} = (1, 0, 1, 1)$ is upper bounded by

$$\begin{aligned} P_E(\mathbf{e}_{14})^{\text{SM}} &\leq 3\left(\frac{1}{1+\gamma_s}\right) + \left(\frac{1}{1+\gamma_s}\right)\left(\frac{1}{1+2\gamma_r}\right) + 3\left(\frac{1}{1+\gamma_s}\right)^2 \\ &\quad + 3\left(\frac{1}{1+\gamma_s}\right)^2\left(\frac{1}{1+2\gamma_r}\right) + \left(\frac{1}{1+\gamma_s}\right)^3 + 3\left(\frac{1}{1+\gamma_s}\right)^3\left(\frac{1}{1+2\gamma_r}\right) \\ &\quad + \left(\frac{1}{1+\gamma_s}\right)^4\left(\frac{1}{1+2\gamma_r}\right) \sim \frac{3}{\gamma_s} \text{ as } \gamma_s, \gamma_r \to \infty \\ P_E(\mathbf{e}_{14})^{\text{TD}} &\leq 3\left(\frac{1}{1+\gamma_s}\right) + \left(\frac{1}{1+\gamma_s}\right)\left(\frac{1}{1+\gamma_r}\right)^2 + 3\left(\frac{1}{1+\gamma_s}\right)^2 \\ &\quad + 3\left(\frac{1}{1+\gamma_s}\right)^2\left(\frac{1}{1+\gamma_r}\right)^2 + \left(\frac{1}{1+\gamma_s}\right)^3 + 3\left(\frac{1}{1+\gamma_s}\right)^3\left(\frac{1}{1+\gamma_r}\right)^2 \\ &\quad + \left(\frac{1}{1+\gamma_s}\right)^4\left(\frac{1}{1+\gamma_r}\right)^2 \sim \frac{3}{\gamma_s} \end{aligned} \tag{C.26}$$

where the error event $\mathbf{e}_{14}$ occurs with the following probability

$$\begin{aligned} P(\mathbf{e}_{14}) &= P(e_1 = 1)P(e_2 = 0)P(e_3 = 1)P(e_4 = 1) \\ &= p_{e,r1}\ (1 - p_{e,r2})\ p_{e,r3}\ p_{e,r4} \end{aligned} \tag{C.27}$$

Table C.15 Codebook for Error Pattern $\mathbf{e}_{15} = (e_1, e_2, e_3, e_4) = (0, 1, 1, 1)$

				SM		TD
x_1	x_2	x_3	x_4	$p_1 = x_1$	$p_2 = x_1$	$p_0 = x_1$
0	0	0	0	0	0	0
0	0	0	1	0	0	0
0	0	1	0	0	0	0
0	1	0	0	0	0	0
1	0	0	0	1	1	1
0	0	1	1	0	0	0
0	1	0	1	0	0	0
1	0	0	1	1	1	1
0	1	1	0	0	0	0
1	0	1	0	1	1	1
1	1	0	0	1	1	1
1	1	1	0	1	1	1
1	1	0	1	1	1	1
1	0	1	1	1	1	1
0	1	1	1	0	0	0
1	1	1	1	1	1	1

The decoding error probability for error pattern $\mathbf{e}_{15} = (0, 1, 1, 1)$ is upper bounded by

$$\begin{aligned}
P_E(\mathbf{e}_{15})^{\text{SM}} &\le 3\left(\frac{1}{1+\gamma_s}\right) + \left(\frac{1}{1+\gamma_s}\right)\left(\frac{1}{1+2\gamma_r}\right) + 3\left(\frac{1}{1+\gamma_s}\right)^2 \\
&\quad + 3\left(\frac{1}{1+\gamma_s}\right)^2\left(\frac{1}{1+2\gamma_r}\right) + \left(\frac{1}{1+\gamma_s}\right)^3 + 3\left(\frac{1}{1+\gamma_s}\right)^3\left(\frac{1}{1+2\gamma_r}\right) \\
&\quad + \left(\frac{1}{1+\gamma_s}\right)^4\left(\frac{1}{1+2\gamma_r}\right) \sim \frac{3}{\gamma_s} \text{ as } \gamma_s, \gamma_r \to \infty \\
P_E(\mathbf{e}_{15})^{\text{TD}} &\le 3\left(\frac{1}{1+\gamma_s}\right) + \left(\frac{1}{1+\gamma_s}\right)\left(\frac{1}{1+\gamma_r}\right)^2 + 3\left(\frac{1}{1+\gamma_s}\right)^2 \\
&\quad + 3\left(\frac{1}{1+\gamma_s}\right)^2\left(\frac{1}{1+\gamma_r}\right)^2 + \left(\frac{1}{1+\gamma_s}\right)^3 + 3\left(\frac{1}{1+\gamma_s}\right)^3\left(\frac{1}{1+\gamma_r}\right)^2 \\
&\quad + \left(\frac{1}{1+\gamma_s}\right)^4\left(\frac{1}{1+\gamma_r}\right)^2 \sim \frac{3}{\gamma_s}
\end{aligned} \tag{C.28}$$

where the error event $\mathbf{e}_{15}$ occurs with the following probability

$$\begin{aligned}
P(\mathbf{e}_{15}) &= P(e_1 = 0)P(e_2 = 1)P(e_3 = 1)P(e_4 = 1) \\
&= (1 - p_{e,r1}) \prod_{i=2}^{4} p_{e,ri}
\end{aligned} \tag{C.29}$$

Table C.16 Codebook for Error Pattern $\mathbf{e}_{16} = (e_1, e_2, e_3, e_4) = (1, 1, 1, 1)$

				SM		TD
x_1	x_2	x_3	x_4	$p_1 = \varnothing$	$p_2 = \varnothing$	$p_0 = \varnothing$
0	0	0	0	$\varnothing$	$\varnothing$	$\varnothing$
0	0	0	1	$\varnothing$	$\varnothing$	$\varnothing$
0	0	1	0	$\varnothing$	$\varnothing$	$\varnothing$
0	1	0	0	$\varnothing$	$\varnothing$	$\varnothing$
1	0	0	0	$\varnothing$	$\varnothing$	$\varnothing$
0	0	1	1	$\varnothing$	$\varnothing$	$\varnothing$
0	1	0	1	$\varnothing$	$\varnothing$	$\varnothing$
1	0	0	1	$\varnothing$	$\varnothing$	$\varnothing$
0	1	1	0	$\varnothing$	$\varnothing$	$\varnothing$
1	0	1	0	$\varnothing$	$\varnothing$	$\varnothing$
1	1	0	0	$\varnothing$	$\varnothing$	$\varnothing$
1	1	1	0	$\varnothing$	$\varnothing$	$\varnothing$
1	1	0	1	$\varnothing$	$\varnothing$	$\varnothing$
1	0	1	1	$\varnothing$	$\varnothing$	$\varnothing$
0	1	1	1	$\varnothing$	$\varnothing$	$\varnothing$
1	1	1	1	$\varnothing$	$\varnothing$	$\varnothing$

The decoding error probability for error pattern $\mathbf{e}_{16} = (1, 1, 1, 1)$ is upper bounded by

$$\begin{aligned} P_E(\mathbf{e}_{16})^{\mathrm{SM}} &\le 4\left(\frac{1}{1+\gamma_s}\right) + 6\left(\frac{1}{1+\gamma_s}\right)^2 + 4\left(\frac{1}{1+\gamma_s}\right)^3 + \left(\frac{1}{1+\gamma_s}\right)^4 \\ &\sim \frac{4}{\gamma_s} \text{ as } \gamma_s, \gamma_r \to \infty \\ P_E(\mathbf{e}_{16})^{\mathrm{TD}} &\le 4\left(\frac{1}{1+\gamma_s}\right) + 6\left(\frac{1}{1+\gamma_s}\right)^2 + 4\left(\frac{1}{1+\gamma_s}\right)^3 + \left(\frac{1}{1+\gamma_s}\right)^4 \sim \frac{4}{\gamma_s} \end{aligned} \tag{C.30}$$

where the error event $\mathbf{e}_{16}$ occurs with the following probability

$$\begin{aligned} P(\mathbf{e}_{16}) &= P(e_1 = 1)P(e_2 = 1)P(e_3 = 1)P(e_4 = 1) \\ &= \prod_{i=1}^{4} p_{e,ri} \end{aligned} \tag{C.31}$$

The corresponding outage probability for each error pattern is given as follows.

Table C.17 Outage Probability $P(\text{out}|\mathbf{e}_i)$ for error pattern $\mathbf{e}_i$, $i = 1, \cdots, 16$

$\mathbf{e}_i$	$P(\mathbf{e}_i)$	SM	TD
$\mathbf{e}_1$	$\prod_{i=1}^{4}(1-p_{ri})$	$p_{ds}\left[1-(1-p_{\text{SM}})\cdot(1-p_{ds})\right]$	$p_{ds}\left[1-(1-p_{\text{TD}})\cdot(1-p_{ds})^3\right]$
$\mathbf{e}_2$	$\prod_{i=1}^{3}(1-p_{ri})p_{r4}$	$p_{ds}\left[1-(1-p_{\text{SM}})\cdot(1-p_{ds})\right]$	$p_{ds}\left[1-(1-p_{\text{TD}})\cdot(1-p_{ds})^2\right]$
$\mathbf{e}_3$	$\prod_{i=1,2,4}(1-p_{ri})p_{r3}$	$p_{ds}\left[1-(1-p_{\text{SM}})\cdot(1-p_{ds})\right]$	$p_{ds}\left[1-(1-p_{\text{TD}})\cdot(1-p_{ds})^2\right]$
$\mathbf{e}_4$	$\prod_{i=1,3,4}(1-p_{ri})p_{r2}$	$p_{ds}\cdot p_{\text{SM}}$	$p_{ds}\left[1-(1-p_{\text{TD}})\cdot(1-p_{ds})^2\right]$
$\mathbf{e}_5$	$\prod_{i=2,3,4}(1-p_{ri})p_{r1}$	p_{ds}	p_{ds}
$\mathbf{e}_6$	$\prod_{i=1,2}(1-p_{ri})\prod_{j=3,4}p_{rj}$	$p_{ds}\left[1-(1-p_{\text{SM}})\cdot(1-p_{ds})\right]$	$p_{ds}\left[1-(1-p_{\text{TD}})\cdot(1-p_{ds})\right]$
$\mathbf{e}_7$	$\prod_{i=1,3}(1-p_{ri})\prod_{j=2,4}p_{rj}$	$p_{ds}\cdot p_{\text{SM}}$	$p_{ds}\left[1-(1-p_{\text{TD}})\cdot(1-p_{ds})\right]$
$\mathbf{e}_8$	$\prod_{i=2,3}(1-p_{ri})\prod_{j=1,4}p_{rj}$	p_{ds}	p_{ds}
$\mathbf{e}_9$	$\prod_{i=1,4}(1-p_{ri})\prod_{j=2,3}p_{rj}$	$p_{ds}\cdot p_{\text{SM}}$	$p_{ds}\left[1-(1-p_{\text{TD}})\cdot(1-p_{ds})\right]$
$\mathbf{e}_{10}$	$\prod_{i=2,4}(1-p_{ri})\prod_{j=1,3}p_{rj}$	p_{ds}	p_{ds}
$\mathbf{e}_{11}$	$\prod_{i=3,4}(1-p_{ri})\prod_{j=1,2}p_{rj}$	p_{ds}	p_{ds}
$\mathbf{e}_{12}$	$\prod_{i=1,2,3}p_{ri}(1-p_{r4})$	p_{ds}	p_{ds}
$\mathbf{e}_{13}$	$\prod_{i=1,2,4}p_{ri}(1-p_{r3})$	p_{ds}	p_{ds}
$\mathbf{e}_{14}$	$\prod_{i=1,3,4}p_{ri}(1-p_{r2})$	p_{ds}	p_{ds}
$\mathbf{e}_{15}$	$\prod_{i=2,3,4}p_{ri}(1-p_{r1})$	$p_{ds}\cdot p_{\text{SM}}$	$p_{ds}\cdot p_{\text{TD}}$
$\mathbf{e}_{16}$	$\prod_{i=1}^{4}p_{ri}$	p_{ds}	p_{ds}

APPENDIX D. EIGENVALUES OF $\Delta X_{RD} \cdot \Delta X_{RD}^H$

In this appendix, we evaluate the eigenvalues of $\Delta X_{RD} \cdot \Delta X_{RD}^H$ for SM and GC mode. Without loss of generality, assume the parity bit $v_{a,k} = 0$ for all k. Then we have

$$\begin{aligned} X_{a,SM} &= \begin{bmatrix} y_{a,1} & y_{a,3} \\ y_{a,2} & y_{a,4} \end{bmatrix} = \begin{bmatrix} \sqrt{E_r} & \sqrt{E_r} \\ \sqrt{E_r} & \sqrt{E_r} \end{bmatrix} \\ X_{a,GC} &= \frac{\sqrt{E_r}}{\sqrt{5}} \begin{bmatrix} \alpha(1+\theta) & \alpha(1+\theta) \\ \bar{\alpha} i(1+\bar{\theta}) & \bar{\alpha}(1+\bar{\theta}) \end{bmatrix} \end{aligned} \tag{D.1}$$

where $y_{a,k} = (-1)^{v_{a,k}} \sqrt{E_r}$ is BPSK constellation corresponding to the parity bit $v_{a,k}$.

If $\{v_{a,l} \oplus v_{b,l}, l = 1, \cdots, 4\}$ is given by $(0, 0, 0, 1)$, it follows that

$$\begin{aligned} X_{b,SM} = \begin{bmatrix} \sqrt{E_r} & \sqrt{E_r} \\ \sqrt{E_r} & -\sqrt{E_r} \end{bmatrix}, \quad \Delta X_{SM} = X_{a,SM} - X_{b,SM} = \begin{bmatrix} 0 & 0 \\ 0 & 2\sqrt{E_r} \end{bmatrix} \\ \Delta X_{SM} \Delta X_{SM}^H = \begin{bmatrix} 0 & 0 \\ 0 & 4E_r \end{bmatrix} \end{aligned} \tag{D.2}$$

for SM mode and

$$\begin{aligned} \Delta X_{GC} &= \frac{2\sqrt{E_r}}{\sqrt{5}} \begin{bmatrix} 0 & \alpha\theta \\ \bar{\alpha} i \bar{\theta} & 0 \end{bmatrix} \\ \Delta X_{GC} \Delta X_{GC}^H &= \frac{4E_r}{5} \begin{bmatrix} |\alpha|^2\theta^2 & 0 \\ 0 & |\bar{\alpha}|^2\bar{\theta}|^2 \end{bmatrix} = \frac{4E_r}{\sqrt{5}} \begin{bmatrix} \theta & 0 \\ 0 & -\theta \end{bmatrix} \end{aligned} \tag{D.3}$$

for GC mode where we used the following equalities.

$$|\alpha|^2\theta^2 = \sqrt{5}\theta, \quad |\bar{\alpha}|^2\bar{\theta}|^2 = -\sqrt{5}\bar{\theta} \tag{D.4}$$

The eigenvalues for other $\{v_{a,l} \oplus v_{b,l}, l = 1, \cdots, 4\}$ combinations can be derived similarly.

APPENDIX E. $g_{GC}(\gamma)$ FOR GOLDEN CODE

$g_{GC}(\gamma)$ for GC mode is given by

$$
\begin{aligned}
&E_{\{\lambda_n\}}\left[\prod_{n=1}^{n_R}\left(1+d_{r,d}^{-\alpha}\lambda_n/4N_0\right)^{-n_D}\right] \\
&=\frac{1}{2^L}\left[1+\frac{4}{\left[(1+\theta\gamma_r/\sqrt{5})(1-\bar{\theta}\gamma_r/\sqrt{5})\right]^{n_D}}+\frac{4}{\left[(1+(1+\sqrt{\tfrac{3}{5}})\gamma_r)(1+(1-\sqrt{\tfrac{3}{5}})\gamma_r)\right]^{n_D}}\right. \\
&+\frac{2}{\left[(1+(1+2\theta)\gamma_r/\sqrt{5})(1-(1+2\bar{\theta})\gamma_r/\sqrt{5})\right]^{n_D}}+\frac{4}{\left[(1+(6+\sqrt{\tfrac{148}{5}})\gamma_r)(1+(6-\sqrt{\tfrac{148}{5}})\gamma_r)\right]^{n_D}} \\
&\left.+\frac{1}{\left[(1+(2\sqrt{5}+3\sqrt{2})\gamma_r)(1+(2\sqrt{5}-3\sqrt{2})\gamma_r\right]^{n_D}}\right]\cdot\Bigg|_{L_{\mathrm{GC}}=4}
\end{aligned}
\tag{E.1}
$$

APPENDIX F. THE ACCURACY OF (6.16) AND (6.17)

In this appendix we discuss the accuracy of the approximations

$$x_k(t-\tau) \simeq x_k(t), \quad k = 1, \cdots, K \tag{F.1}$$

and

$$n_i(t-\tau) \simeq n_i(t), \quad i = 1, \cdots, N_R. \tag{F.2}$$

The accuracy of the approximation in (F.1) can be measured by the normalized mean square error (MSE)

$$\frac{E[|x_k(t) - x_k(t-\tau)|^2]}{R_{xx}(0)} = 2[1 - R_{xx}(\tau)/R_{xx}(0)] \tag{F.3}$$

where $R_{xx(\tau)} = E[x_k(t)x_k^*(t-\tau)]$ is the autocorrelation function of $x_k(t)$. For rectangular pulse shaping, it can be shown that

$$R_{xx}(\tau) = R_{xx}(0)\left(1 - \frac{|\tau|}{T}\right), \quad \text{for } |\tau| < T \tag{F.4}$$

where T is the symbol duration [76]. Therefore, the normalized MSE is

$$\begin{aligned} \frac{E[|x_k(t) - x_k(t-\tau)|^2]}{R_{xx}(0)} &= 2\left[1 - \frac{R_{xx}(\tau)}{R_{xx}(0)}\right] && \text{(F.5)} \\ &= \frac{2|\tau|}{T}, \quad \text{for } |\tau| < T && \text{(F.6)} \\ &= \frac{3}{2f_cT} && \text{(F.7)} \\ &\ll 1. && \text{(F.8)} \end{aligned}$$

For example, when f_c is 1GHz and the symbol duration T is 10^{-6} second, corresponding to the symbol rate of 1M symbols per second, the normalized MSE is 1.5×10^{-3}, which is negligibly small.

For raised-cosine pulse shaping, the autocorrelation function of $x_k(t)$ is given by [77]

$$R_{xx}(\tau) = T\left[\mathrm{sinc}(\tau/T)\cdot\frac{\cos(\alpha\pi\tau/T)}{1-(2\alpha\tau/T)^2} - \frac{\alpha}{4}\cdot\mathrm{sinc}(\alpha\tau/T)\cdot\frac{\cos(\pi\tau/T)}{1-(\alpha\tau/T)^2}\right], \tag{F.9}$$

where $\mathrm{sinc}(x) = \sin(\pi x)/(\pi x)$. For $f_c = 1\mathrm{GHz}$ and $T = 10^{-5}$ the normalized MSE is 2.1×10^{-4}, and for $f_c = 1\mathrm{GHz}$ and $T = 10^{-6}$ it is zero. Hence, the accuracy of the approximation in (F.1) is even higher for the raised-cosine pulse shaping.

A similar argument can be made for (F.2). Suppose $n_i(t)$ is a low-pass, wide-sense stationary random process with a flat power spectral density over a bandwidth of W, where W is much smaller than f_c. Then, it can be shown that $R_{n_in_i}(\tau) = R_{n_in_i}(0)\sin(\pi\tau W)/(\pi\tau W)$. Hence, the normalized MSE is

$$\frac{E[|n_i(t)-n_i(t-\tau)|^2]}{R_{n_in_i}(0)} = 2\left[1-\frac{\sin(\pi\tau W)}{\pi\tau W}\right] \tag{F.10}$$

$$\approx \frac{1}{3}(\pi\tau W)^2 \tag{F.11}$$

$$\ll 1 \tag{F.12}$$

where the approximation in (F.11) follows from the Taylor expansion $\sin(x) \approx x - x^3/6$. Since, for $\tau = 3/(4f_c)$, $\tau W = 3W/(4f_c) \ll 1$, the approximation error in (F.2) is also negligibly small. For example, when f_c is 1GHz and the symbol duration T is 10^{-6} second, corresponding to the bandwidth W of 10^6. the normalized MSE is 1.85×10^{-6}.

APPENDIX G. THE ACCURACY OF (6.22) AND (6.23)

In this appendix we discuss the accuracy of the approximations in (6.22) and (6.23). If we let

$$\Delta x_k(t) = x_k(t-\tau) - x_k(t), \quad k = 1, \cdots, K \tag{G.1}$$

$$\Delta n_i(t) = n_i(t-\tau) - n_i(t), \quad i = 1, \cdots, N_R \tag{G.2}$$

then it follows from (6.14), (6.15), and (6.20) that

$$\begin{aligned} y_1(t) &= Re\{[x_1(t) + w_{11}n_1(t) + w_{21}n_2(t)]e^{j2\pi f_c t}\} \\ &+Re\{jw_{11,I}[h_{11}\Delta x_1(t) + h_{21}\Delta x_2(t) + \Delta n_1(t)]e^{j2\pi f_c t}\} \\ &+Re\{jw_{21,I}[h_{12}\Delta x_1(t) + h_{22}\Delta x_2(t) + \Delta n_2(t)]e^{j2\pi f_c t}\}. \end{aligned} \tag{G.3}$$

Down converting $y_1(t)$ into the baseband (through the RF chain) yields

$$\begin{aligned} z_1(t) &= [x_1(t) + w_{11}n_1(t) + w_{21}n_2(t)] \\ &+jw_{11,I}[h_{11}\Delta x_1(t) + h_{21}\Delta x_2(t) + \Delta n_1(t)] \\ &+jw_{21,I}[h_{12}\Delta x_1(t) + h_{22}\Delta x_2(t) + \Delta n_2(t)] \end{aligned} \tag{G.4}$$

where the first term on the right hand side of (G.4) is for the conventional receiver and the second and the third terms are present only for the proposed receiver. Therefore, the signal-to-interference-plus-noise-ratio (SINR) for the conventional receiver, given $\mathbf{h}$, is given by

$$\text{SINR}_c(\mathbf{h}) = \frac{\gamma}{|w_{11}|^2 + |w_{21}|^2} \tag{G.5}$$

where $\gamma = E[|x_1(t)|^2]/E[|n_i(t)|^2]$ is the signal-to-noise ratio per receive antenna, and that for the proposed receiver is given by

$$\begin{aligned}
&\mathrm{SINR}_p(\mathbf{h}) \\
= \;& E[|x_1(t)|^2]/\{(|w_{11}|^2+|w_{21}|^2)E[|n_i(t)|^2] \\
&+(|w_{11,I}|^2E[|\Delta n_1(t)|^2]+|w_{21,I}|^2E[|\Delta n_2(t)|^2]) \\
&+(|w_{11,I}h_{11}+w_{21,I}h_{12}|^2)E[|\Delta x_1(t)|^2] \\
&+(|w_{11,I}h_{21}+w_{21,I}h_{22}|^2)E[|\Delta x_2(t)|^2]\} \\
= \;& \{(|w_{11}|^2+|w_{21}|^2)\gamma^{-1} \\
&+(|w_{11,I}|^2+|w_{21,I}|^2)(\pi\tau W)^2/3\cdot\gamma^{-1} \\
&+(|w_{11,I}h_{11}+w_{21,I}h_{12}|^2 \\
&+|w_{11,I}h_{21}+w_{21,I}h_{22}|^2)\cdot 2|\tau|/T\}^{-1}
\end{aligned} \tag{G.6}$$

where we used the equalities $E[|\Delta x_i(t)|^2]/E[|x_i(t)|^2] = 2|\tau|/T$ and $E[|\Delta n_i(t)|^2]/E[|n_i(t)|^2] \approx (\pi\tau T)^2/3$. Hence, it follows from (G.5) and (G.6) that the ratio between $\mathrm{SINR_c}$ and $\mathrm{SINR_p}$, given $\mathbf{h}$, is given by

$$\begin{aligned}
&\frac{\mathrm{SINR_c}(\mathbf{h})}{\mathrm{SINR_p}(\mathbf{h})} \\
= \;& 1+\frac{|w_{11,I}|^2+|w_{21,I}|^2}{|w_{11}|^2+|w_{21}|^2}\frac{(\pi\tau W)^2}{3} \\
&+\frac{|w_{11,I}h_{11}+w_{21,I}h_{12}|^2+|w_{11,I}h_{21}+w_{21,I}h_{22}|^2}{|w_{11}|^2+|w_{21}|^2} \\
&\cdot\frac{2|\tau|\gamma}{T}.
\end{aligned} \tag{G.7}$$

For i.i.d. Rayleigh flat fading channels, Monte Carlo simulation shows that

$$E\left[\frac{|w_{11,I}|^2+|w_{21,I}|^2}{|w_{11}|^2+|w_{21}|^2}\right] = \frac{1}{2} \tag{G.8}$$

$$E\left[\frac{|w_{11,I}h_{11}+w_{21,I}h_{12}|^2+|w_{11,I}h_{21}+w_{21,I}h_{22}|^2}{|w_{11}|^2+|w_{21}|^2}\right] = \frac{2}{3}. \tag{G.9}$$

Hence, it follows from (G.7)-(G.9) that the average ratio between $\mathrm{SINR_c}$ and $\mathrm{SINR_p}$ is given by

$$\frac{\mathrm{SINR_c}}{\mathrm{SINR_p}} = 1+\frac{1}{6}(\pi\tau W)^2+\frac{4}{3}\frac{|\tau|\gamma}{T}. \tag{G.10}$$

BIBLIOGRAPHY

[1] J. N. Laneman and G. W. Wornell, "Distributed Space-Time Coded Protocols for Exploiting Cooperative Diversity in Wireless Networks", in *IEEE Trans. Inform. Theory*, vol. 49, no. 10, pp. 2415-2425, Oct. 2003.

[2] G. Kramer and A. J. vanWijngaarden, "On the white Gaussian multiple-access relay channel", in *Proc. 2000 IEEE Int. Symp. Inform. Theory*, pp.40, Jun. 2000.

[3] L. Sankaranarayanan, G. Kramer, and N. B. Mandayam, "Capacity theorems for the multiple-access relay channel", in *Proc. of Allerton Conference on Communication, Control, and Computing*, Oct. 2004.

[4] K. Azarian, H. E. Gamal, and P. Schniter, "On the optimality of the ARQ-DDF protocol", *IEEE Trans. Inform. Theory*, pp. 1718 - 1724, Apr. 2006.

[5] D. Chen and J.N.Laneman, "The diversity-multiplexing tradeoff for multiple-access relay channel", in *Proc. of Conf. on Information Sciences and Systems (CISS)*, Mar. 2006.

[6] M. Yuksel and E. Erkip. "Multi-antenna cooperative wireless systems: A diversity multiplexing tradeoff perspective", *IEEE Trans. Inform. Theory*, pp. 3371 - 3393, Oct. 2007.

[7] N. Prasad and X. Wang, "Outage minimization and fair rate allocation for the multiple access relay channel", in *Proc. of IEEE ISIT*, pp. 1333 - 1337, 2008.

[8] J.N. Laneman, D.N.C. Tse, and G.W. Wornell, "Cooperative diversity in wireless networks: Efficient protocols and outage behavior", in *IEEE Trans. Inform. Theory*, pp. 3062 - 3180, Dec. 2004.

[9] K. Azarian, H. El Gamal, and P. Schniter, "On the achievable diversity-multiplexing tradeoff in half-duplex cooperative channels", in *IEEE Trans. Inform. Theory*, vol. 51, pp. 41524172, Dec. 2005.

[10] S. Yang and J.-C. Belfiore, "Optimal spacetime codes for the MIMO amplify-and-forward cooperative channel", in *IEEE Trans. Inform. Theory*, vol. 53, pp. 647663, Feb. 2007.

[11] M. Yukselc and E. Erkip, "Multiple-Antenna Cooperative Wireless Systems: A Diversity-Multiplexing Tradeoff Perspective", in *IEEE Trans. Inform. Theory*, vol.53, pp.3371-3393, Oct. 2007.

[12] Y. Chen, S. Kishore, and J. Li, "Wireless diversity through network coding", in *Proc. of IEEE Wireless Communications and Networking Conference (WCNC)*, May 2006.

[13] X. Bao and J. Li, "Matching code-on-graph with network-on-graph: adaptive network coding for wireless relay networks", in *Proc. of Allerton Conference on Communication, Control, and Computing*, Sept.2005.

[18] C. Hausl and P.Dupraz, "Joint network-channel coding for the multiple-access relay channel", in *Proc. of IEEE SECON*, pp. 817 - 822, 2006.

[19] A. Chakrabarti, A. Baynast, A.Sabharwal, and B. Aazhang, "Low density parity check codes for the relay channel", *IEEE JSAC*, pp. 280-291, Feb. 2007.

[16] S.W. Kim, "Tradeoffs in random network coded multiple-access relay networks", *IEEE, Wireless Network Coding Conference (WiNC)*, pp.1-6, June 2010.

[17] B. Xingkai, L. Jing, "Adaptive network coded cooperation (ANCC) for wireless relay networks: matching code-on-graph with network-on-graph", *IEEE Trans. Wireless Communications*, vol.7, pp.574-583, Feb. 2008.

[18] F. Ono and K. Sakaguchi, "Space time coded MIMO network coding", *Personal, Indoor and Mobile Radio Communications (PIMRC)*, pp.1-5, Sept. 2008.

[19] H. Shiwen, L. Chunguo, and Y. Luxi, "Lattice reduction aided MIMO two way relay network coding", *IEEE 10th International Conference on Signal Processing (ICSP)*, pp.1471-1474, Oct. 2010.

[20] M. Vajapeyam and U. Mitra, "A hybrid space-time coding scheme for cooperative networks", in *Proc. Allerton Conf.*, Monticello, IL, Sep. 2004.

[21] A. Bletsas, A. Khisti, D. Reed, and A. Lippman, "A simple cooperative diversity method based on network path selection", in *IEEE J. Sel. Areas Commun.*, vol. 24, pp. 659672, Mar. 2006.

[22] D.H. Woldegebreal and H. Karl, "Multiple-Access Relay Channel with Network Coding and Non-Ideal Source-Relay Channels", in *ISWCS 2007*, pp.732-736, 17-19 Oct. 2007

[23] S. W. Peters and R. W. Heath, Jr., "Switching between antenna selection and spatial multiplexing in the nonregenerative MIMO relay channel", in*Proc. Asilomar Conf. Signals, Syst., Comput., Pacific Grove, CA*, Oct. 2008.

[24] K.T. Truong and R.W. Heath, "Multimode Antenna Selection for MIMO Amplify-and-Forward Relay Systems", in *IEEE Trans. Signal Processing*, vol.58, pp.5845-5859, Nov. 2010

[25] E. M. Yeh and R. Berry, "Throughput optimal control of cooperative relay networks", in *Proc. of International Symposium on Information Theory*, pp. 1206–1210, 2005.

[26] H. Ochiai, P. Mitran, V. Tarokh, "Variable-Rate Two-Phase Collaborative Communication Protocols for Wireless Networks", in *IEEE Trans. Inform. Theory*, vol.52, pp.4299-4313, Sept. 2006

[84] Y. Chen, S. Kishore, and J. Li, "Wireless diversity through network coding", in *Proc. of IEEE Wireless Communications and Networking Conference (WCNC)*, May 2006.

[85] X. Bao and J. Li, "Matching code-on-graph with network-on-graph: adaptive network coding for wireless relay networks", in *Proc. of Allerton Conference on Communication, Control, and Computing*, Sept.2005.

[86] S.W. Kim, "Tradeoffs in random network coded multiple-access relay networks", *IEEE, Wireless Network Coding Conference (WiNC)*, pp.1-6, June 2010.

[30] B. Xingkai, L. Jing, "Adaptive network coded cooperation (ANCC) for wireless relay networks: matching code-on-graph with network-on-graph", *IEEE Trans. Wireless Communications*, vol.7, pp.574-583, Feb. 2008.

[87] F. Ono and K. Sakaguchi, "Space time coded MIMO network coding", *Personal, Indoor and Mobile Radio Communications (PIMRC)*, pp.1-5, Sept. 2008.

[88] H. Shiwen, L. Chunguo, and Y. Luxi, "Lattice reduction aided MIMO two way relay network coding", *IEEE 10th International Conference on Signal Processing (ICSP)*, pp.1471-1474, Oct. 2010.

[89] M. Vajapeyam and U. Mitra, "A hybrid space-time coding scheme for cooperative networks", in *Proc. Allerton Conf.*, Monticello, IL, Sep. 2004.

[90] A. Bletsas, A. Khisti, D. Reed, and A. Lippman, "A simple cooperative diversity method based on network path selection", in *IEEE J. Sel. Areas Commun.*, vol. 24, pp. 659672, Mar. 2006.

[91] D.H. Woldegebreal and H. Karl, "Multiple-Access Relay Channel with Network Coding and Non-Ideal Source-Relay Channels", in *ISWCS 2007*, pp.732-736, 17-19 Oct. 2007

[92] S. W. Peters and R. W. Heath, Jr., "Switching between antenna selection and spatial multiplexing in the nonregenerative MIMO relay channel", in*Proc. Asilomar Conf. Signals, Syst., Comput., Pacific Grove, CA*, Oct. 2008.

[93] K.T. Truong and R.W. Heath, "Multimode Antenna Selection for MIMO Amplify-and-Forward Relay Systems", in *IEEE Trans. Signal Processing*, vol.58, pp.5845-5859, Nov. 2010

[38] E. M. Yeh and R. Berry, "Throughput optimal control of cooperative relay networks", in *Proc. of International Symposium on Information Theory*, pp. 1206–1210, 2005.

[39] H. Ochiai, P. Mitran, V. Tarokh, "Variable-Rate Two-Phase Collaborative Communication Protocols for Wireless Networks", in *IEEE Trans. Inform. Theory*, vol.52, pp.4299-4313, Sept. 2006

[94] D. Tse and P. Viswanath, "Fundamentals of Wireless Communication", Cambridge University Press, 2005

[95] T. Cover, R. McEliece, and E. Posner, "Asynchronous multiple-access channel capacity", in *IEEE Trans. Inform. Theory*, vol.27, pp.409-413, July 1981

[78] G. Kramer and A. J. vanWijngaarden, "On the white Gaussian multiple-access relay channel", in *Proc. 2000 IEEE Int. Symp. Inform. Theory*, pp.40, Jun. 2000.

[79] L. Sankaranarayanan, G. Kramer, and N. B. Mandayam, "Capacity theorems for the multiple-access relay channel", in *Proc. of Allerton Conference on Communication, Control, and Computing*, Oct. 2004.

[44] K. Azarian, H. E. Gamal, and P. Schniter, "On the optimality of the ARQ-DDF protocol", *IEEE Trans. Inform. Theory*, pp. 1718 - 1724, Apr. 2006.

[45] D. Chen and J.N.Laneman, "The diversity-multiplexing tradeoff for multiple-access relay channel", in *Proc. of Conf. on Information Sciences and Systems (CISS)*, Mar. 2006.

[46] M. Yuksel and E. Erkip. "Multi-antenna cooperative wireless systems: A diversity multiplexing tradeoff perspective", *IEEE Trans. Inform. Theory*, pp. 3371 - 3393, Oct. 2007.

[47] N. Prasad and X. Wang, "Outage minimization and fair rate allocation for the multiple access relay channel", in *Proc. of IEEE ISIT*, pp. 1333 - 1337, 2008.

[84] Y. Chen, S. Kishore, and J. Li, "Wireless diversity through network coding", in *Proc. of IEEE Wireless Communications and Networking Conference (WCNC)*, May 2006.

[85] X. Bao and J. Li, "Matching code-on-graph with network-on-graph: adaptive network coding for wireless relay networks", in *Proc. of Allerton Conference on Communication, Control, and Computing*, Sept.2005.

[87] C. Hausl and P.Dupraz, "Joint network-channel coding for the multiple-access relay channel", in *Proc. of IEEE SECON*, pp. 817 - 822, 2006.

[88] A. Chakrabarti, A. Baynast, A.Sabharwal, and B. Aazhang, "Low density parity check codes for the relay channel", *IEEE JSAC*, pp. 280-291, Feb. 2007.

[86] S.W. Kim, "Tradeoffs in random network coded multiple-access relay networks", *IEEE, Wireless Network Coding Conference (WiNC)*, pp.1-6, June 2010.

[53] L. Luzzi, G. R.B. Othman, J.C. Belfiore, E. Viterbo, "Golden space-time block coded modulation" *Information Theory Workshop*, pp.86-90 May 2008

[54] R. W. Heath, Jr. and A. J. Paulraj, "Switching between diversity and multiplexing in MIMO systems", *IEEE Trans. on Communications*, vol. 53, no. 6, pp. 962-968, June 2005.

[55] L. Mroueh, S. Rouquette-Leveil, G. Rekaya-Ben Othman, J.C. Belfiore, "On the performance of the Golden code in BICM-MIMO and in IEEE 802.11n cases", in *Asilomar Conference on Signals, Systems and Computers (ACSSC)*, pp.1544 - 1548, Nov. 2007.

[56] M. K. Simon and M. S. Alouini, "Digital Communication over fading channels: A Unified Approach to Performance Analysis", Wiley, 2000.

[57] V. Tarokh, N. Seshadri, A.R. Calderbank, "Space-time codes for high data rate wireless communication: performance criterion and code construction", *IEEE Transactions on Information Theory*, vol.44, no.2, pp.744-765, Mar 1998.

[58] D. Gesbert, M. Shafi, D. Shiu, P. Smith, and A. Naguib, "From theory to practice: An overview of space-time coded MIMO wireless systems", *IEEE J. Select. Areas. Commun.*, pp. 281 - 302, Apr. 2003.

[59] J. H. Winter, "Smart antennas for wireless systems", *IEEE Personal Commun. Mag.*, vol. 5, pp. 23 - 27, Feb. 1998.

[60] G. D. Golden, G. J. Foschini, R. A. Valenzuela, and P. W. Wolniansky, "Detection algorithm and initial laboratory results using the V-BLAST space-time communication architecture,", *Electron. Lett.*, vol. 35, no. 1, pp. 14 - 15, 1999.

[61] S. W. Kim and K. P. Kim, "Log-likelihood-ratio-based detection ordering in V-BLAST", *IEEE Trans. Commun.*, vol. 54, no. 2, pp. 302 - 307, Feb. 2006.

[62] R. Heath and A. Paulraj, "Switching between diversity and multiplexing in MIMO systems", *IEEE Trans. Commun.*, vol. 53, no. 6, pp. 962 - 968, June 2005.

[63] V. Tarokh, A. Naguib, N. Seshadri and A. R. Caldebank, "Combined Array Processing and Space-Time Coding", *IEEE Trans. Inform. Theory*, vol. 45, no. 4, pp. 1121 - 1128, may 1999.

[64] V. Kuhn, "Wireless Communications over MIMO Channels", Wiley, pp. 306, 2006.

[65] G. H. Golub and C. F. Van Loan, "Matrix Computations", The John Hopkisns Univ. Press, pp. 219, 1996.

[66] J.H.Winters, "Smart antennas for wireless systems," *IEEE Personal Communications*, Volume: 5 , Issue: 1 pp. 23-27, Feb. 1998.

[67] X.Zhang, A.F.Molish, and S-Y Kung, "Variable-phase-shift-based RF-baseband codesign for MIMO antenna selection," *IEEE Tr. on Signal Processing*, vol. 53, no. 11, pp. 4091-4103, Nov. 2005.

[68] F. Tzeng, A. Jahanian, and P. Heydari, "A universal code-modulated path-sharing multi-antenna receiver," *Proc. of IEEE Wireless Comm. and Networking Conf.*, Apr. 2008.

[69] H. Rafati and B. Razavi, "A receiver architecture for dual-antenna systems," *IEEE J. Solid-State Circuits*, vol. 42, no. 6, pp. 1291-1299, Jun. 2007.

[70] E. Biglieri, "Coding for Wireless Channels (Information Technology: Transmission, Processing and Storage) ," Springer, 2005.

[71] T. L. Marzetta, "BLAST training: estimating channel characteristics for high-capacity space-time wireless," *Proc. 37th Annual Allerton Conference Communications, Control, and Computing*, pp. 958-966, 1999.

[72] B. Hassibi and B. M. Hochwald, "How much training is needed in multiple-antenna wireless links?," *IEEE Tr. Inf. Theory*, vol. 49, no. 4, pp. 951-963, Apr. 2003.

[73] C. Wang, K. S. Au, R. D. Murch, W. H. Mow, R. S. Cheng, and V. Lau, "On the Performance of the MIMO Zero-Forcing Receiver in the Presence of Channel Estimation Error," *IEEE Tr. Wireless Commun.*, vol. 6, no. 3, pp. 805-810, March 2007.

[74] A. Gorokhov, D. A. Gore, A. J. Paulraj, "Receive antenna selection for MIMO spatial multiplexing: theory and algorithms," *IEEE Tr. Signal Processing*, vol. 51, no. 11, pp. 2796-2807, Nov 2003.

[75] S. Sanayei, A. Nosratinia, "Antenna selection in MIMO systems," *IEEE Communications Magazine*, vol. 42, no. 10, pp. 74-80, Oct. 2004.

[76] B. P. Lathi, Z. Ding, "Modern Digital and Analog Communication Systems," Oxford University Press, 2009.

[77] L. M. Tavares, G. N. Tavares, "Comments on "Performance of Asynchronous Band-Limited DS/SSMA Systems"," *IEICE Tr. on Commun.*, vol. E81-B, no. 9, pp. 1782-1784, Sept. 1998.

[78] G. Kramer and A. J. vanWijngaarden, "On the white Gaussian multiple-access relay channel", in *Proc. 2000 IEEE Int. Symp. Inform. Theory*, pp.40, Jun. 2000.

[79] L. Sankaranarayanan, G. Kramer, and N. B. Mandayam, "Capacity theorems for the multiple-access relay channel", in *Proc. of Allerton Conference on Communication, Control, and Computing*, Oct. 2004.

[80] J.N. Laneman, D.N.C. Tse, and G.W. Wornell, "Cooperative diversity in wireless networks: Efficient protocols and outage behavior", in *IEEE Trans. Inform. Theory*, pp. 3062 - 3180, Dec. 2004.

[81] K. Azarian, H. El Gamal, and P. Schniter, "On the achievable diversity-multiplexing tradeoff in half-duplex cooperative channels", in *IEEE Trans. Inform. Theory*, vol. 51, pp. 41524172, Dec. 2005.

[82] S. Yang and J.-C. Belfiore, "Optimal spacetime codes for the MIMO amplify-and-forward cooperative channel", in *IEEE Trans. Inform. Theory*, vol. 53, pp. 647663, Feb. 2007.

[83] M. Yukselc and E. Erkip, "Multiple-Antenna Cooperative Wireless Systems: A Diversity-Multiplexing Tradeoff Perspective", in *IEEE Trans. Inform. Theory*, vol.53, pp.3371-3393, Oct. 2007.

[84] Y. Chen, S. Kishore, and J. Li, "Wireless diversity through network coding", in *Proc. of IEEE Wireless Communications and Networking Conference (WCNC)*, May 2006.

[85] X. Bao and J. Li, "Matching code-on-graph with network-on-graph: adaptive network coding for wireless relay networks", in *Proc. of Allerton Conference on Communication, Control, and Computing*, Sept.2005.

[86] S.W. Kim, "Tradeoffs in random network coded multiple-access relay networks", *IEEE, Wireless Network Coding Conference (WiNC)*, pp.1-6, June 2010.

[87] F. Ono and K. Sakaguchi, "Space time coded MIMO network coding", *Personal, Indoor and Mobile Radio Communications (PIMRC)*, pp.1-5, Sept. 2008.

[88] H. Shiwen, L. Chunguo, and Y. Luxi, "Lattice reduction aided MIMO two way relay network coding", *IEEE 10th International Conference on Signal Processing (ICSP)*, pp.1471-1474, Oct. 2010.

[89] M. Vajapeyam and U. Mitra, "A hybrid space-time coding scheme for cooperative networks", in *Proc. Allerton Conf.*, Monticello, IL, Sep. 2004.

[90] A. Bletsas, A. Khisti, D. Reed, and A. Lippman, "A simple cooperative diversity method based on network path selection", in *IEEE J. Sel. Areas Commun.*, vol. 24, pp. 659672, Mar. 2006.

[91] D.H. Woldegebreal and H. Karl, "Multiple-Access Relay Channel with Network Coding and Non-Ideal Source-Relay Channels", in *ISWCS 2007*, pp.732-736, 17-19 Oct. 2007

[92] S. W. Peters and R. W. Heath, Jr., "Switching between antenna selection and spatial multiplexing in the nonregenerative MIMO relay channel", in *Proc. Asilomar Conf. Signals, Syst., Comput., Pacific Grove, CA*, Oct. 2008.

[93] K.T. Truong and R.W. Heath, "Multimode Antenna Selection for MIMO Amplify-and-Forward Relay Systems", in *IEEE Trans. Signal Processing*, vol.58, pp.5845-5859, Nov. 2010

[94] D. Tse and P. Viswanath, "Fundamentals of Wireless Communication", Cambridge University Press, 2005

[95] T. Cover, R. McEliece, and E. Posner, "Asynchronous multiple-access channel capacity", in *IEEE Trans. Inform. Theory*, vol.27, pp.409-413, July 1981